National Library of Canada
Bibliothèque nationale du Canada

Canadian Theses Service
Service des thèses canadiennes

Ottawa, Canada
K1A 0N4

NOTICE

The quality of this microform is heavily dependent upon the quality of the original thesis submitted for microfilming. Every effort has been made to ensure the highest quality of reproduction possible.

If pages are missing, contact the university which granted the degree.

Some pages may have indistinct print especially if the original pages were typed with a poor typewriter ribbon or if the university sent us an inferior photocopy.

Reproduction in full or in part of this microform is governed by the Canadian Copyright Act, R.S.C. 1970, c. C-30, and subsequent amendments.

AVIS

La qualité de cette microforme dépend grandement de la qualité de la thèse soumise au microfilmage. Nous avons tout fait pour assurer une qualité supérieure de reproduction.

S'il manque des pages, veuillez communiquer avec l'université qui a conféré le grade.

La qualité d'impression de certaines pages peut laisser à désirer, surtout si les pages originales ont été dactylographiées à l'aide d'un ruban usé ou si l'université nous a fait parvenir une photocopie de qualité inférieure.

La reproduction, même partielle, de cette microforme est soumise à la Loi canadienne sur le droit d'auteur, SRC 1970, c. C-30, et ses amendements subséquents.

NL 339 (r. 88/04) c

Canada

A Computer Technique for Heating Control Analysis and Application to Radiant Heating

Jian G. Shou

A thesis

in

The Centre for Building Studies

Presented in Partial Fulfilment of the Requirements

For the Degree of Master of Applied Science

Concordia University

Montreal, Quebec, Canada

November 1991

©Jian G. Shou, 1991

National Library of Canada
Bibliothèque nationale du Canada

Canadian Theses Service
Service des thèses canadiennes

Ottawa, Canada
K1A 0N4

The author has granted an irrevocable non-exclusive licence allowing the National Library of Canada to reproduce, loan, distribute or sell copies of his/her thesis by any means and in any form or format, making this thesis available to interested persons.

L'auteur a accordé une licence irrévocable et non exclusive permettant à la Bibliothèque nationale du Canada de reproduire, prêter, distribuer ou vendre des copies de sa thèse de quelque manière et sous quelque forme que ce soit pour mettre des exemplaires de cette thèse à la disposition des personnes intéressées.

The author retains ownership of the copyright in his/her thesis. Neither the thesis nor substantial extracts from it may be printed or otherwise reproduced without his/her permission.

L'auteur conserve la propriété du droit d'auteur qui protège sa thèse. Ni la thèse ni des extraits substantiels de celle-ci ne doivent être imprimés ou autrement reproduits sans son autorisation.

ISBN 0-315-73686-0

Canada

ABSTRACT

A Computer Technique for Heating Control Analysis and Application to Radiant Heating

Jian G. Shou

System performance of a building may be improved by considering the interactions between the building, the HVAC system and its control at the design stage. A technique for analysis of these interactions has been developed, specifically for heating and its control.

A building model is represented with a detailed thermal network which includes both distributed parameter elements, such as thermal mass, and lumped elements, such as the room air thermal capacitance. Laplace transfer functions for the building are obtained from the discrete frequency response data by means of a modified least-squares polynomial fitting method. Together with the transfer functions for heating and control elements, the overall system transfer function is determined through block diagram algebra.

The overall system transfer function is studied in the frequency domain for control tuning. The transient response of the heating system is then determined with a stepwise numerical Laplace transform inversion. The technique developed has been applied to electric radiant panel heating systems. Numerical and experimental results have indicated that the technique, implemented on personal computer, is an efficient tool for heating control analysis. Its major advantage is that it enables us to perform the analysis of the

interactions between the building, the heating system and the control system. Different building design options can thus be evaluated based on a relative basis.

Experimental studies in an outdoor test-room have been conducted to study the control of a radiant heating system with an air temperature sensor or with an operative temperature sensor. The results from both the computer simulations and the measurements indicate that special consideration of system stability should be given to the design of a radiant heating system with operative temperature control. The computer technique developed was shown to be helpful in tuning a radiant heating control system, as well as for evaluation of design options.

ACKNOWLEDGEMENTS

I would like to express my deepest gratitude to Dr. Andreas K. Athienitis, my thesis supervisor, for his expert guidance and support during my graduate studies.

Also, I would like to thank Joseph Zilkha for his technical assistance in the installation of the test facilities.

This research was made possible through the support of the Centre for Building Studies (CBS), Concordia University. Many thanks also to CanRay Ltd. for providing the radiant heating panels used in this study.

Finally, special appreciation goes to my parents, my family and Shuling for their encouragement and support.

TABLE OF CONTENTS

CHAPTER 4. ANALYSIS OF HEATING CONTROL SYSTEM

CHAPTER 5. CONTROL OF RADIANT PANEL HEATING

CHAPTER 6. CONCLUSION

I IST OF FIGURES

LIST OF TABLES

NOMENCLATURE

A area (m^2).

A_s effective sensing area of long wave radiant exchange (m^2).

C_a specific heat of air (J/kg·K).

C_i zero of a transfer function.

$\{D\}$ vector relating T_e to $\{T\}$.

$[D_{mr}]'$ matrix relating T_{mr} to $\{T_{sf}\}$.

E error function in the least-squares fitting.

F^*_{ij} radiation exchange factor between surface i and j.

F_{ij} view factor between surface i and j.

$F(s,i)$ view factor between a sensor and surface i.

$G_{c,p}$ transfer function representing a proportional controller.

$G_{c,pi}$ transfer function representing a proportional integral controller.

G_f transfer function representing a final control element.

G_p transfer function representing a heating system.

H_s transfer function representing a temperature sensor.

$I(\omega)$ imaginary part of a discrete frequency response.

K thermal conduction coefficient ($W/m^2 \cdot °C$).

K_f magnitude ratio of a final control element (W/mA).

$K_{s,p}$ system proportional gain or $K_{s,p} = K_p \cdot K_f$ (W/°C).

K_p proportional controller gain factor (mA/°C).

K_h capacity of a heating system (W).

K_u ultimate gain (W/°C)

M order of a numerator polynomial in transfer function model.

$M(\omega)$ magnitude ratio between the output and input.

N order of a denominator polynomial in transfer function model.

P_u ultimate period (second).

Q heat flow (W).

$\{Q\}$ vector of room nodal heat sources.

Q_c heat flow due to conduction (W).

Q_r heat flow due to radiation (W).

$R(\omega)$ real part of a discrete frequency response.

S_i pole of a transfer function.

T temperature (°C).

T_{air} room air temperature (°C).

T_e operative temperature (°C).

T_g room globe temperature (°C).

T_{mr} mean radiant temperature (°C).

T_m temperature measured in the feedback loop (°C).

$\{T\}$ vector of room interior nodal temperatures.

$\{T_{sf}\}$ vector of room surface temperature (°C).

U heat conductance ($W/m^2 \cdot °C$).

U_0 conductance between inside and outside air ($W/m^2 \cdot °C$).

U_{ij} conductance between node i and node j (W/m·°C).

U(s) Laplace transform of a input signal.

W_{IL} weighting factor for the iterative least-squares fitting.

X horizontal distance.

{X} vector relating heat sources and operative temperature.

X^0 initial condition vector for stepwise algorithm.

X(i) operative temperature transfer function (°C/W).

[Y] matrix of admittance relating nodal temperatures and heat sources.

Y(i,j) component admittance between node i and j (W/°C).

Y(s) Laplace transform of an output signal.

[Z] matrix of impedance relating heat sources and nodal temperatures.

Z(i,j) room air temperature transfer function (°C/W).

a_i coefficients of numerator polynomial.

b_j coefficients of denominator polynomial.

e base of natural logarithms.

h time step for numerical inversion of the Laplace transform.

h_c convective heat transfer coefficient (W/m^2·°C).

h_r radiative heat transfer coefficient (W/m^2·°C).

h_t combined heat transfer coefficient or $h_t = h_c + h_r$ (W/m^2·°C).

j $(-1)^{1/2}$.

q heat flow (W).

q^+ radiosity (W/m^2).

s Laplace operator.

t time (second).

t_d dead time of a component (second).

$t_{f,d}$ time constant of a final control element (second).

SUBSCRIPTS

c conduction.

g globe.

L number of iterations.

p proportional.

r radiation.

sp set point.

SUPERSCRIPT

0 initial condition.

GREEKS

α thermal diffusivity (m^2/s).

$\alpha(\omega)$ real part of a complex.

$\beta(\omega)$ imaginary part of a complex.

γ $(s/\alpha)^{1/2}$.

δ proportional band (°C).

ε longwave emissivity.

$\varepsilon(j\omega)$ error message at discrete frequency.

$\varepsilon(t)$ deviation between the setpoint and measured temperature (°C).

ξ damping coefficient of a second order system.

ρ longwave reflectivity.

σ Stefan-Boltzmann constant ($W/m^2 K^4$).

τ_i integral time constant (second).

τ_s time constant of a temperature sensor (second).

τ_h time constant of a heating system (second).

Φ phase angle (degree).

ω frequency (rad/s).

ω_{co} crossover frequency (rad/s).

CHAPTER 1

INTRODUCTION

1.1 Introduction

Analysis of building thermal dynamics is traditionally performed separately from the design of HVAC systems and their controls. Most studies have been focused individually on the three aspects of building thermal performance: predicting building load and estimating energy consumption, designing HVAC systems, and determining control components and control strategies. Various investigators have developed different room models to describe the building thermal response. Most of these models are too simple to deal with the dynamic thermal process. Furthermore, the control system is treated as an "add-on" to the building mechanical system instead of as an integral part of the building and its HVAC system.

The search for energy-efficient and high performance building systems should not only embrace the component dynamics of each element in the building system, but also the interactions between them. It becomes evident that the success of implementing efficient energy management and control strategies is coupled with the understanding of the overall system performance. The nature of the interactions between the system components has established the need for a unified procedure to study the performance of the building, the HVAC system and its control as one thermal system. During the past ten years, some efforts have been made to tackle the problem of the integration of the mechanical and control systems with transient heat transfer through the building's

structure (Thompson 1981, Miller 1982, Hartman 1988, Dexter 1988, Zhang et al. 1988). One of the most important elements in the building system is the envelope, which has a significant influence on the system performance. For instance, thermal mass in the envelope has the function of storing thermal energy and reducing the room temperature swings caused by fast changes in the ambient temperature, high solar gains and intermittent heating. Energy savings can be achieved by effective use of the storage capacity of the thermal mass, such as the use of a night setback in the thermostat setpoint.

However, the room envelope models used for study of system dynamics are often oversimplified in terms of radiation, as well as the transient effects related to building thermal mass (Zhang et al. 1988). As reported by Borresen (1981), use of oversimplified models for rooms in selecting control parameters will result in conservative values for the control parameters. The optimum control of the HVAC systems requires fully understanding of building thermal dynamics. The total integrated dynamic thermal response analysis of a building system is considered as an effective tool only when all the major parameters affecting the system are understood and included in the study. One such detailed analysis program is HVACSIM$^+$ (Clark et al. 1985), which analyzes a building system through time domain simulation. However, the program needs a large amount of input data and requires high computation times; it becomes a cumbersome tool to use when there are numerous design options.

Alternatively, frequency domain techniques and associated Fourier series periodic methods have been used in building energy analysis. A program using a detailed room model is BEEP (Building Energy and Environment Program) (Athienitis, 1988), which

has employed thermal network theory and efficient computer formulation techniques. The room interior radiant exchanges, as well as the thermal mass in the envelope, are modelled accurately. However, the building thermal response is only obtained by solving the detailed thermal network at discrete frequencies. This makes difficult the application of the thermal network model to building system control analysis which requires a continuous form of Laplace transfer functions for buildings.

In this study, an important objective is to develop a computer method for the derivation of a continuous form of room transfer functions in the Laplace domain from the discrete frequency response data generated by BEEP and then to use these transfer functions for thermal control studies. If a room transfer function is available, the overall system transfer function of a building system can be obtained by integrating the component transfer functions with block diagram algebra. Following this approach, the detailed thermal network model used for energy analysis can be applied to building system control studies. The key feature of the approach is to use one detailed building model for both thermal control studies and building energy analysis. The building, its HVAC system, and the control system are considered as one thermal dynamic system, with all components represented by Laplace transfer functions. Thus, load calculations as well as transient numerical simulation and control parameter estimations are readily performed, which permits comparative study of control algorithms for energy efficiency and thermal comfort.

As an application, the method developed for the study of a building thermal system and its control will be applied to radiant heating. Unlike convective heating

systems, such as baseboard heating, the radiant heating system provides heat into a space mainly by radiation. Most of the heat is absorbed by the thermal mass of the building and its contents, and then released to the space by means of radiation and convection. However, the methods for the calculation of radiant heating loads and the control of radiant heating systems are similar to those for convective heating systems (ASHRAE Handbook 1987). The surface temperatures of the inside walls are assumed to be the same as the room air temperature. As a result, the effect of the mean radiant temperature on the thermal comfort of occupants is neglected. Studies have shown that the mean radiant temperature may differ significantly from room air temperature, often by more than 3°C (Athienitis and Dale 1987). Therefore, the conventional approach for radiant heating design and the heating system controls must be improved.

Recently, several researchers have suggested a new design method based on mean radiant temperature (Kalisperis et al. 1990). However, the potentially beneficial control of radiant heating systems using an operative temperature sensor has not been investigated analytically. This is partially due to the lack of an efficient modelling technique and a method to derive the operative temperature transfer functions for rooms. In this study, the thermal network model employed represents room thermal mass and interior radiant exchanges in detail, with which a radiant heating system and its control can be studied efficiently.

1.2 Objectives

A unified analysis tool is desirable for both building energy analysis and system

control studies. The building envelope, the HVAC system and the control components should be considered dynamically interrelated. As an important element, a room should be modelled in detail so that both thermal mass and interior radiant heat exchanges can be accurately taken into account. The same detailed room model will be used for both energy analysis and control system studies. The present study will be confined to the heating applications and primarily the electric radiant panel heating. The objectives of this research are the following:

1. To develop an efficient method for the estimation of room transfer functions in the Laplace domain from the discrete frequency response data of buildings, which is determined with the program BEEP.

2. To extend the application of building thermal network models to the study of building thermal control; thus both energy analysis and thermal dynamic studies can be performed with a detailed room model, which represents transient heat conduction in each wall and room interior radiant exchanges accurately.

3. To conduct theoretical and experimental studies of radiant heating control based on air temperature or operative temperature sensor, which will reveal the effects of the two types of temperature control on the system performance and provide a guideline for design applications.

1.3 Overview of thesis

The literature review will be summarized in chapter 2 to provide the reader with an overview of the present status of the room modelling, the building system simulation and the radiant heating applications.

In chapter 3, a thermal network model for rooms, which has been used in the program BEEP, will be discussed as a background for room modelling. It models thermal mass and room interior radiant exchanges in detail. However, this detailed thermal network program can only generate discrete frequency response data. In order to obtain a continuous form of room Laplace transfer functions for the analysis of building thermal controls, an interpolation method is employed based on a modified least-squares fitting technique. Representative results for a room are then given.

The integration of the building envelope, the heating system and the control components into one thermal system is presented in chapter 4. The overall Laplace transfer function of a system is derived from its component transfer functions through block diagram algebra. The control system stability is analyzed using a frequency domain technique. The transient response of the system is obtained with a numerical Laplace transform inversion technique. A computer program HEATCON is also presented in this chapter for the study of heating system control.

Comparisons of the transient responses of radiant heating systems through both computer simulations and experimental results are given in chapter 5, following a description of the test facilities and experimental setup. The effect of different controller gains are investigated with the radiant heating controls based on either air temperature

sensor or globe temperature sensor (an approximation to an operative temperature sensor).

Finally, the conclusions on the analysis procedure and the computer technique developed are summarized in chapter 6. Extensions of the present work are then recommended.

CHAPTER 2

LITERATURE REVIEW

2.1 Introduction

The investigation of the dynamic characteristics of building systems has been a topic of research for a long time. Significant efforts have been made to conduct both experimental and theoretical simulations of individual components of HVAC systems and control elements. The aim was to achieve a better understanding of the dynamics of individual components in building systems, such as the dynamics of the buildings, the heating and cooling coils, the control valves, etc..

Recently, the studies of building thermal dynamics have been towards the integration of the components including the building envelope, the HVAC system and its control. This is mainly due to the recognition that the building thermal dynamic characteristics have significant effects on HVAC system operation. Poor design of a control loop, which links the building thermal behaviour and the HVAC system, may adversely affect the thermal comfort level, and lead to increased use of energy by forcing the HVAC system to operate in an uneconomic manner (Borresen 1981). Further energy savings in buildings may be realized through better design and optimal control of the building systems. The control system dynamics have a strong influence on the energy consumption patterns of a building; the study of control system dynamics may lead to the derivation of control strategies for energy saving while maintaining a thermal comfort level.

Close examination of the dynamic interactions between HVAC system, building and the control system as an integrated thermal system is still at its early stage. This chapter will review the major techniques for building system simulation and analysis, as well as the different room models for thermal control analysis. A specific type of the heating application - radiant heating system, will also be discussed.

2.2 Building system simulation

There are two general approaches for building thermal system simulation. In the first approach, the system is analyzed through time domain simulation using finite difference or transform based techniques based on the convolution theorem (response factor methods). The advantage of the finite difference approach is that both linear systems and non-linear systems can be modelled. However, in order to represent some distributed components in the system such as the thermal mass, discretization with lumped parameter models is usually employed. The larger the number of nodes taken, the more close the approximation will be to the distributed components. Sometimes, it is required to take a large number of nodes and very small time steps to avoid numerically induced oscillations in the solution, which leads to computational inefficiency. On the other hand, very small time steps may cause significant truncation error (Borresen 1981). In this case, variable time steps may have to be used.

One detailed simulation program is HVACSIM$^+$, which has been primarily developed as a research tool for whole building system studies. The approach HVACSIM$^+$ takes in the simulation is to have variable time steps for HVAC components and control

system, and a user-defined constant time step for the building envelope (Park et al. 1985; Clark 1985). The user can compose a system by selecting individual components and controls, which provides the flexibility to compare various systems and examine different control strategies. However, the program requires large amounts of data to conduct a detailed simulation, which may not be available at the design stage. Besides, there are needs to examine or evaluate different design alternatives at the design stage and thus the program becomes a cumbersome tool to use when there are numerous design options.

Alternatively, another approach can be used which involves frequency domain analysis and simulation. It has been an approach that is often employed in periodic models for passive solar analysis and building load calculations (Kimura 1977). The discrete frequency domain method has proven its efficiency in building energy analysis in conjunction with network theory (Athienitis 1985, Haghighat and Athienitis 1988). The interests in frequency domain techniques stem from their potential advantages over time domain techniques. Some important advantages of frequency domain methods are summarized:

1. They are very flexible in that they can be used for either analysis or simulation, while time domain methods cannot be used for analysis without simulation.

2. Because there is no time step involved, frequency domain methods provide less expensive and more efficient solutions than time domain methods.

3. No discretization is required for the distributed parameter components. This is an important advantage in building modelling in which a significant amount of thermal mass may be present.

The major problem with frequency domain methods has been the difficulty of modelling non-linear behaviour. In practice, linearization of the problem undertaken is generally an acceptable compromise in engineering. Depending on the objectives, one may evaluate th pros and cons of the two approaches and choose the one that best suites his study. The majority of the studies in which non-linear models are considered generally use the time domain analysis. On the other hand, frequency domain techniques are more appropriate for linear models.

To perform a dynamic simulation of a building system and its control, the following procedure is usually followed:

1. Mathematical models are developed to represent the components of the integrated system. The detail with which the models describe the actual components, however, has a significant effect over the results of studies performed, as well as the computational efficiency.

2. These individual models are then be integrated into the representations of the actual system through the use of sets of differential equations or use of Laplace domain block diagram algebra.

3. Finally, the resulting set of differential equations or a system transfer function must be determined. By changing room materials and system parameters, different design options can be analyzed and evaluated. The outputs from the study may include the transient responses, state variables and system parameters.

2.3 Room modelling

HVAC system operation depends strongly on the building dynamic characteristics. As pointed out by Thempson (1981), the model describing the thermal behaviour of the building for control studies may vary widely in complexity. It could be for example a simple model, which considers only the air mass, or a relatively detailed model that takes into account interior radiant exchanges and thermal storage effects (Borresen 1981; Zhang et al. 1988).

Most room models represent radiation heat exchanges and thermal capacity of the walls in a very approximate manner (Mehta 1980; Wood 1980). As such, less information about the building thermal characteristics can be drawn from the dynamic analysis. In order to improve the building system performance, a knowledge of the building dynamics is necessary, which may be achieved by detailed modelling of the building's thermal behaviour (Zaheer-uddin 1990). Programs such as DOE-2 and BLAST have improved room models, but are primarily concerned with the load calculation of the building, instead of considering dynamic interactions between the building, the HVAC system and the control loop (BLAST 1983; DOE-2 1981). These models are often complex and not suitable for the analysis or design of a control system. Furthermore, these models are

merely used for room air temperature analysis. The control of operative temperature, which is important to maintain the thermal comfort of occupants, has not been investigated in detail.

A common method of studying a heating system for a building is to use energy simulation tools, such as BLAST and DOE-2. The use of such a tool allows us to investigate various convective heating systems. Generally, these programs lack the capability to simulate a radiant heating system. Recently, a radiant heating system model has been proposed for BLAST (Maloney et al. 1988). However, the room model employed requires iterative calculation of each surface temperature, which results in high computational times, particularly for large buildings.

Alternatively, an efficient thermal network model, which handles the radiation-convection heat transfer in the building and thermal storage effects in detail, has been developed and implemented in an energy analysis program BEEP (Building Energy and Environment Program) (Athienitis et al. 1988). This program has been compared with TARP (a response factor program which is a research version of BLAST) by Haghighat and Athienitis (1988). The key concepts employed in modelling a building are network theory and efficient computer formulation and solution techniques which utilize representation of building components such as walls, windows and rooms by subnetworks. Radiant exchanges among the room interior surfaces, as well as the thermal mass, are modelled in detail. Mean radiant temperature of a room is determined accurately. As a result, the thermal dynamic response of the room can be analyzed either in terms of air temperature or operative temperature, which provides an efficient analytical tool for

passive solar and radiant heating analysis.

2.4 Radiant heating and its control

Radiant heating systems have been used in commercial and residential buildings for several decades. During the past few years, the applications have increased and many articles have been published on the investigations of radiant heating systems with respect to thermal comfort and energy efficiency.

The study of human comfort sensation has been an area of extensive research activity (Fanger 1972; Olesen et al. 1980). Thermal comfort may be predicted with a comfort equation, which considers six parameters: activity level, clothing, space air temperature, mean radiant temperature, air velocity and humidity. Despite the completeness of the equation, the thermal comfort of a space is mainly controlled in terms of air temperature, mean radiant temperature, humidity and , at most, air movement. One of the important indices to predict overall thermal comfort is "operative temperature", which is defined as "the uniform temperature of an enclosure in which an occupant would exchange the same amount of heat by radiation plus convection as in the actual non-uniform environment" (ASHRAE Standard 55-81). It is approximately equal to the average of the space air temperature and the mean radiant temperature weighted by the respective heat transfer coefficients. Operative temperature generally indicates how people sense the thermal comfort level of their environment.

Traditionally, radiant heating systems have been sized based on the heat loss of an enclosure at some specified room air temperature. This air temperature is usually the

same one as what would be used in the design of a convective heating system (ASHRAE Handbook 1987). During the operation, the control of the heating system is based on the feedback from the room air temperature sensor. This procedure ignores the fact that an occupant's thermal comfort is directly related to the operative temperature of the environment. With radiant heating, the mean radiant temperature of the space is usually higher than the space air temperature, the average temperature of the room. Some experiments have indicated that mean radiant temperature of a room may differ significantly from room air temperature, often by more than 3°C (Athienitis and Dale 1987). Therefore, radiant heating allows the space air temperature to be set a few degrees lower than convective heating and still maintain acceptable levels of thermal comfort. As a result, neither the control nor the design based solely on air temperature for radiant heating systems has been justified.

An analytical study by Zmeureanu et al. (1988) indicates that the application of the conventional calculation method will overestimate the heating loads, thus the equipment size. Some experimental and analytical comparisons of energy requirements have also been made (Bryan 1981; Berglund 1982; Jones 1989; Chen 1990). However, the cost-effectiveness of a radiant heating is still uncertain in many circumstances because of its complexity. In addition, radiant heating systems with operative temperature control have not been investigated. Few projects have been conducted to study the radiant heating controls in detail and their dynamic relationships with the building enclosures. As pointed out by Berglund (1982), potential applications exist for energy savings and performance improvement with radiant heating in transient conditions. An efficient tool for the analysis

will help us to study such applications, and to evaluate different design options and control strategies at the design stage.

CHAPTER 3

DETERMINATION OF ROOM TRANSFER FUNCTIONS

3.1 Introduction

Many efforts have been made to develop various room models for building system simulation. Recently, a detailed thermal network model has been developed by Athienitis and used in a building energy analysis program BEEP (Athienitis 1988). The model represents thermal mass in the building envelope and room interior radiant exchanges accurately (Athienitis 1988).

Frequency domain techniques and associated Fourier series periodic methods are often used in building energy analysis (Haghighat and Athienitis 1988). They may be primarily categorized into two groups - literal analysis and discrete frequency analysis. Literal analysis is applicable to problems in which the analytical solutions can be obtained. However, the method is impossible for the analysis of complex thermal networks, such as the detailed room model used in BEEP. Instead, an energy balance is solved at discrete frequencies, a computationally more efficient procedure.

The design of thermal control systems for buildings is usually performed separately from the building energy analysis. An integrated (building - HVAC system - control) system analysis requires the transfer functions of every component in the system. As a result, a continuous form of Laplace transfer functions for the room has to be derived from the discrete frequency response. This is achieved by fitting a Laplace transfer function model to the discrete frequency domain data.

With this approach, the application of the thermal network model (used for energy analysis) can be extended to the system control study by means of a transfer function technique. The same room model can be used in the control study, as well as in the energy analysis. The method to derive the room transfer functions from such a detailed room model, a major contribution of this thesis, will be fully addressed in this chapter.

3.2 Background

Before the introduction of the method for determination of the room transfer function, the thermal network model will be briefly discussed. Thermal networks are analogues to electrical networks, the temperature being analogous to the voltage and the heat flow analogous to current. In the frequency domain modelling of building heat transfer, two types of passive components can be identified (Athienitis 1986):

1. Two-terminal components: These components represent thermal coupling between two nodes (terminals). In the case of convective coupling the nodes represent a surface and a fluid, or two fluid masses at different temperatures, such as infiltration. In the case of radiation coupling, the nodes link two surfaces exchanging energy. Conductive coupling is also represented by a two-terminal component if the relevant wall layer has negligible thermal capacitance, such as insulation materials.

The constitutive equation for a two-terminal component can be expressed in matrix form:

$$\begin{vmatrix} T_i \\ Q_i \end{vmatrix} = \begin{vmatrix} 1 & 1/U \\ 0 & 1 \end{vmatrix} \begin{vmatrix} T_j \\ Q_j \end{vmatrix} \quad . \tag{3.1}$$

where T_i and Q_i are the temperature and heat source at node i; T_j and Q_j are temperature and heat source at node j. Heat conductance U for different cases of heat transfer can be calculated as follows:

1. Convection between a surface j and air i:

$$U = A_j \, h_c$$

2). One-dimensional conduction:

$$U = \frac{A_j \, K}{X}$$

3). Radiative exchange between surfaces i and j:

$$U = 4 \, \sigma \, T_m^3 \, A_i \, F_{ij}^*$$

The term $4T_m^3$ is the linearization factor for radiation and F^*_{ij} is the radiation exchange factor. Linearization of the radiation exchange process is generally accurate enough because the total temperature variation in rooms, on an absolute scale, is relatively small. This assumption is widely accepted and used in simulations.

2. Three-terminal components: One dimensional heat diffusion through a massive slab is physically the same process as conduction through a non-massive component. However, because of the heat storage in the thermal mass, an additional node is needed as a reference to quantify the thermal state of the slab. Thus, the heat stored can be determined with the temperatures of two surfaces relative to the reference node.

For a detailed building simulation, thermal storage effects of mass in an enclosure have to be taken into account and walls are treated as three terminal components, two of the terminals (nodes) being the interior and exterior surfaces and the third being the reference node. The constitutive equation for three-terminal model can be expressed in different forms. The one frequently encountered is the cascade form. It is derived by taking the Laplace transform of the one-dimensional heat diffusion equation, which can be solved to relate heat flux and temperature at one surface to those at the other surface, without discretizing (Kimura 1977):

$$\begin{vmatrix} T_1 \\ Q_1 \end{vmatrix} = \begin{vmatrix} D & B \\ C & D \end{vmatrix} \begin{vmatrix} T_2 \\ -Q_2 \end{vmatrix} \quad . \qquad (3.2)$$

The elements of the storage mass cascade matrix are given by: $D=\cosh(\gamma X)$, $B=\sinh(\gamma X)/(k\gamma)$ and $C=(k\gamma)\sinh(\gamma X)$. The quantity k is the storage mass thermal conductivity and γ is equal to $(s/\alpha)^{1/2}$, s being the Laplace transform variable and α being the storage mass thermal diffusivity. For frequency domain analysis, s is set equal to $j\omega$, where $j=(-1)^{1/2}$ and ω is the frequency. The cascade matrix for a multilayered wall is obtained by multiplying the cascade matrix for consecutive layers. Usually the

temperatures of interest are either the inside or the outside temperatures. In this way, the wall interior temperatures are easily eliminated.

A large thermal network can be viewed as composed of subnetworks connected at their nodes, such as the nodes representing the walls, windows, floor and ceiling. A linear subnetwork connected to a network at only two terminals can be represented by its Norton equivalent (Athienitis et al. 1990). It consists of a heat source and an admittance connected in parallel between the two terminals. The heat source is the short-circuit heat flow at the node and the admittance is the subnetwork equivalent admittance as seen from the connection nodes. Often, an exterior wall is assumed to be made up of an inner layer of storage mass of uniform thermal properties and another massless layer, also of uniform thermal properties. By applying two-terminal model and three-terminal model in cascade, matrix equation (3.3) is obtained relating the temperatures and the heat flows at the inside and outside surfaces:

$$\begin{vmatrix} T_1 \\ Q_1 \end{vmatrix} = \begin{vmatrix} D & B \\ C & D \end{vmatrix} \begin{vmatrix} 1 & 1/U \\ 0 & 1 \end{vmatrix} \begin{vmatrix} T_2 \\ -Q_2 \end{vmatrix} \quad . \tag{3.3}$$

Depending on the objectives, a given room may be modelled in different ways. For a detailed room model, all massive walls, floor and ceiling are modelled by individual three-terminal distributed parameter elements. A room with its detailed thermal network model is illustrated in figure 3.1. An energy balance for a detailed model is expressed in the admittance form (Athienitis et al. 1990):

$$\begin{vmatrix} sC_a+\Sigma Uij+U_a & -U12 & -U13 & -U14 & -U15 & -U16 & -U17 & -U18 \\ -U12 & Y_{2a}+\Sigma U2j & -U23 & -U24 & -U25 & -U26 & -U27 & -U28 \\ -U13 & -U23 & Y_{3a}+\Sigma U3j & -U34 & -U35 & -U36 & -U37 & -U38 \\ -U14 & -U24 & -U34 & Y_{4a}+\Sigma U4j & -U45 & -U46 & -U47 & -U48 \\ -U15 & -U25 & -U35 & -U45 & Y_{5a}+\Sigma U5j & -U56 & -U57 & -U58 \\ -U16 & -U26 & -U36 & -U46 & -U56 & Y_{6a}+\Sigma U6j & -U67 & -U68 \\ -U17 & -U27 & -U37 & -U47 & -U57 & -U67 & Y_{7a}+\Sigma U7j & -U78 \\ -U18 & -U28 & -U38 & -U48 & -U58 & -U68 & -U78 & Y_{8a}+\Sigma U8j \end{vmatrix} \begin{vmatrix} T1 \\ T2 \\ T3 \\ T4 \\ T5 \\ T6 \\ T7 \\ T8 \end{vmatrix} = \begin{vmatrix} Q1 \\ Q2 \\ Q3 \\ Q4 \\ Q5 \\ Q6 \\ Q7 \\ Q8 \end{vmatrix}$$

or $$[Y]\{T\} = \{Q\}. \qquad (3.4)$$

Here, heat flows $\{Q\}$ and temperatures $\{T\}$ at the nodes, are vectors with elements Q_i and T_i corresponding to nodes (i=1,2..N) of the network. Admittance matrix [Y] is a square matrix of order N. The diagonal entry Y(i,i) is equal to the sum of the component admittances connected to node i. Off diagonal entry Y(i,j) is the sum of component admittance/conductance connected between nodes i and j, multiplied by -1.

An alternative form of the nodal equation is the impedance form:

$$\{T\} = [Z]\ \{Q\} \qquad (3.5)$$

where $[Z] = [Y]^{-1}$. The first row of the matrix [Z], the impedance transfer function Z1j(s), represents the effects of sources Q(j) at node j on room air temperature T1(s) (node 1 representing room air) by equation (3.6):

$$T1(s) = \sum_{j=1}^{8} Z1j(s)\ Q(j) \quad . \qquad (3.6)$$

For example, the effects of heat sources at air (node 1) and floor (node 7) on room air (node 1) temperature can be shown as

$$T1(s) = Z11(s)\ Q(1) + Z17\ Q(7).$$

For a detailed room model, the room transfer functions Z1j(s) can not be easily obtained

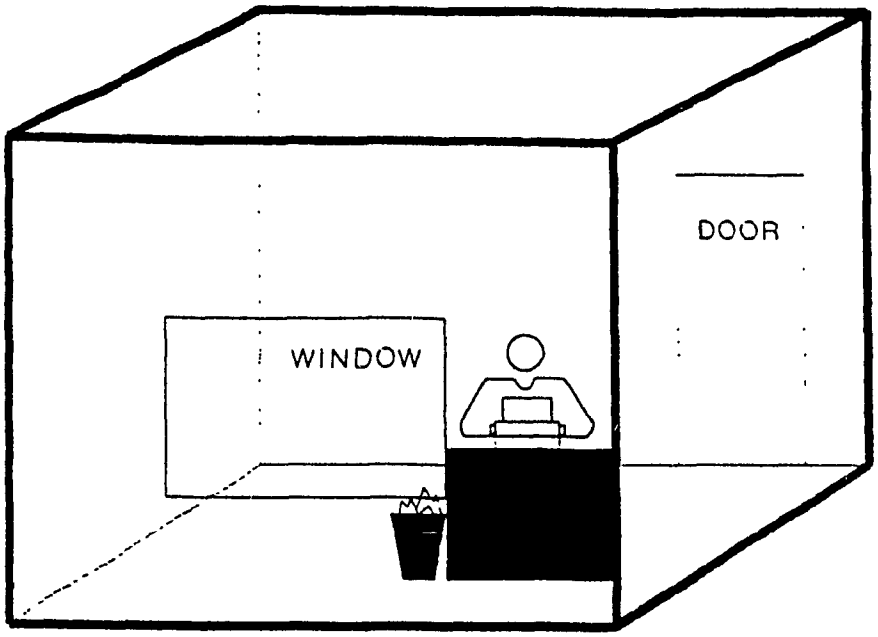

(a)

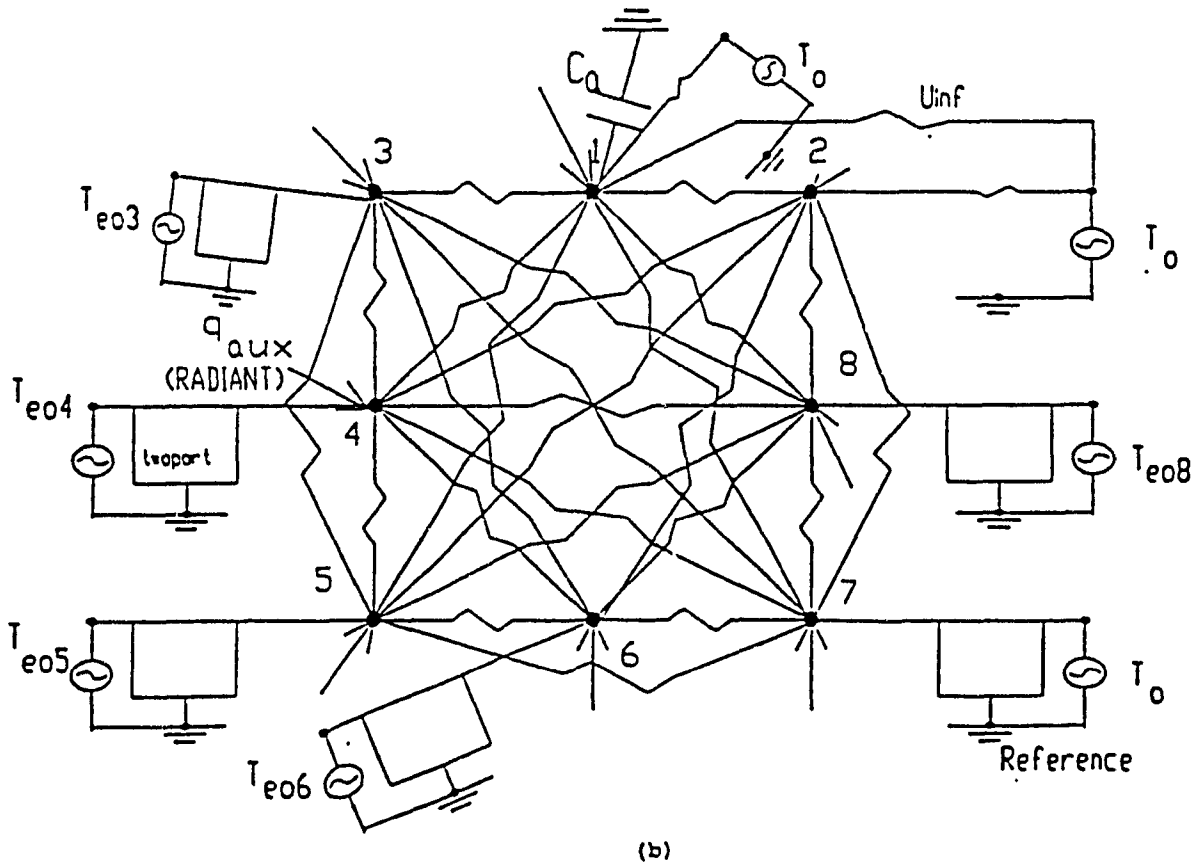

(b)

Figure 3.1 (a) A simple room, (b) room thermal network (nodes: 1=room air, 2-8 are interior surfaces - 2=window, 3=front wall, 4=ceiling, 5=right wall, 6=back wall, 7=floor, 8=left wall; arrows indicate heat sources, $T_{..}$=sol-air temperature, $T_{.}$=outside temperature).

from the complex matrix (3.4) with an analytical method. They are determined at specific frequencies by inversion of the nodal admittance matrix.

As explained in chapter 2, operative temperature is more closely related to the occupant's thermal comfort. The key to determining the operative temperature is to have a detailed model for interior radiant heat exchanges. The weighting factors for the individual surface temperatures need to be calculated accurately. The longwave radiant heat gain as sensed at a location in the room is given by

$$q_s = A_s \varepsilon_s [(q_1^+ F(S,1) + \ldots + q_i^+ F(S,i)) - \sigma T_s^4] \qquad (3.7)$$

where A_s is the effective sensing area, q^+ represents radiosity, i is the surface number (=1...i), and T_s is the temperature of the sensor (or object/person). The mean radiant temperature T_{mr} is defined by the equivalent energy balance:

$$q_s = A_s \varepsilon_s \sigma (T_{mr}^4 - T_s^4) \quad . \qquad (3.8)$$

For simplicity, the sensor is assumed to be located in the centre of the room, and the view factors F(s,i) between the sensor and surface i are approximated as equal to A_i/A_t (A_t=room area). If the effect of location within the room is to be studied, the factors F(s,i) must be calculated more accurately.

The mean radiant temperature in the room can be finally derived (Athienitis and Shou 1991) as

$$T_{mr} = [D_{mr}]' \{T_{sf}\} \qquad (3.9)$$

with row vector $[D_{mr}]'$ given by:

$$[D_{mr}]' = (\varepsilon / A_t)\ [A]'\ [M]^{-1} \qquad (3.10)$$

where [A] = [A,...A_r] (transpose of the area vector), $\{T_{sf}\}$ = [T(2),...T(8)]' (the surface temperature vector) and M(i,j) = I(i,j) - ρ_i F(i,j).

By definition, operative temperature can also be expressed as (note that T_{air} is the temperature at node 1 T(1)):

$$T_o = \frac{h_c}{h_r+h_c}\ T_{air} + \frac{h_r}{h_r+h_c}\ T_{mr} \quad . \qquad (3.11)$$

Substituting equation (3.9) into (3.11), we obtain:

$$T_o = \frac{h_c}{h_c+h_r}\ T_{air} + \frac{h_r}{h_c+h_r}\ \{D_{mr}\}' \{T_{sf}\} = \{D\}'\{T\} \qquad (3.12)$$

where {D}' = [D(1),...D(8)], while {T}=[T(1),T(2),...T(8)]' (the nodal temperature vector including air temperature and surface temperatures). Examination of equation (3.12) reveals that the weighting factors D(i) are as follows: the weight D(1) for the room air temperature is equal to $h_c/(h_r+h_c)$. The entries D(2)...D(8) reflect the relative weighting factors of the surface temperatures in the mean radiant temperature times the ratio $h_r/(h_r+h_c)$; they are therefore determined by multiplying vector $[D_{mr}]'$ by $h_r/(h_r+h_c)$.

The operative temperature is a scalar function of nodal temperatures [T(1)...T(8)], which is in turn a function of the source vector {Q}. Therefore, operative temperature is related to heat sources through a transfer function vector {X}, which denotes the effects

of source elements Q(i) on the operative temperature, and it can be determined as follows:

$$Te = \{D\}' [Y]^{-1} \{Q\} = \{X\}'\{Q\} \tag{3.13}$$

where

$\{X\} = [Y]^{-1} \{D\}$.

In this way, the operative temperature in a room can be accurately determined without the need to solve for the individual wall temperatures. The vector {D} is a function of room geometry and surface properties, it is evaluated only once for a room. Since the admittance matrix [Y] is a function of the room construction and frequency, it has to be determined at different frequencies. Thus, the operative temperature transfer vector {X} is obtained at specific frequencies.

3.3 A new method for estimation of transfer functions from discrete frequency responses

For a detailed room model, the air temperature transfer matrix [Z] or the operative temperature transfer vector {X} can be obtained at specific frequencies by inversion of the admittance matrix. However, it is impossible to directly use these discrete values of a building frequency response for the analysis of the building systems, such as the stability study of the control loops with the Laplace transfer function technique. A continuous form of the Laplace transfer functions of the rooms is desired for the dynamic analysis of building thermal systems. The thermal dynamics of a room have significant implications in system stability analysis and control parameter selection. In fact, the derivation of a continuous Laplace transfer function is the first step toward the analysis

of the overall thermal system.

Room transfer functions representing the essential aspects of building thermal characteristics should provide the capacity of predicting the dynamic building thermal response. Although in practice most building thermal processes are non-linear in nature, linear models for such systems are often used because of their simplicity. In this study, a time-invariant linear model is employed and the Laplace transfer function G(s) is usually expressed by a ratio of two polynomials, as follows:

$$G(s) = \frac{a_0+a_1 s+a_2 s^2+\ldots+a_m s^m}{b_0+b_1 s+b_2 s^2+\ldots b_n s^n} \quad . \qquad (3.14)$$

A convenient method of presenting the response data at various frequencies is to use a log-log plot for the amplitude ratios, accompanied by a semilog plot for the phase angles. Such plots are called Bode diagrams. The frequency method for identification of linear system transfer functions is often based on the Bode diagrams of frequency response. If the transfer function of the system is G(s), then the frequency response is obtained by replacing s=jω, i.e.,

$$G(j\omega) = \frac{Y(j\omega)}{U(j\omega)} = M(\omega)\ e^{j\phi(\omega)} \qquad (3.15)$$

where M is the ratio of the magnitudes, and ϕ is the phase shift between the output and the input. Now, we are concerned with the determination of room models (transfer functions) from discrete frequency response data. The problem is represented diagrammatically in figure 3.2.

Equation (3.14) can usually be decomposed into factors for both the numerator and

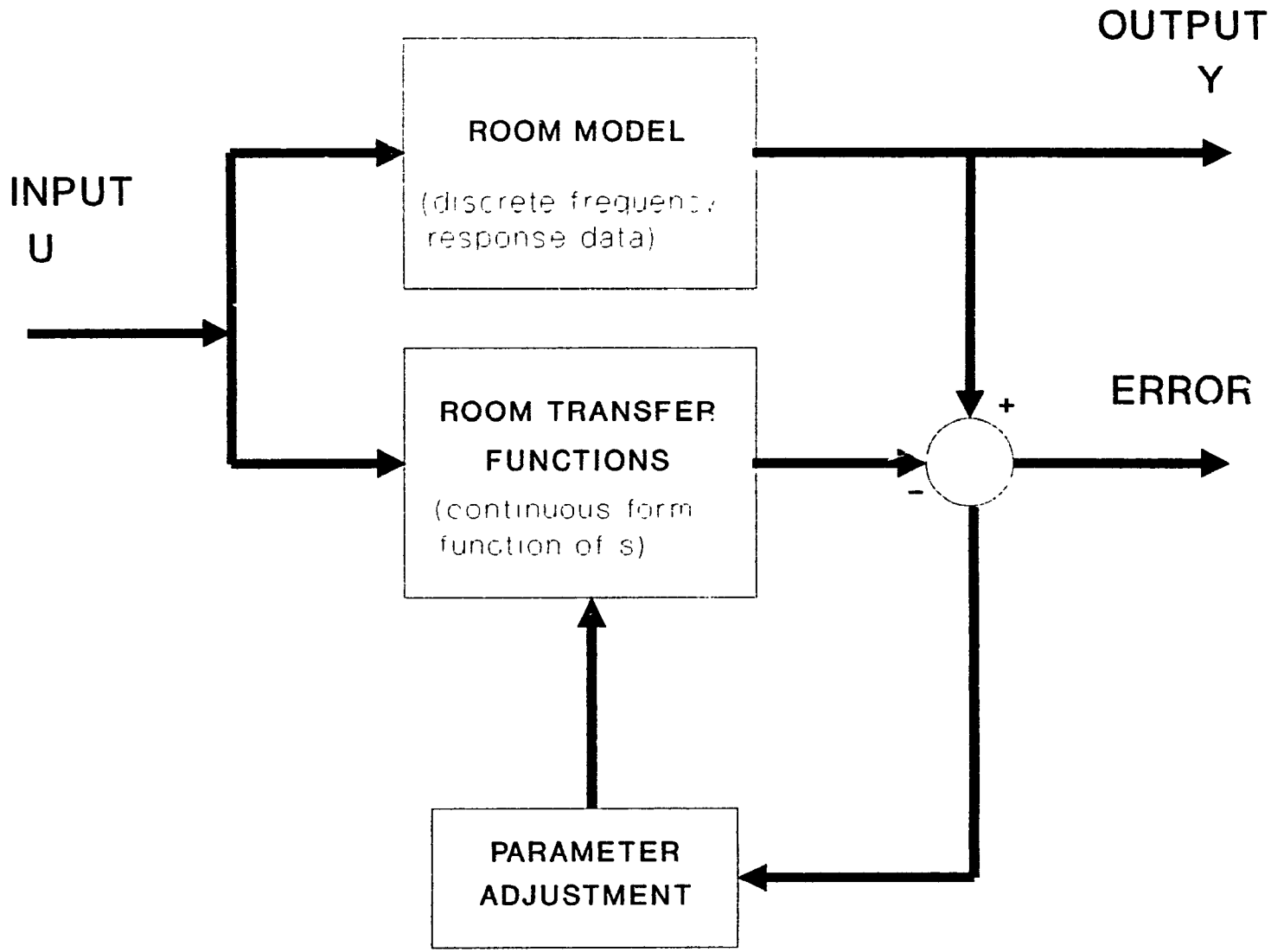

Figure 3.2 Structure of iterative transfer function fitting mehtod.

the denominator as follows:

$$G(s) = \frac{K(s+c_1)(s+c_2)\ldots(s+c_m)}{(s+s_1)(s+s_2)\ldots(s+s_n)} \quad . \qquad (3.16)$$

In the equation, c_1, c_2,..., c_m and s_1, s_2,..., s_n are zeros and poles of the transfer function, respectively. The form is called Bode's decomposition or pole-zero form. Note that if G(s) has a complex term in poles or zeros, then the second order term appears in the above decomposition. For example, if the pole of equation (3.16) has a complex conjugate, such as $s_j=\alpha+j\beta$ and $s_{j+1}=\alpha-j\beta$, then the denominator of G(s) may be factored in equation (3.17):

$$\prod_{i=1}^{n}(s+s_i)(s+s_j)(s+s_{j+1})$$
$$=[(s-\alpha)^2+\beta^2]\prod_{i=1}^{n}(s+s_i) \qquad (3.17)$$
$$=\frac{1}{T^2}[(Ts)^2+2\zeta Ts+1]\prod_{i=1}^{n}(s+s_i)$$

where $T=1/(\alpha^2+\beta^2)^{1/2}$ and $\zeta=-\alpha/(\alpha^2+\beta^2)^{1/2}$. The determination of a transfer function can usually be conducted using the Bode diagram. It is based on the estimations of the poles and zeros graphically. For a system of higher order, it is not easy to estimate the transfer function from the frequency response plots, particularly if the poles and zeros are not far apart. Secondly, the method does not provide any means to optimize the model or establish its accuracy.

A general method will be developed to find a continuous form of transfer function

with iterations according to some accuracy criterion as represented by figure 3.2. The proposed method is based on the technique of complex interpolation developed by Levy (1959), which will be modified to provide more accurate results. The weighted least squares error between the frequency response of the room and that of the fitted model is taken as the criterion for optimization.

In the following derivation, a general impedance transfer function Z(jω) given at specific frequencies is used to obtain the air temperature transfer function Z(s) and the method developed will be the same for deriving the operative temperature transfer functions X(s). From the discussion in section 3.2, we know that air temperature transfer matrix [Z] is obtained through inversion of the admittance matrix [Y]. If Z(jω) is the actual discrete frequency response data generated by BEEP, it can be represented by the sum of its real and imaginary parts:

$$Z(j\omega)=R(\omega)+jI(\omega)\ . \tag{3.18}$$

For a time invariant linear room model, a transfer function can be generally represented in the frequency domain as follows:

$$\begin{aligned} G(j\omega) &= \frac{\sum_{i=0}^{m} a_i (j\omega)^i}{\sum_{j=0}^{n} b_j (j\omega)^j} \\ &= \frac{(a_0-a_2\omega^2+a_4\omega^4-\ldots)+j\omega(a_1-a_3\omega^3+a_5\omega^4-\ldots)}{(b_0-b_2\omega^2+b_4\omega^4-\ldots)+j\omega(b_1-b_3\omega^2+b_5\omega^4,\ldots)} \\ &= \frac{(\alpha+j\omega\beta)}{(\sigma+j\omega\tau)} \\ &= \frac{M(j\omega)}{N(j\omega)} \end{aligned} \tag{3.19}$$

where a_i and b_j are the unknown coefficients of various powers of s. The numerical difference between the two functions G(jω) and Z(jω) represents the fitting error , that is

$$\begin{aligned} \varepsilon(j\omega) &= Z(j\omega) - G(j\omega) \\ &= Z(j\omega) - \frac{M(j\omega)}{N(j\omega)} \end{aligned} \quad . \tag{3.20}$$

Multiplying both sides of equation (3.20) by N(jω), we obtain

$$\begin{aligned} N(j\omega)\varepsilon(j\omega) &= N(j\omega)Z(j\omega) - M(j\omega) \\ &= \alpha(\omega) + j\beta(\omega) \end{aligned} \tag{3.21}$$

where $\alpha(\omega)$ and $\beta(\omega)$ are functions of the frequency and of the unknown coefficients a_i and b_j. The magnitude (absolute value) of the deviation can be expressed as:

$$\begin{aligned} |N(j\omega)\varepsilon(j\omega)| &= |\alpha(\omega) + j\beta(\omega)| \\ &= \sqrt{\alpha^2(\omega) + \beta^2(\omega)} \end{aligned} \quad . \tag{3.22}$$

Let us define E as the error function, summed over the range of the discrete frequencies:

$$E = \sum_{i=1}^{k} [\alpha^2(\omega_i) + \beta^2(\omega_i)] \quad . \tag{3.23}$$

Examination of equation (3.18) and (3.19) reveals that $a_0=Z(\omega=0)$ and $b_0=1$. Because the steady-state value of Z, that is $Z(\omega=0)$, is known, a_0 does not need to be evaluated. Equation (3.23) is now differentiated with respect to each unknown coefficients a_i and b_j, and the results set equal to zero to find the minimum. The result is a set of linear

simultaneous algebraic equations, which can be expressed by matrix equation (3.24a):

$$\begin{vmatrix} L_2 & 0 & -L_4 & .. & -S_2 & T_3 & S_4 & .. \\ 0 & -L_4 & 0 & .. & T_3 & S_4 & -T_5 & .. \\ L_4 & 0 & -L_6 & .. & -S_4 & T_5 & S_5 & .. \\ ... & & & & & & & \\ -S_2 & -T_3 & S_4 & .. & U_2 & 0 & -U_4 & .. \\ T_3 & -S_3 & -T_5 & .. & 0 & U_4 & 0 & .. \\ -S_4 & -T_5 & S_6 & .. & U_4 & 0 & -U_6 & .. \\ .. & & & & & & & \end{vmatrix} \begin{vmatrix} a_1 \\ a_2 \\ a_3 \\ .. \\ a_m \\ b_1 \\ b_2 \\ b_3 \\ .. \\ b_n \end{vmatrix} = \begin{vmatrix} T_1 \\ S_2-L_2 \\ T_3 \\ .. \\ .. \\ .. \\ -T_1 \\ U_2-S_2 \\ .. \end{vmatrix} \qquad (3.24a)$$

where L_h, S_h, T_h and U_h are the elements of the matrix defined by equation (3.24b):

$$\begin{aligned} L_h &= \sum_{i=0}^{k} \omega_i^h \\ S_h &= \sum_{i=0}^{k} \omega_i^h R_i \\ T_h &= \sum_{i=0}^{k} \omega_i^h I_i \\ U_h &= \sum_{i=0}^{k} \omega_i^h (R_i^2 + I_i^2) \end{aligned} \qquad (3.24b)$$

The subscripts n and m are the orders of the polynomial functions N(jω) and M(jω), respectively. The numerical values of the unknown coefficients can thus be obtained from matrix (3.24a). However, the optimum fitting may not be obtained with this approach because of the following serious deficiencies:

1. If the discrete frequency response data span over several decades, a good fit can

not be achieved at low frequencies, because lower frequency data have little influence on the fitting.

2. N(jω) could vary widely through the frequency range fitted, and large errors could be introduced.

3. The parameters thus obtained are not optimized in terms of model accuracy. The order of the fitting model has to be chosen in advance and the method does not provide guidelines for the choice.

In order to overcome the above shortcomings, the model is improved through an iterative approach (Fig 3.2). The error defined in equation (3.20) can be weighted by the ratio of the denominator polynomial evaluated in the current iteration to the denominator evaluated in the previous iteration:

$$\begin{aligned} \varepsilon_i &= \frac{\varepsilon(j\omega_i) N(j\omega_i)_L}{N(j\omega_i)_{L-1}} \\ &= \frac{Z(j\omega_i) N(j\omega_i)_L - M(j\omega_i)_L}{N(j\omega_i)_{L-1}} \end{aligned} \tag{3.25}$$

where L is the number of iterations.

A modified least square error criterion can be defined as a product of ε_i and weighting factor W_{iL}:

$$E_L = \sum_{i=1}^{k} |Z(j\omega_i) N(j\omega_i)_L - M(j\omega_i)_L|^2 W_{iL} \quad . \quad (3.26)$$

where the weighting factor is defined as

$$W_{iL} = \frac{1}{|N(j\omega_i)_{L-1}|^2} \quad . \quad (3.27)$$

The weighting factor is determined by the denominator polynomial evaluated in the previous iteration (initially assumed to be 1). With this method, the squared error is weighted more evenly at all frequencies. The local errors may be minimized (Salem Al-Assadi 1989). The new error function can be solved with the same procedure discussed before and optimum fitting shall be achieved by iterations in terms of the accuracy required.

Substantial insight into the building thermal behaviour may be obtained by studying the magnitude and phase angle of the important transfer functions. Consider, for example, the transfer functions Z17 and X7 in the detailed model, which represent the effects of heat sources at node 7 (floor) on the air temperature or operative temperature of node 1, respectively:

$$Z17 = \left.\frac{Tair(s)}{Q(s)floor}\right| \text{all other sources set equal to 0.}$$

$$X7 = \left.\frac{Te(s)}{Q(s)floor}\right| \text{all other sources set equal to 0.}$$

The magnitudes of Z17 or X7 represent the magnitude of the room air temperature response or operative temperature response due to heat sources at the floor. The phase

angles of the transfer functions indicate the response delay caused by thermal mass. A building with large amount of thermal mass can reduce the room temperature swings caused by change of heating load or ambient temperature. On the other hand, the thermal lag effect may result in system oscillation if the control parameters are not selected properly as shown later in this thesis.

As an example, the technique presented above will be applied to the derivation of the transfer functions of a test room. The detailed thermal properties and geometry of the room will be given in chapter 5, which describes experimental work with this room. Figures 3.3 - 3.10 depict the variations of magnitudes and phase angles (Bode plots) for discrete frequency response data. The magnitudes are nondimensionlized by dividing with the steady state (ω=0) values of the transfer functions. The magnitudes and phase angles calculated with the transfer functions are compared with the exact values generated from the discrete frequency response data.

Figure 3.3 illustrates the fitting of transfer function Z11(s) by using lower model order (numerator order M=1, denominator order N=2). However, a larger discrepancy happens in the frequency range of 1 - 10 cycles per day. Figure 3.4 indicates that the fitting accuracy will not be improved by simply increasing the model order. An iterative process is needed in order to improve the fitting results. The search of the model order and the required number of iterations is conducted based on the criterion of least-squares error. In our case, an order of four or less has been found to be adequate for a building thermal network model with the maximum percent error of $\pm$3% for the magnitude ratios and the maximum error of $\pm$0.01 degree for the phase angles. The number of iterations

is dependent on the specific discrete frequency data. In figure 3.5, the transfer function model Z11(s) is optimized with only two iterations. The fitted function corresponding to figure 3.5 is:

$$Z11(s) = \frac{4.8\times10^{-2}+180s+1.05\times10^{5}s^{2}+3.09\times10^{6}s^{3}}{1+1.8\times10^{4}s+1.7\times10^{7}s^{2}+3\times10^{3}s^{3}+7.5\times10^{10}s^{4}}$$

Similar results for Z14(s), Z17(s), X1(s), X4(s) and X7(s) are shown in figure 3.6, 3.7, 3.8, 3.9 and 3.10. The figures have indicated an excellent agreement between the fitted functions and the exact discrete frequency response data with an accuracy of ±1%.

Examination of figure 3.5 and 3.8 reveals that larger phase angles with X1 have been observed in the frequency range less than 30 cycles per day. This implies that the operative temperature variation caused by heated air has a slower response than air temperature at lower frequencies. However, at high frequencies, the thermal capacity of walls has little effect on the operative temperature response. As a result for short-term changes, the operative temperature has similar magnitudes and phase angles as air temperature response. For heat sources at wall surfaces, such as node 4 for radiant ceiling heating and node 7 for radiant floor heating, the operative temperature response is faster than air temperature response, especially in the frequency range larger than 30 cycles per day. This is clearly indicated by comparison of figures 3.9 and 3.10 with figures 3.6 and 3.7, respectively. Smaller phase angles of X4 and X7 are observed at high frequencies in figure 3.6 and 3.7. Because thermal capacity has little effect at high frequencies, a fast response of ceiling or floor surface temperature and operative temperature is expected.

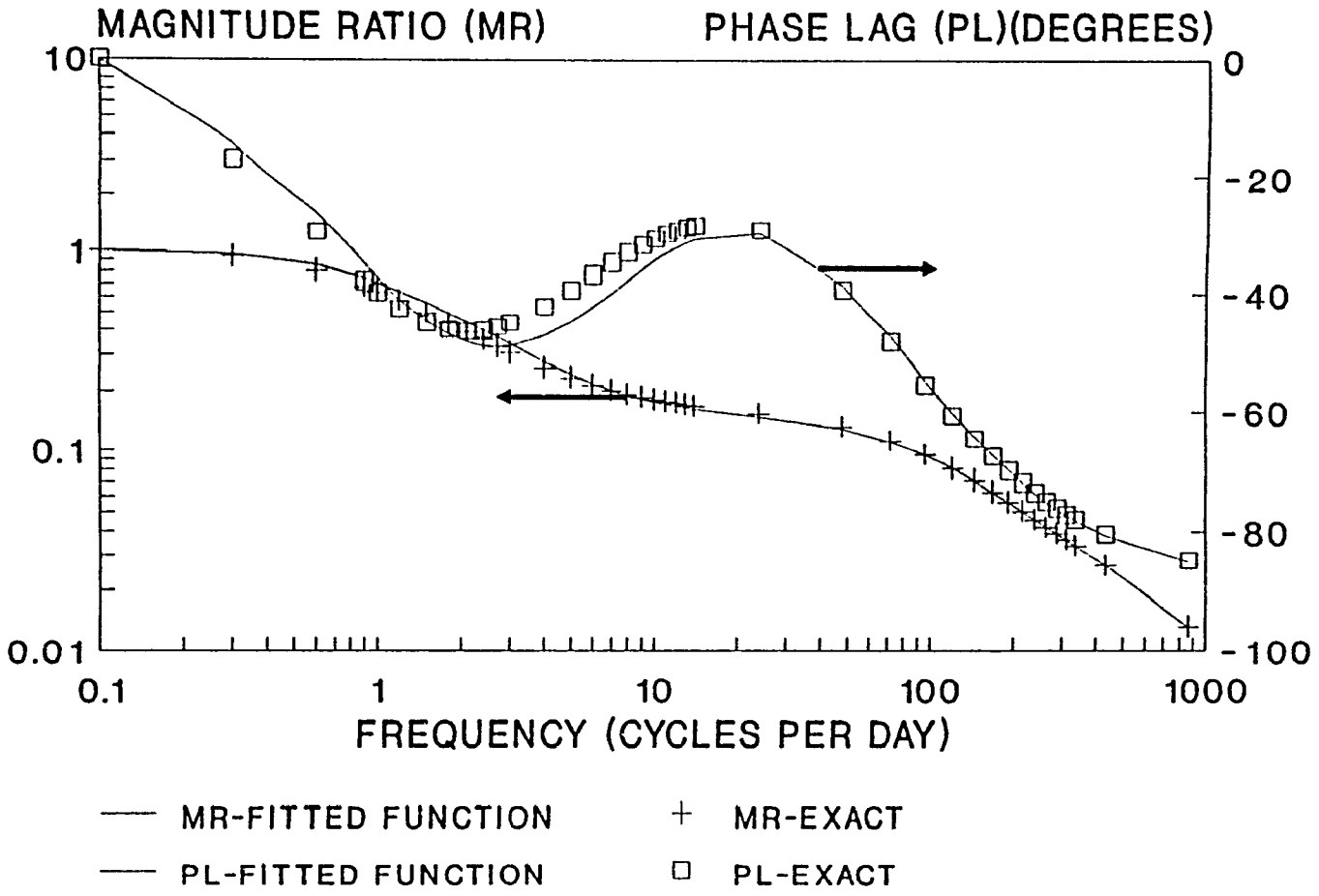

Figure 3.3 Exact discrete frequency response and fitted first order transfer function (m=1, n=2) for Z11(s) with one iteration.

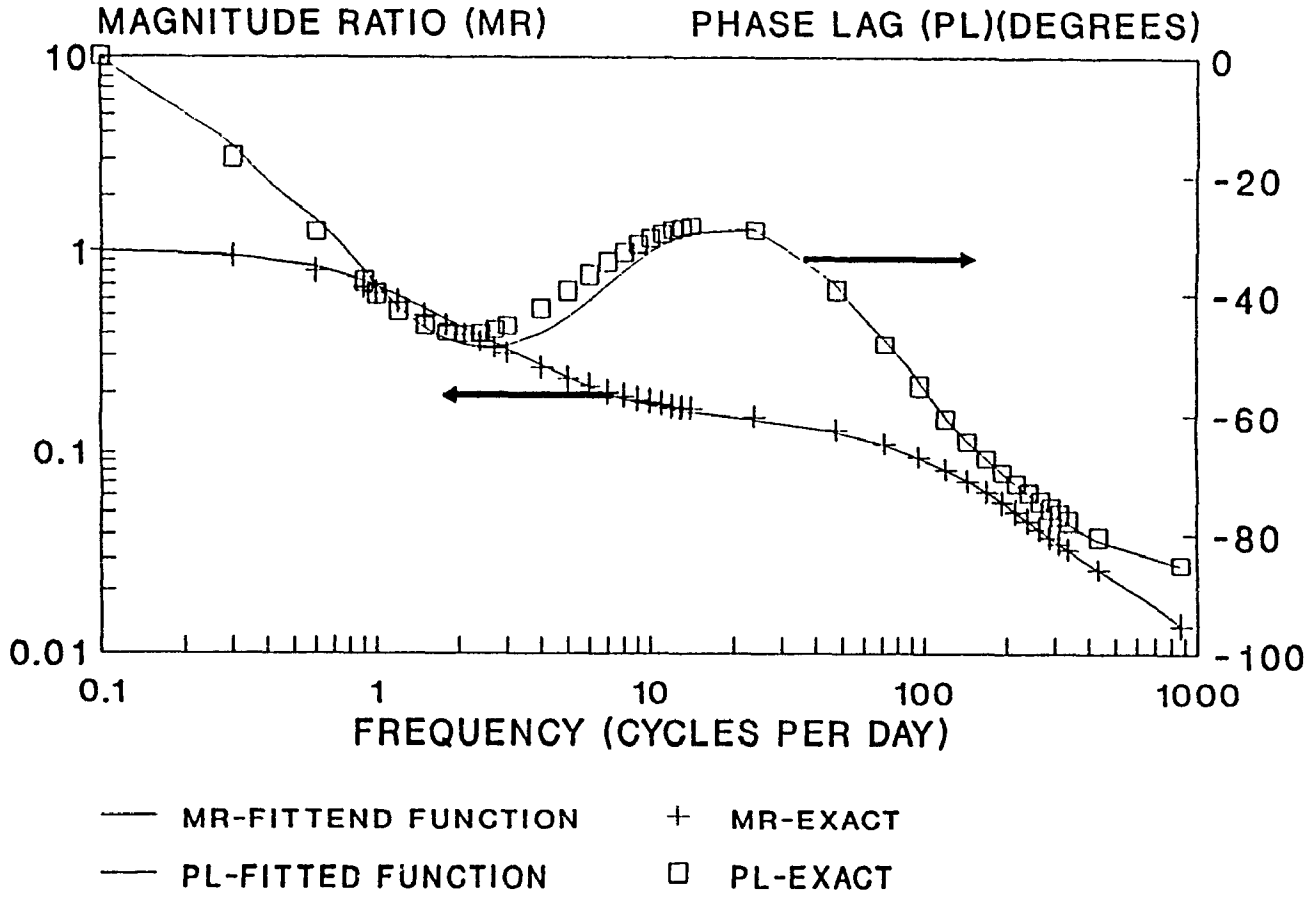

Figure 3.4 Exact discrete frequency response and fitted fourth order transfer function (m=3, n=4) for Z11(s) with one iteration.

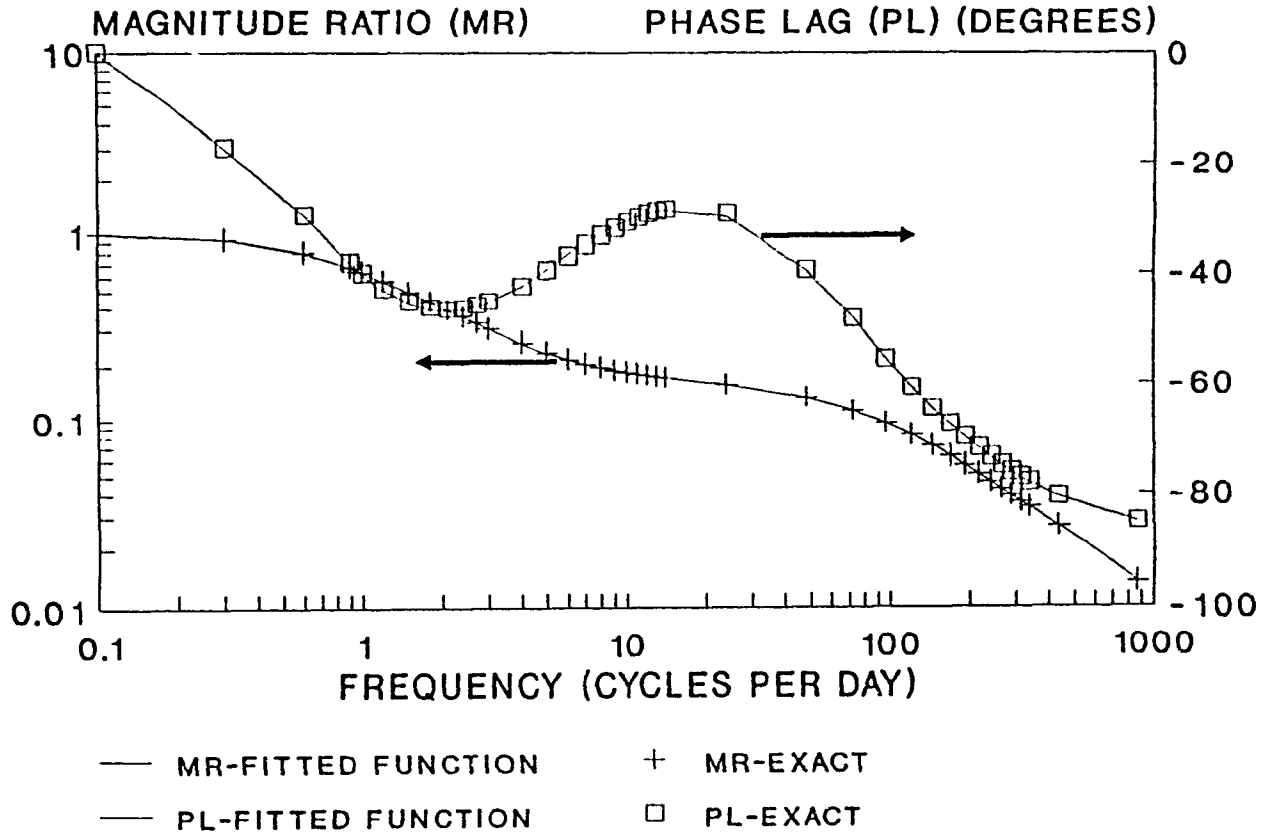

Figure 3.5 Exact discrete frequency response and fitted fourth order transfer function (m=3,n=4) for Z11(s) with two iterations.

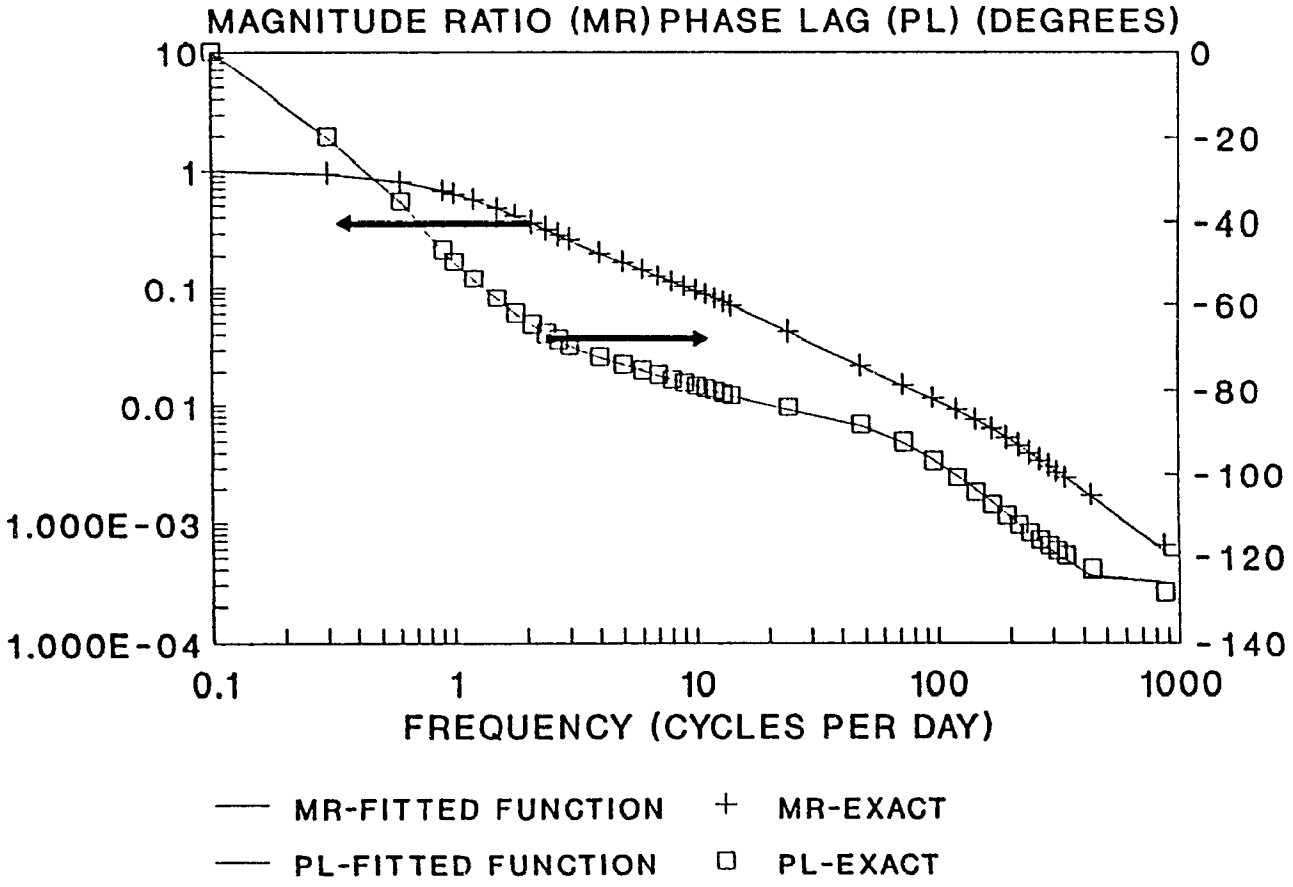

Figure 3.6 Exact discrete frequency response and fitted fourth order transfer function (m=3, n=4) for Z14(s) with two iterations.

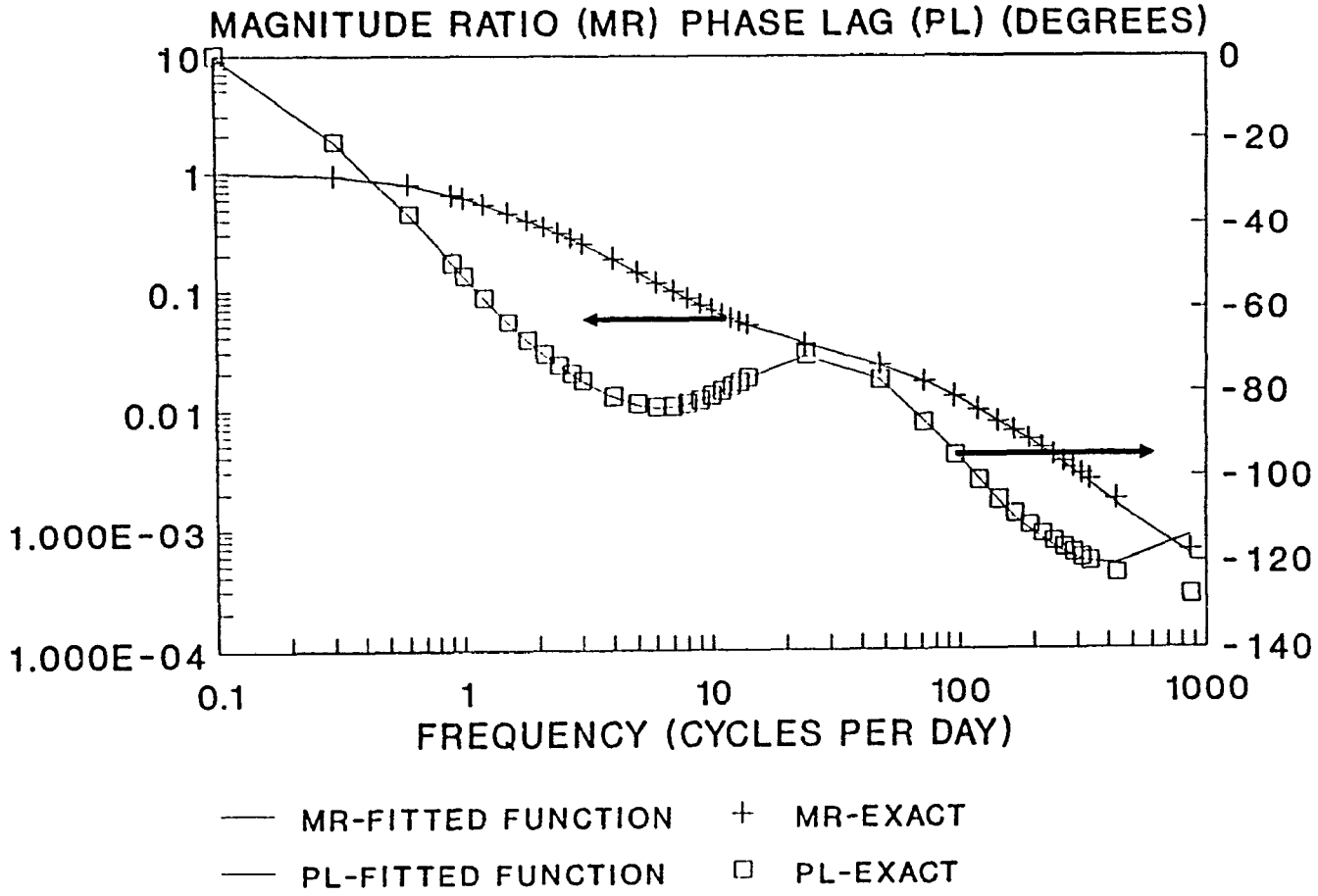

Figure 3.7 Exact discrete frequency response and fitted fourth order transfer fucntion (m=3,n=4) for Z17(s) with three iterations

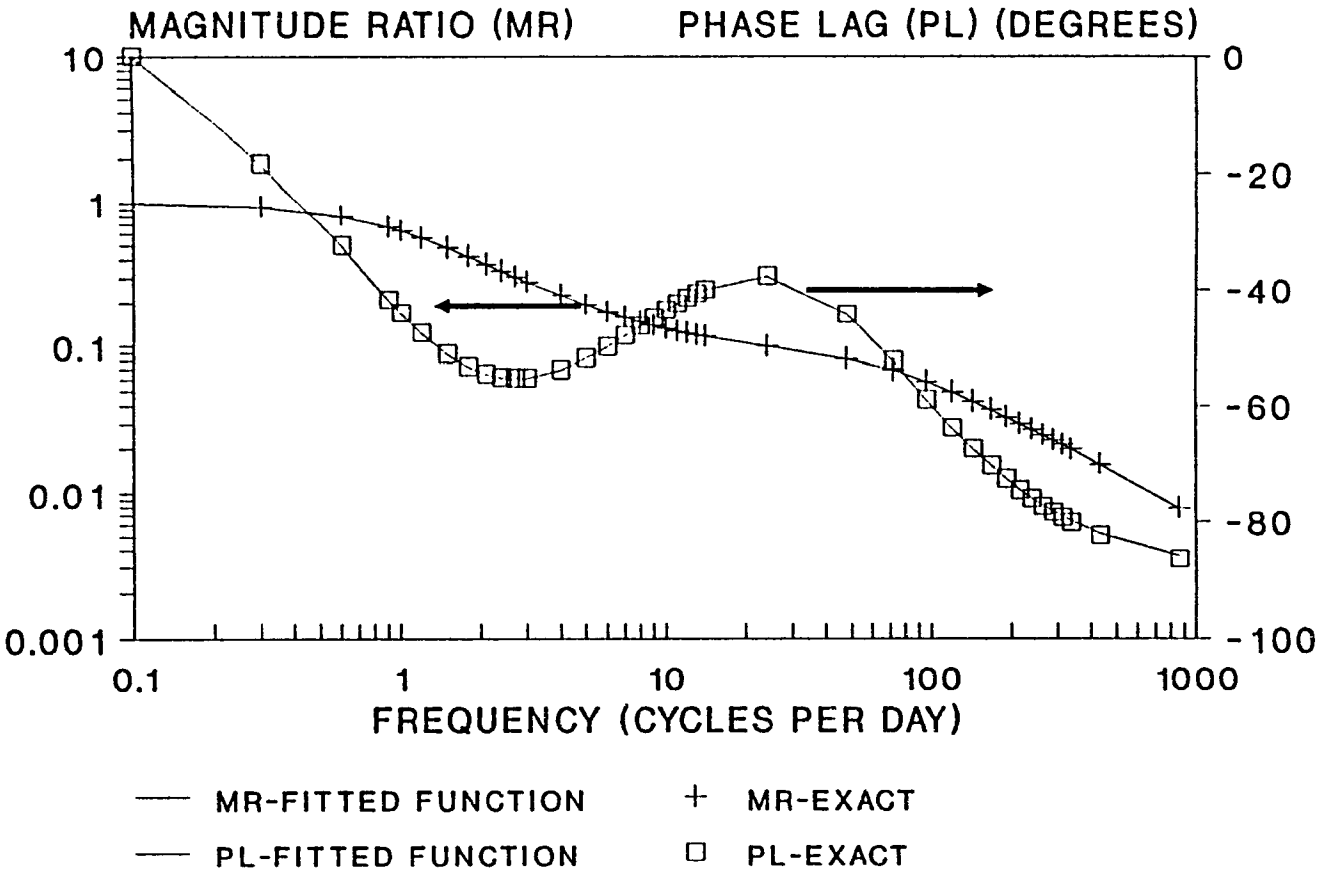

Figure 3.8 Exact discrete frequency response and fitted third order transfer function (m=2,n=3) for X1(s) with three iterations

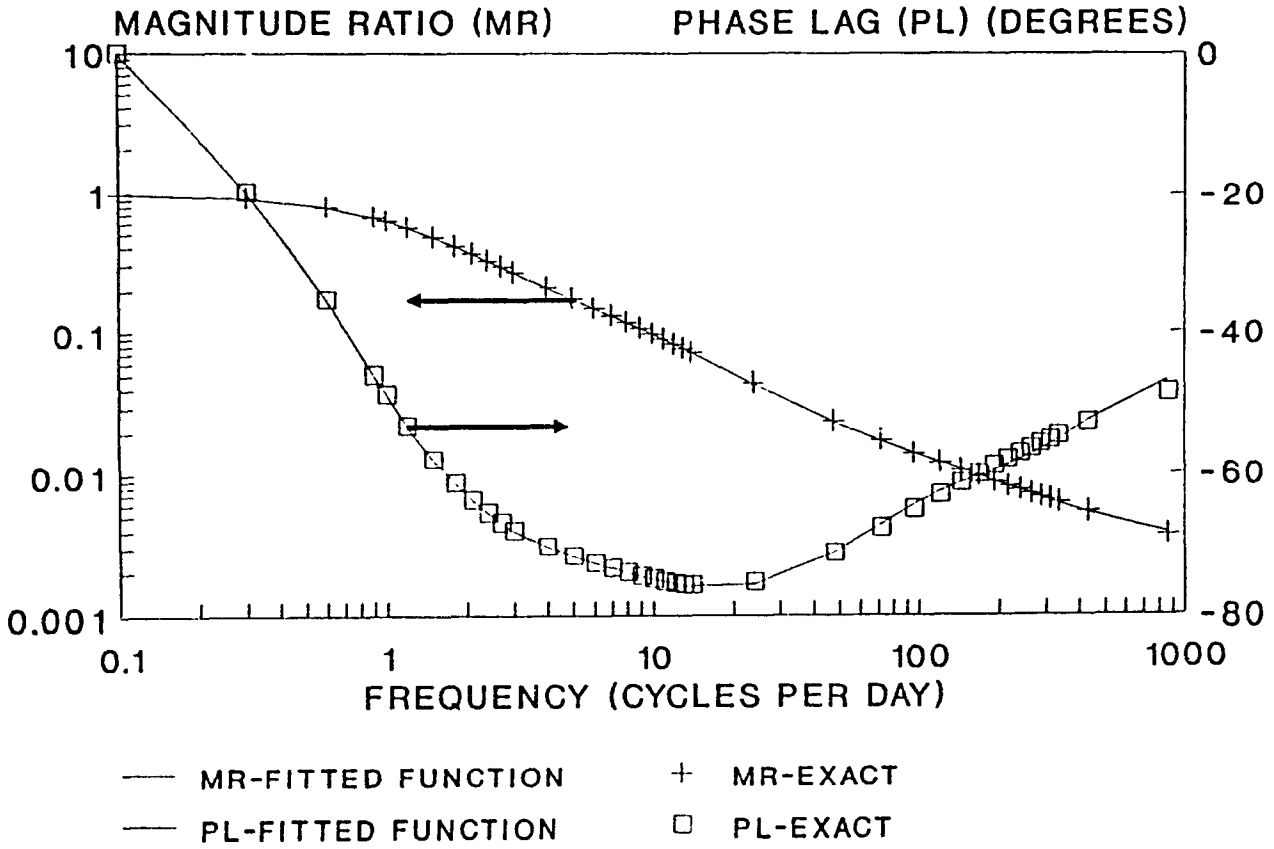

Figure 3.9 Exact discrete frequency response and fitted fourth order transfer function (m=3, n=4) for X4 with three iterations.

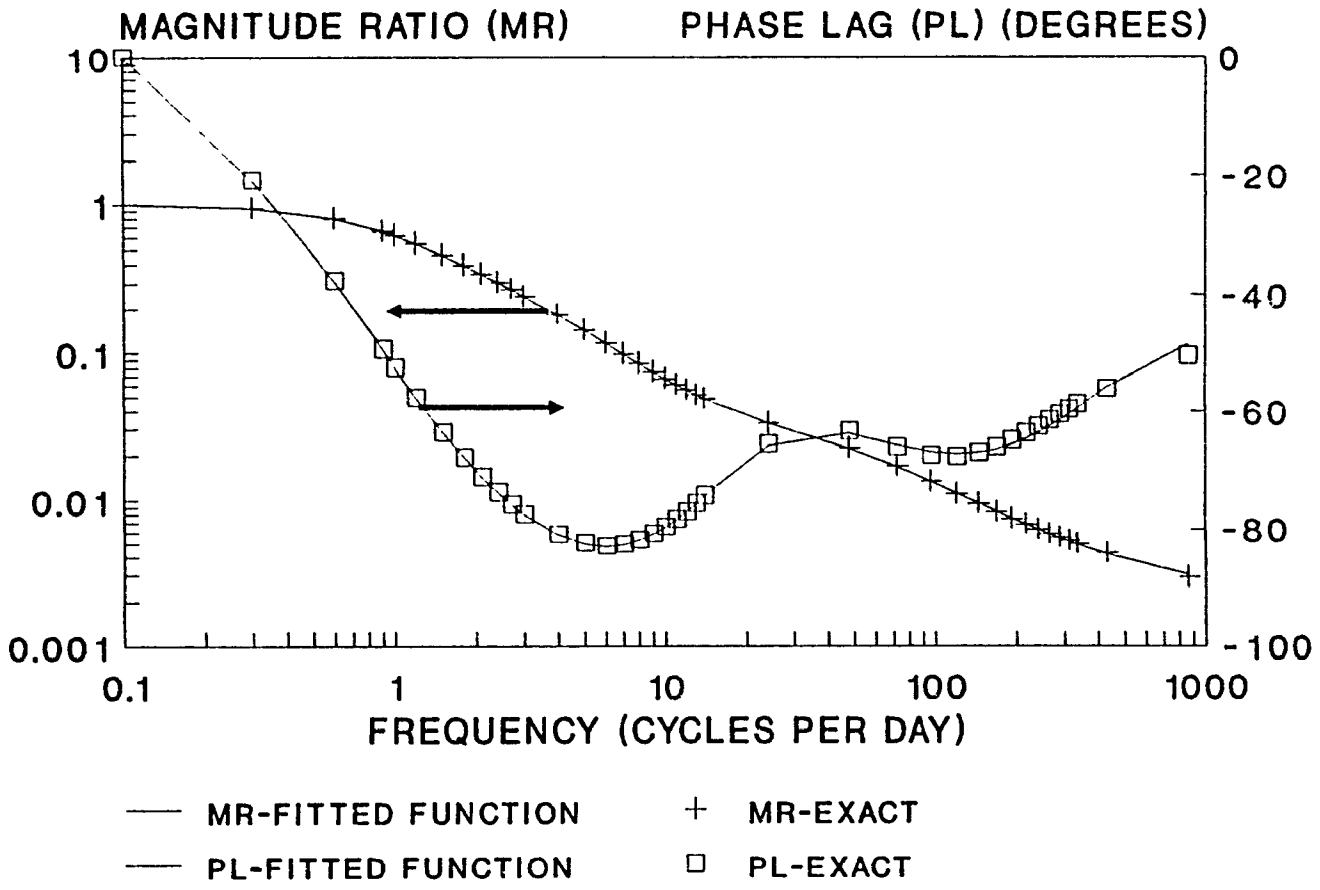

Figure 3.10 Exact discrete frequency response and fitted fourth order transfer function (m=3,n=4) for X7(s) with three iterations.

Both the frequency response data and the room transfer functions have revealed significant thermal dynamic characteristics of the room.

The Laplace transfer function technique is an efficient tool for the integrated analysis of the building envelope, the HVAC system and the control components. During the synthesis of the system transfer function, it is necessary to employ the continuous form of the component Laplace transfer functions. Usually they are obtained by estimating the poles and zeros of the transfer functions with a graphical technique. This is not only difficult, but almost impossible for a detailed room model. The modified least-squares method proposed in this study has made it possible to find the room Laplace transfer functions from a detailed thermal network model using a computer method. Accurate transfer functions can generally be obtained by optimizing the polynomial coefficients with an iterative approach developed.

CHAPTER 4

ANALYSIS OF HEATING CONTROL SYSTEM

4.1 Introduction

Dynamic building thermal studies usually employ simplified room models with which the effects of the thermal mass, as well as the radiant heat exchanges, are not modelled in detail. Nevertheless, a computer simulation of the total integrated thermal response of a building system may not be an effective tool unless all the important parameters affecting the dynamic operation are included.

In this chapter, a transfer function technique is presented for the study of the dynamic characteristics of a heating control system. The building thermal network, which models the thermal mass effects and the radiant heat exchanges in detail, is employed (Athienitis et al. 1990). The transfer functions for the room are then obtained by means of a modified least squares technique as discussed in chapter 3. The transfer functions for heating systems and various control components are based on the established models in the literature that have been widely used in detailed simulations. After combining each component transfer function in the system with block diagram algebra, the overall system transfer function is readily obtained. The effects of the different system parameters can be assessed, which may include various time constants of the components and the different controller gains in the system. For instance, a stable operation of the heating system may be ensured by proper choice of the system parameters, such as the gain for proportional control.

4.2 System analysis with transfer function technique

It was discussed in chapter 2 that the analysis of a building system can be conducted either in the time domain or in the frequency domain. The non-linearity in the system can be theoretically dealt with by time domain techniques. However, the temporal response of a system is inefficient to determine analytically with time domain techniques, especially in the case of a high-order system. However, there are many graphical or analytical methods available in the frequency domain, all suitable for the analysis and design of linear control systems. In practice, linearization of building systems is an acceptable approximation for the purpose of efficient frequency domain analysis or design. It is important to realize that once the analysis and design are carried out in the frequency domain, the time domain properties of the system can be interpreted based on the relationships that exist between the time domain and the frequency domain characteristics. Therefore, an important reason for conducting heating control system analysis and design in the frequency domain is that numerous analysis tools available offer flexibility and ease of use.

The starting point of the frequency domain analysis is the formation of the component transfer functions, which are the mathematical descriptions and modelling of the processes or components in the systems. In general, given a process or a component, the set of variables that identify the dynamic characteristics should first be defined. These variables are interrelated through established physical laws which lead to equations of various forms. Depending upon the nature of the process, the equations that relate the variables can be algebraic equations, differential equations, etc.. The transfer functions of

interest are usually obtained from the Laplace domain energy balance. A building heating control system normally consists of a heating system (such as a baseboard heater or radiant heating panels), possibly an energy distribution system such as a fan/duct system, a controller, a final control element and a temperature sensor. In this study, an electric heating system, such as electric radiant panel heating and electric baseboard heating, with linear control components is assumed. The transfer functions for the physical components are given below.

Controllers:

The main purpose of a controller used in HVAC applications is to minimize the process deviation from a setpoint. Two types of controllers are used extensively in HVAC systems - proportional (P) controller and proportional integral (PI) controller. A proportional controller transfer function is the proportional gain (K_p). The control action C_p is proportional to the error:

$$C_p = K_p\, e(t) \qquad (4.1)$$

where $\varepsilon(t)$ is the error message equal to the difference between the setpoint and measured temperature.

A proportional-integral controller is described by the proportional gain (K_p) and the integral time (τ_i). The control action C_{pi} is proportional to the error, as well as to the integral of the error:

$$C_{pi} = K_p\, e(t) + K_p \int \frac{e(t)}{\tau_i} dt \ . \qquad (4.2)$$

The Laplace transfer functions for P and P-I control are given by:

$$G_{c,p} = \frac{C_p(s)}{e(s)} = K_p \qquad (4.3)$$

and

$$G_{c,pi} = \frac{C_{pi}(s)}{e(s)} = K_p \left(1 + \frac{1}{\tau_i s}\right) \ . \qquad (4.4)$$

Temperature sensors:

A temperature sensor is an essential element for detecting any deviations of controlled temperature from a setpoint. Generally, the temperature sensor response can be modelled by the following first order differential equation:

$$\frac{dT_s}{dt} = \frac{T_m - T_s}{\tau_s} \qquad (4.5)$$

where T_s = sensor output temperature, T_m = measured temperature and τ_s = sensor time constant.

The Laplace transfer function of the sensor is given by:

$$H_s = \frac{T_s(s)}{T_m(s)} = \frac{1}{1 + \tau_s s} \ . \qquad (4.6a)$$

A transport delay may also be included if the distance between the sensor and the controller is significant:

$$H_s = \frac{e^{-\tau_{s,d}}}{1+\tau_s \cdot s} \qquad (4.6b)$$

where $\tau_{s,d}$ is the time delay (dead time) due to the time needed for the temperature change in the air to be transmitted over the distance (mixing time delay).

Final control elements:

A final control element accepts a control message from the controller and implements the control action according to the preset control algorithm or circuit/mechanism. Depending upon the nature of a heating system, it could be a control valve, an on/off switch or a silicon controlled rectifier (SCR), etc.. For a linear element, the input-output relationship of the component may be described by a translated function in the Laplace domain:

$$G_f(s) = K_f e^{-t_{f,d} s} \qquad (4.7)$$

where $t_{f,d}$ is the time delay (dead time) and K_f is the magnitude ratio of the component.

Heating system:

It is the heating system supplying heat to the controlled environment, which

generally falls into one of two categories -- convective heating systems, such as baseboard heating, and radiant heating systems, such as radiant panel heating. This study will be confined to electric radiant panel heating and electric baseboard heating, which can be modelled as a first-order element:

$$\tau_h \frac{dY}{dt} + Y = K_h f(t) \qquad (4.8)$$

where Y(t) is the heating output from a heating element and K_h f(t) is the power supplied. The Laplace transfer function for equation (4.8) is expressed by:

$$G_p = \frac{Y(s)}{f(s)} = \frac{K_h}{\tau_h s + 1} \quad . \qquad (4.9)$$

For electric heating K_h represents the capacity of the heating system, while τ_h is the time constant of the heating system reflecting its thermal inertia.

A block diagram is a useful tool in transfer function analysis and is often used by engineers to represent a system. It can be used to represent the composition of the system. If the mathematical and functional relationships of all the system components are known, the block diagram can be utilized as an information flow chart to represent the interactions throughout the system. Furthermore, if all the system components are assumed to be linear, the overall system transfer function can be obtained by means of block diagram algebra.

For instance, the block diagram in figure 4.1 represents a heating system with air temperature control. Major components of the system are described by the transfer

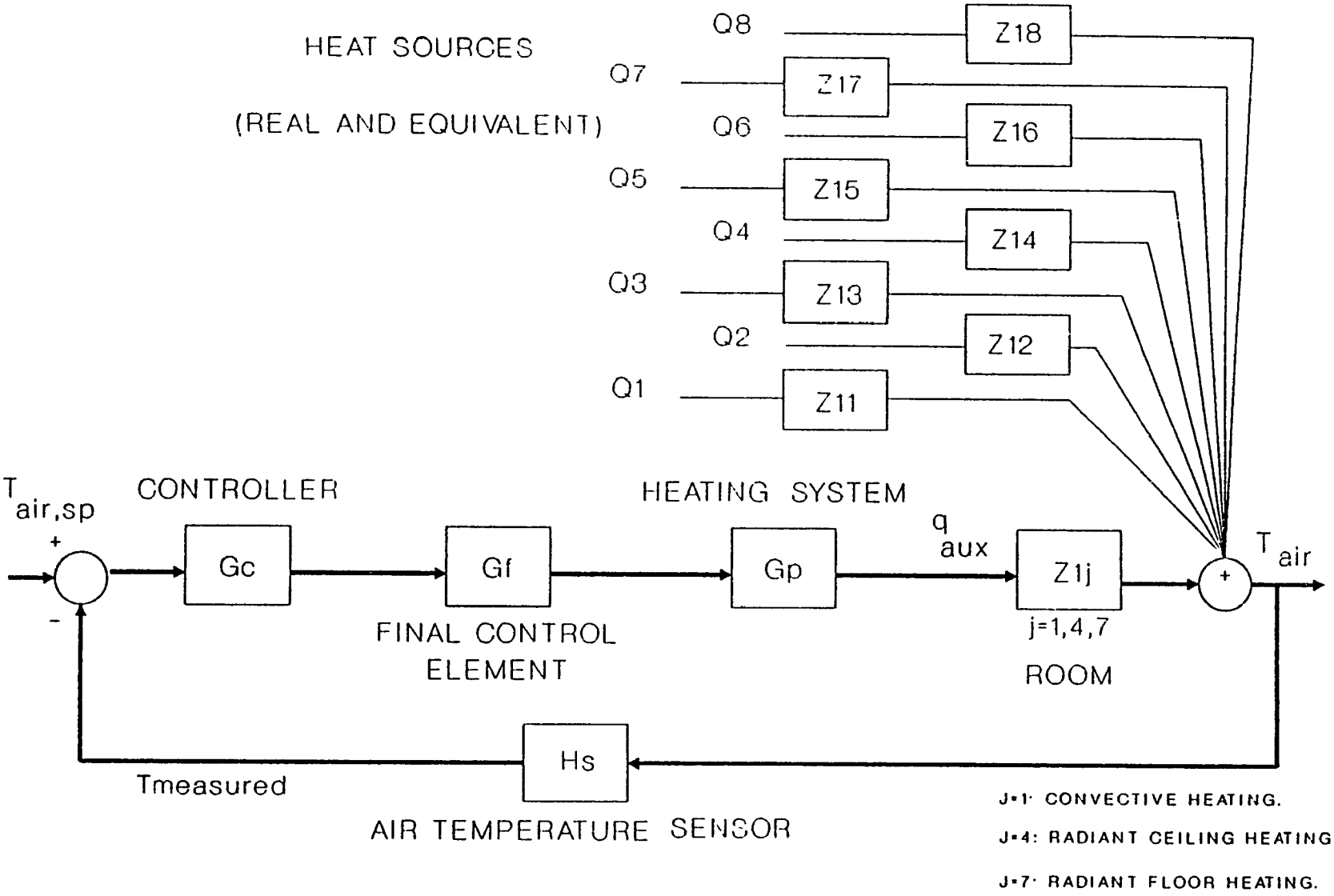

Figure 4.1 Block diagram of a heating control system

function blocks, such as the controller (G_c), the final control element (G_f), the heating system (G_p), the temperature sensor (H_s), room transfer functions Z1j, etc.. The transfer function relating temperature to auxiliary heat is Z1j, such as Z11 (room air) in the case of convective heating, or Z17 (floor) in the case of radiant floor heating. The heat gains or losses of the room are also indicated in the block diagram, such as Q1, Q2, etc.. The room temperature is measured by a temperature sensor and is then compared with a temperature setpoint. Any deviation of the room temperature from the setpoint will activate the final control element through the controller. Finally, the energy input level into the heating system is regulated in order to meet the load or setpoint changes.

The resulting room temperature variation as a function of the heat sources and temperature setpoint is obtained by block diagram algebra from figure 4.1:

$$T_{air} - T_{air,sp} \frac{G_c\, G_f\, G_p\, Z(1,j)}{1+G_c\, G_f\, G_p\, Z(1,j)\, H_s} + \sum_{j=1}^{8} \frac{Q_j\, Z(1,j)}{1+G_c\, G_f\, G_p\, Z(1,j)\, H_s} \tag{4.10}$$

where the first term indicates the room air temperature change due to setpoint, and the second term indicates the temperature response due to the load changes. The denominator $\{1+G_c\ G_f\ G_p\ Z(1,j)\ H_s\}$ is the characteristic equation, which determines the stability of the heating control system. A loop transfer function of an overall system is defined as the product of all the component transfer functions in the control loop, i.e, $G_c\ G_f\ G_p\ Z(1,j)\ H_s$, which may be used for stability analysis (Stephanopoulos 1981).

Using the input-output relation of a transfer function, the power of the heating system and the auxiliary heat for a room can be determined, respectively, by equations

(4.11a) and (4.11b):

$$Power = \frac{T_{air}}{Z(1,j)\ G_p} \qquad (4.11a)$$

$$q_{aux} = \frac{T_{air}}{Z(1,j)} \qquad (4.11b)$$

The presence of measuring devices, controllers and final control elements may change the dynamic characteristics of a process, such as a building heating system. For example, a nonoscillatory building heating process may acquire oscillatory behaviour using proportional or proportional plus integral control system with improper selection of the controller parameters. The system oscillation may adversely affect the thermal control, as well as destroy control components. Thus, the objective of the design of a feedback control system is to select the control components, to study the system performance and to tune its controller. If a control system is stable, the value of the room temperature will remain at its setpoint. A fast response control system will eliminate disturbances, such as due to load changes, and quickly return the room temperature to its setpoint. In general, the increase of the response speed may endanger the system stability. The speed of the system response and its stability should be carefully evaluated.

In every control configuration, the controller is the most active element that receives the information from the measurement and takes appropriate control action to adjust the value of the manipulated variable, such as the heat output in a heating system. Obviously, the controller parameters have direct influence over the system dynamics.

Controller parameter tuning typically involves the selection of proportional and integral constants. Conservative tuning of the parameters yields sluggish response of the system, while oversizing may destabilize the system operation.

There are numerous methods for stability analysis in control engineering, most of which require the analysis of the characteristic equation of the system, such as the Routh-Hurwitz criterion and the root-locus analysis. Control parameter tuning is usually conducted in the field, such as the process reaction curve method, which is primarily experimental and uses real process data from the system's response.

In this study, a frequency response method will be applied, which has been proposed by Ziegler and Nichols (1942). The method is based on the Bode stability criterion, which states that a feedback control system is unstable if the amplitude ratio of the corresponding loop transfer function is larger than one at the crossover frequency ω_{co}, with which the phase lag of the loop transfer function is equal to 180°. The Bode stability criterion has indicated how the feedback controllers should be tuned in order to avoid unstable behaviour. It also constitutes a measure of how far the system is from instability.

To select the proper controller parameters, such as the proportional gain, the following procedure is proposed by Ziegler and Nichols:

1. The loop transfer function of the system is constructed, which is equal to the product of all the component transfer functions in the control loop.

2. Using proportional control only, a unit setpoint change is introduced and the

proportional gain is varied until the system oscillates continuously at its crossover frequency ω_{co}.

3. If M is the amplitude ratio of the system's response at the crossover frequency, the following two quantities are calculated:

$$K_u = \frac{1}{M} \tag{4.12}$$

$$P_u = \frac{2\pi}{\omega_{co}} \tag{4.13}$$

where K_u is the ultimate gain and P_u is the ultimate period.

4. Stable operation of the system can be achieved by selecting the controller parameters based on the ultimate gain and the ultimate period. For proportional control alone, the controller gain is set equal $K_u/2$. For a proportional plus integral controller, the gain factor is $K_u/2.2$, while the integral time constant is $P_u/1.2$ (Stephanopoulos 1981).

4.3 Transient response with the stepwise numerical Laplace transform inversion

The Laplace transfer function technique provides us a convenient tool for frequency response analysis by simply substituting the Laplace variable s with the frequency variable $j\omega$. Transient response is equally important because it reveals time

domain properties. For instance, it is desirable to study the dynamic behaviour and energy consumption of the different heating systems or to investigate a heating system with different types of temperature controls.

Many numerical methods are available for obtaining the time domain response from the Laplace transformed equation, such as equations (4.10) and (4.11). They generally require the determination of poles and residues which are not only tedious but may be computationally prohibitive if multipoles exist. A numerical method proposed by Singhal and Vlach (1981) can be used to compute the transient response of a linear time invariant system described by its transfer function without determining poles or residues. It is equivalent to a high order, absolutely stable numerical integration.

The numerical Laplace transform inversion technique has been applied to the building system analysis (Stylianou 1989). The method is very efficient since no discretization of distributed elements, such as a massive slab, is required. It also allows the use of dead time (time delay) without any artificial manipulation of the constants present, as is required if other numerical methods are used (Clark 1985). Further, it can be readily incorporated within a program for frequency response analysis because the transfer functions are already determined as function of s (=$j\omega$).

However, a major shortcoming of this technique is that the results of the inversion are accurate only for small time. The accuracy will deteriorate with the increase of the time span. In order to maintain the accuracy throughout the time period, Vlach and Singhal (1981) proposed a stepping algorithm. The basic philosophy is to achieve the Laplace inversion step by step, taking the previous result as a new initial condition.

To use the stepping algorithm, the Laplace transfer function to be inverted must be represented as a ratio of two polynomials. If the overall transfer function of the heating system is considered in the form of A(s)/B(s), the response may be expressed as:

$$Y(s) = U(s)\ \frac{A(s)}{B(s)} = U(s)\ \frac{\sum_{i=1}^{m} a_i\ s^{i-1}}{s^n + \sum_{i=1}^{n} b_i\ s^{i-1}} \qquad (4.14)$$

where U(s) is the Laplace transform of the input signal and Y(s) is the Laplace transform of the output.

If a system has a time delay (dead time) τ_d due to the transportation lag, such as duct or pipe, the dead time term can be approximated as a ratio of two polynomials:

$$e^{-\tau_d s} = \frac{(1-\tau_d s/2)}{(1+\tau_d s/2)} \quad .$$

As a result, the process still can be approximated by the ratio of two polynomials. This approximation is accurate enough for the purpose of engineering analysis (Truxal 1955).

An auxiliary transfer function X(s) is defined as:

$$X(s) = \frac{U(s)}{B(s)} \qquad (4.15)$$

or

$$(s^n + b_n\ s^{n-1} + \ldots + b_1)\ X(s) = U(s) \quad . \qquad (4.16)$$

The original output of the response is given as

$$Y(s) = A(s)\ X(s) = \left(\sum_{i=1}^{m} a_i s^{i-1}\right)\ X(s) \quad . \qquad (4.17)$$

Since multiplication by s in the Laplace domain corresponds to differentiation in the time domain, a set of variables $x_1, x_2,...,x_n$ in the time domain can be introduced such that the equation (4.16) be expressed in matrix form:

$$\begin{vmatrix} X'_1 \\ X'_2 \\ \cdots \\ X'_n \end{vmatrix} = \begin{vmatrix} 0 & 1 & 0 & 0 & \cdots \\ 0 & 0 & 1 & 0 & \cdots \\ \cdots & & & & \\ -b_1 & -b_2 & -b_3 & \cdots\cdots & -b_n \end{vmatrix} \begin{vmatrix} X_1 \\ X_2 \\ \cdots \\ X_n \end{vmatrix} + \begin{vmatrix} 0 \\ 0 \\ \cdots \\ 1 \end{vmatrix} U \qquad (4.18)$$

or

$$X' = A\ X + B\ U \qquad (4.19)$$

where A has the form shown in equation (4.18) and B is a vector with all zeros except for the last which is unity. Taking the Laplace transform, we get the frequency domain system:

$$(sI-A)\ X(s) = B\ U(s) + X^{o} \qquad (4.20)$$

where X^{o} is an initial condition vector.

The auxiliary transfer function X(s) at each step can be solved by applying

triangular decomposition to (sI-A), and using the forward and backward substitution technique (Singhal and Vlach 1981). The Laplace transform inversion of this auxiliary transfer function may be obtained at each time step h with the numerical Laplace transform inversion technique (see Appendix A):

$$X_i(h) = -\frac{1}{h} \sum_{i=1}^{m'} Re[K_i' X_i(\frac{Z_i}{h})] \quad . \tag{4.21}$$

The accuracy of the inversion will not be impaired because a smaller constant time step can be used to satisfy the accuracy requirement. Finally, the system response shown by equation (4.17) has the equivalent time domain response:

$$Y(t) = \sum_{i=1}^{m} a_i X_i \tag{4.22}$$

where a_i is the coefficient of the transfer function numerator and X_i is the Laplace inversion of the auxiliary transfer function.

4.4 HEATCON: a computer program for heating control analysis

A computer program named HEATCON has been developed as part of this study. The program provides several tools for the design and analysis of a heating control system:

1. The transient response of the room air temperature or operative temperature

without temperature control can be determined by introducing heat sources in the room. At this stage, the room thermal response is considered as an "open loop", which means that no temperature control system is involved. The open loop temperature response can be used to compare the effects of different types of building envelopes and constructions, such as the amount of the thermal mass used in a room, on the room thermal response.

2. The loop transfer function of the overall system with proportional control only can be constructed, with which the frequency response analysis is performed to determine the ultimate amplitude at the crossover frequency. Based on the ultimate amplitude and the crossover frequency, the controller parameters for proportional control or proportional integral control are estimated using the Ziegler-Nichols tuning method.

3. Given the component transfer functions and the control parameters, the overall transfer function of the heating system is readily obtained with block diagram algebra. Here, a "closed loop" system is considered, which means that there is a feedback element added to the system. The room temperature is measured and the control devices are actuated to bring about a change. The corrective action continues until the room temperature is brought to a setpoint. The transient response of this closed loop system is calculated in response to the temperature setpoint change by means of the Laplace transform inversion technique. Finally,

the energy consumption of the heating system and the auxiliary heat into the room can be estimated.

The structure of the program HEATCON is illustrated in figure 4.2. The data needed to perform an analysis of a heating control system are divided into two groups: information for room, and information for control and heating systems. The room information, such as the thermal properties and geometric parameters, is input into the separate program BEEP (Athienitis 1988) to generate discrete frequency response data and to perform building energy analysis. On the other hand, the parameters of heating system and control elements are input into the program HEATCON. Two types of heating systems, convective heating and radiant ceiling or radiant floor heating, are considered in the program. The control systems used in the simulation are the proportional control and the proportional integral control.

As indicated by figure 4.2, the discrete frequency response data generated by BEEP are used to obtain the Laplace transfer functions of a room. The program HEATCON incorporates both frequency and time domain techniques in the study of heating control systems. The stability analysis is perfomed with frequency domain technique and the system response is obtained with numerical Laplace transform inversion.

As an example, a theoretical study is given to analyze the thermal storage effects and different heating systems in a simple room with dimension 2.4 m in depth, 3 m in width and 2.8 m in height. The insulation of the room is 2.2 RSI on vertical walls and

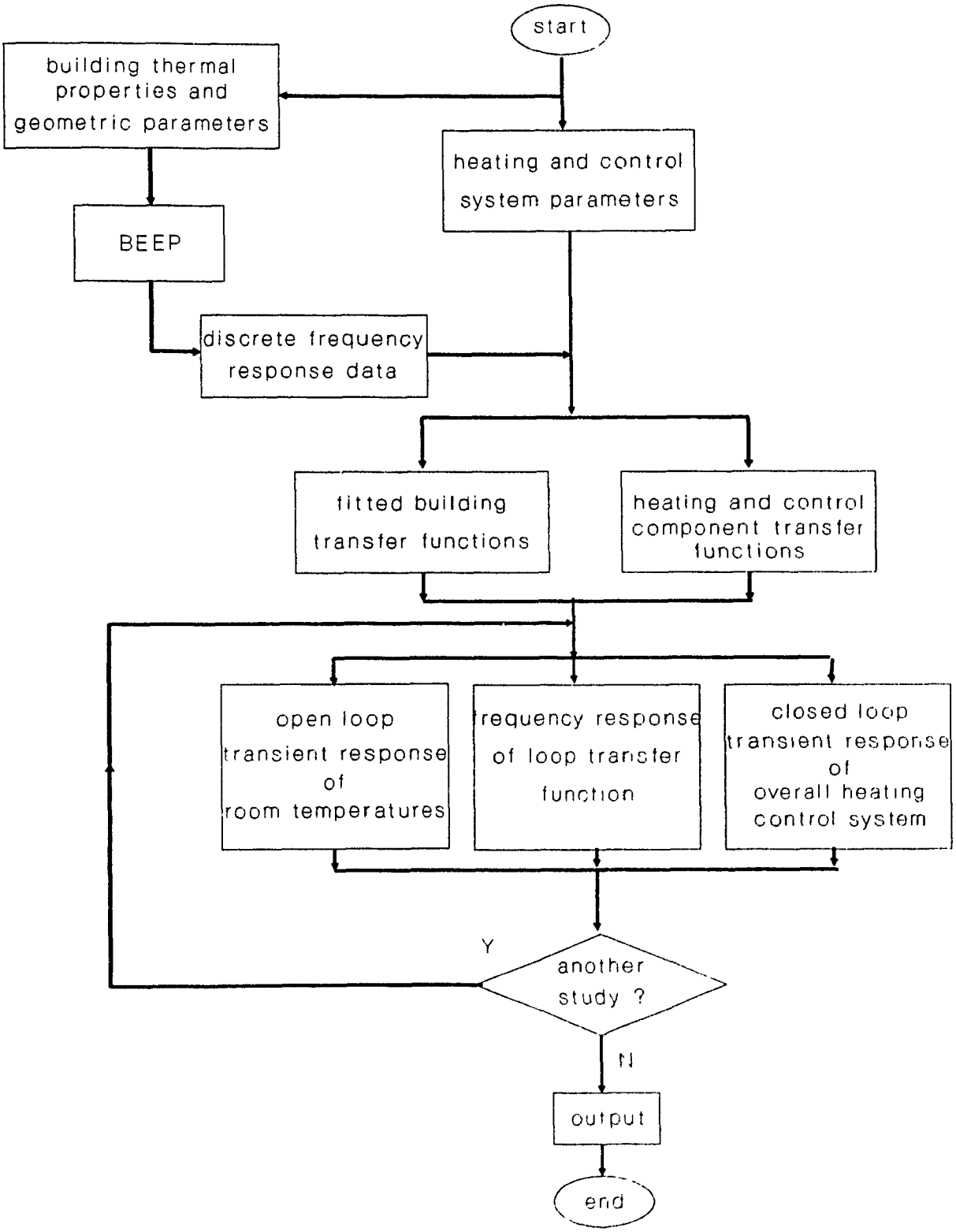

Figure 4.2 Flow chart of the program HEATCON

3.6 RSI on the ceiling and floor. The floor could be furnished with low mass material such as wood or higher thermal capacity material such as gypsum board. The thermal response will be significantly affected by the thermal storage mass in the room. This can be clearly shown in figure 4.3. Given a step heat input (100 W) into the room, a faster temperature response with low mass floor (16 mm plywood) is predicted, which has a time constant of 4.8 hours. In contrast, a slower temperature response is expected with the gypsum board (30 mm) covered floor and the time constant is about 8.5 hours. In figure 4.4, the block diagram representing the baseboard heating system with air temperature control is illustrated. In order to simplify the problem, only auxiliary heat is considered in the study. The similar block diagram representing the radiant ceiling panel heating with operative temperature control is shown in figure 4.5. It should be noticed that two different room transfer functions, as well as two different control variables, are used in the two block diagrams. For the baseboard heating with air temperature control, the room transfer function Z11 is used because the auxiliary heat is directly delivered into room air (node 1). On the other hand, the room transfer function X4 is employed in the case of the radiant ceiling (node 4) heating with operative temperature control. The proportional control for the heating systems is implemented through a silicon controlled rectifier (SCR) by a computerized data acquisition and control system. The time constant of the radiant ceiling panels and cover material is 280 seconds, and the baseboard time constant is 60 seconds. The air temperature sensor and globe temperature sensor (as an approximation to operative temperature sensor) time constants are 16 seconds and 270 seconds, respectively.

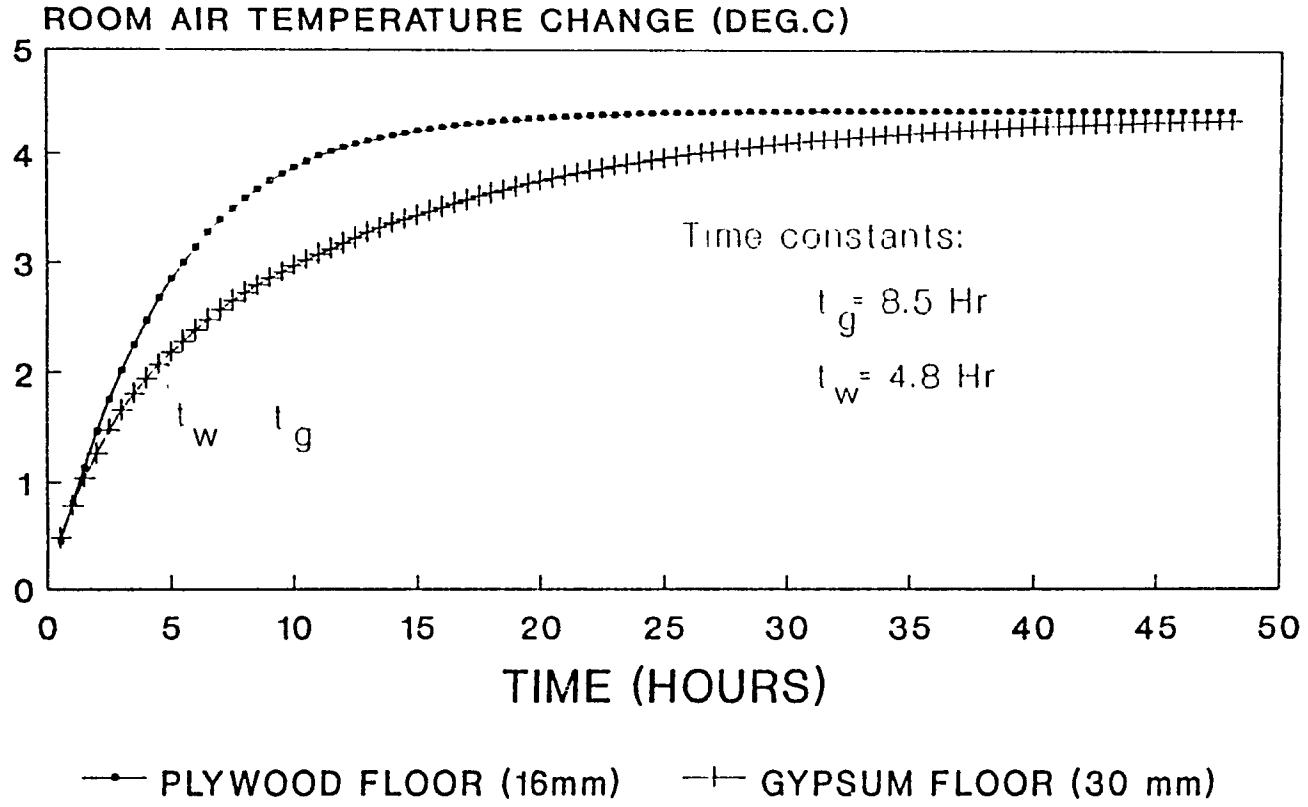

Figure 4.3 Effect of floor thermal mass (plywood and gypsum board) on room temperature response to step input of radiative gains (100 W) at the floor surface (node 7).

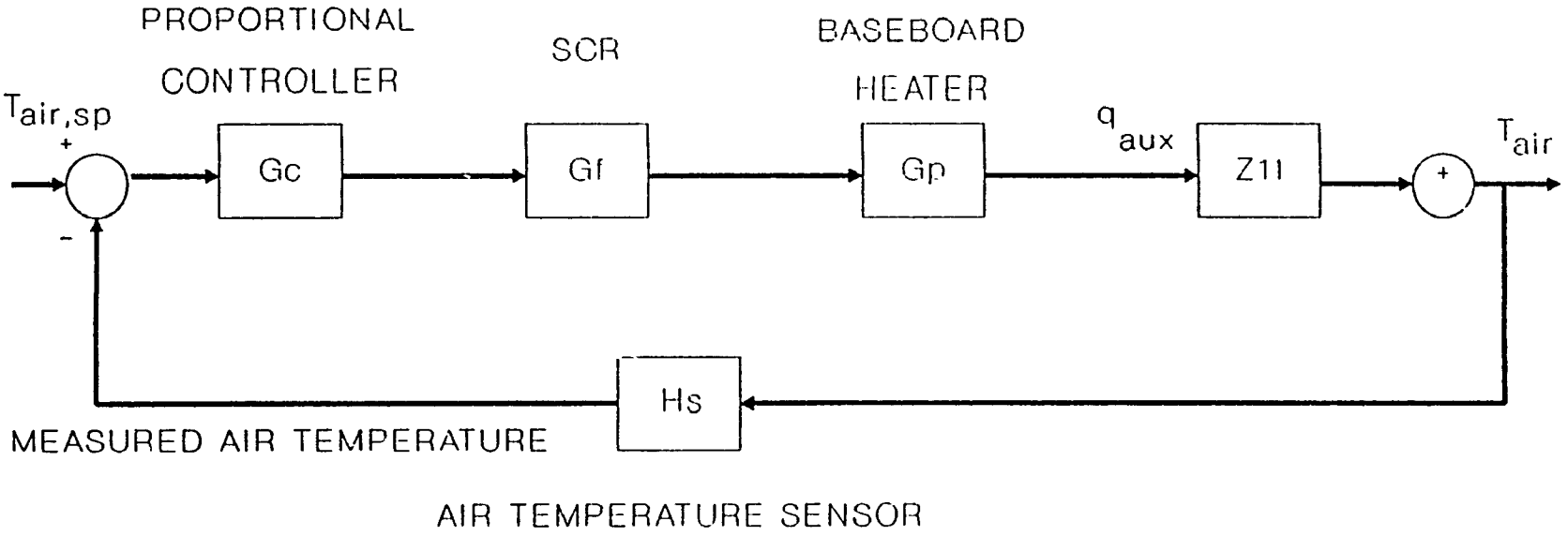

Figure 4.4 Block diagram of a baseboard heating system with air temperature control.

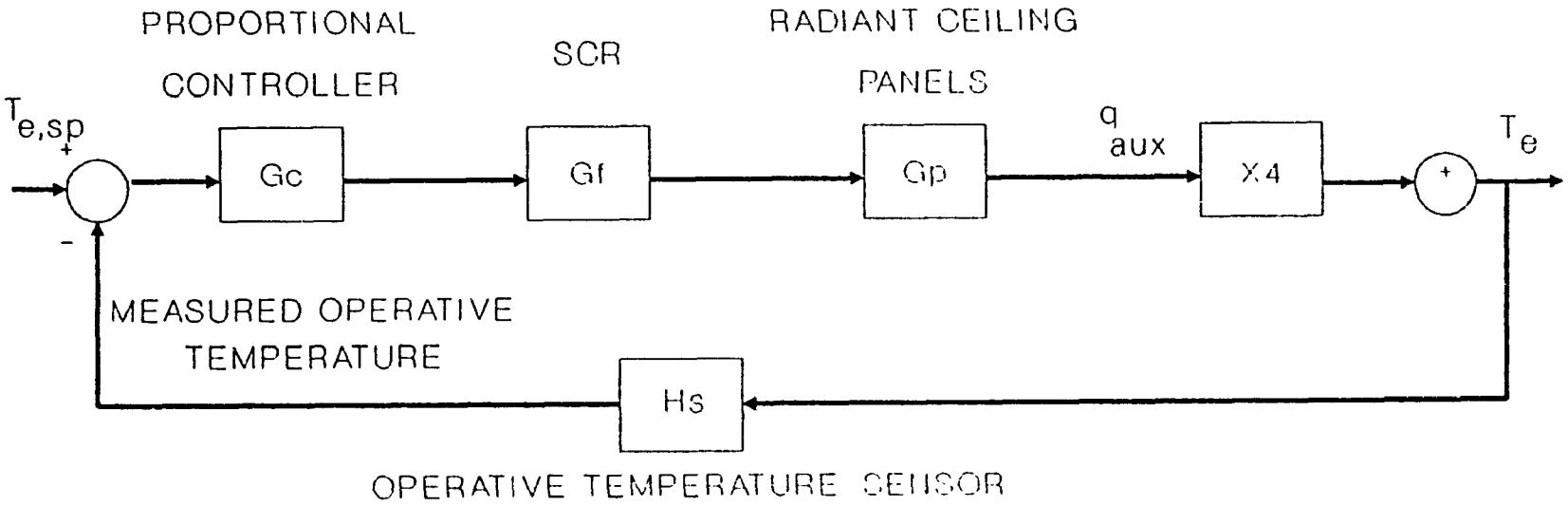

Figure 4.5 Block diagram of a radiant ceiling heating system with operative temperature control.

In order to obtain the ultimate gains at the stability limit for the two heating systems, the program HEATCON has been employed. The results indicate that no crossover frequency exists for the baseboard heating with air temperature control because of its small time constant. This means that no matter how large the proportional gain used, the baseboard heating system with air temperature control always operates in a stable manner. By contrast, for radiant ceiling panel, there is a crossover frequency and the corresponding ultimate gain is 4,420 W/°C. Following the Ziegler-Nichols tuning method, a proportional gain 2,210 W/°C is chosen, which is half the ultimate gain.

The room temperature responses due to one degree temperature step rise in the setpoint were simulated with HEATCON. The proportional gains used in the simulation of baseboard heating were 1,000 W/°C, 500 W/°C and 250 W/°C. For the simulation of radiant ceiling heating, proportional gains were 2,210 W/°C (tuned with Ziegler-Nichols method), 1,000 W/°C and 500 W/°C. The simulation results for both baseboard heating and radiant heating with different proportional gains are plotted in figure 4.6 and figure 4.7.

It is seen that the larger the proportional gain, the faster the temperature response and the smaller the control offset which is the difference between the setpoint and the actual room temperature under stable conditions. As shown in figure 4.6, fast response of the baseboard heating is obtained with the proportional gain 1,000 W/°C and the rise time (the time required for the response to reach its setpoint for the first time) is about 1.2 minutes. However, the room temperature never reaches the setpoint with the proportional gain 500 W/°C and 250 W/°C, and the offset temperature is 0.1°C

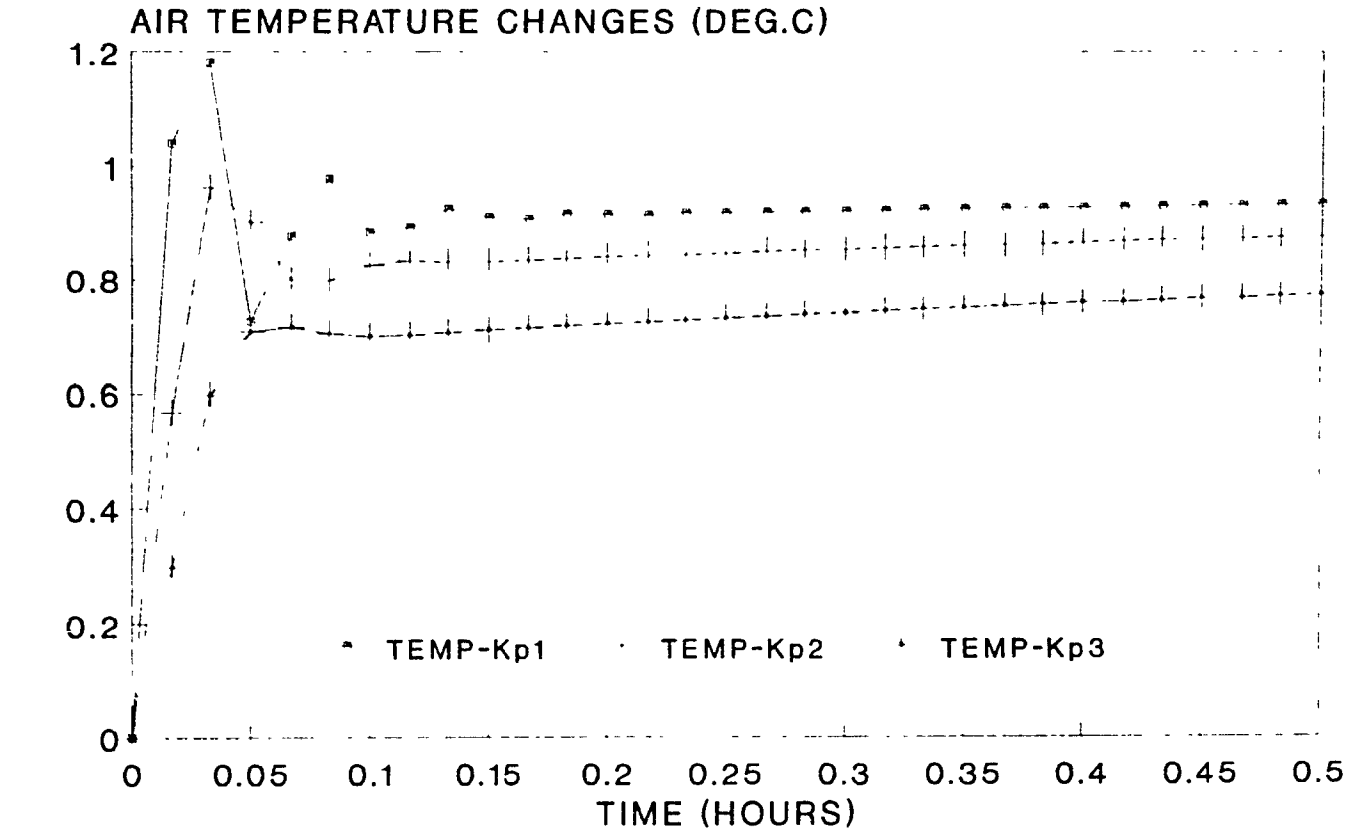

Kp1=1000 W/DEG.C
Kp2=500 W/DEG.C
Kp3=250 W/DEG.C

Figure 4.6 Simulation results of air temperature changes due to one degree setpoint change for a baseboard heating system with different proportional gains.

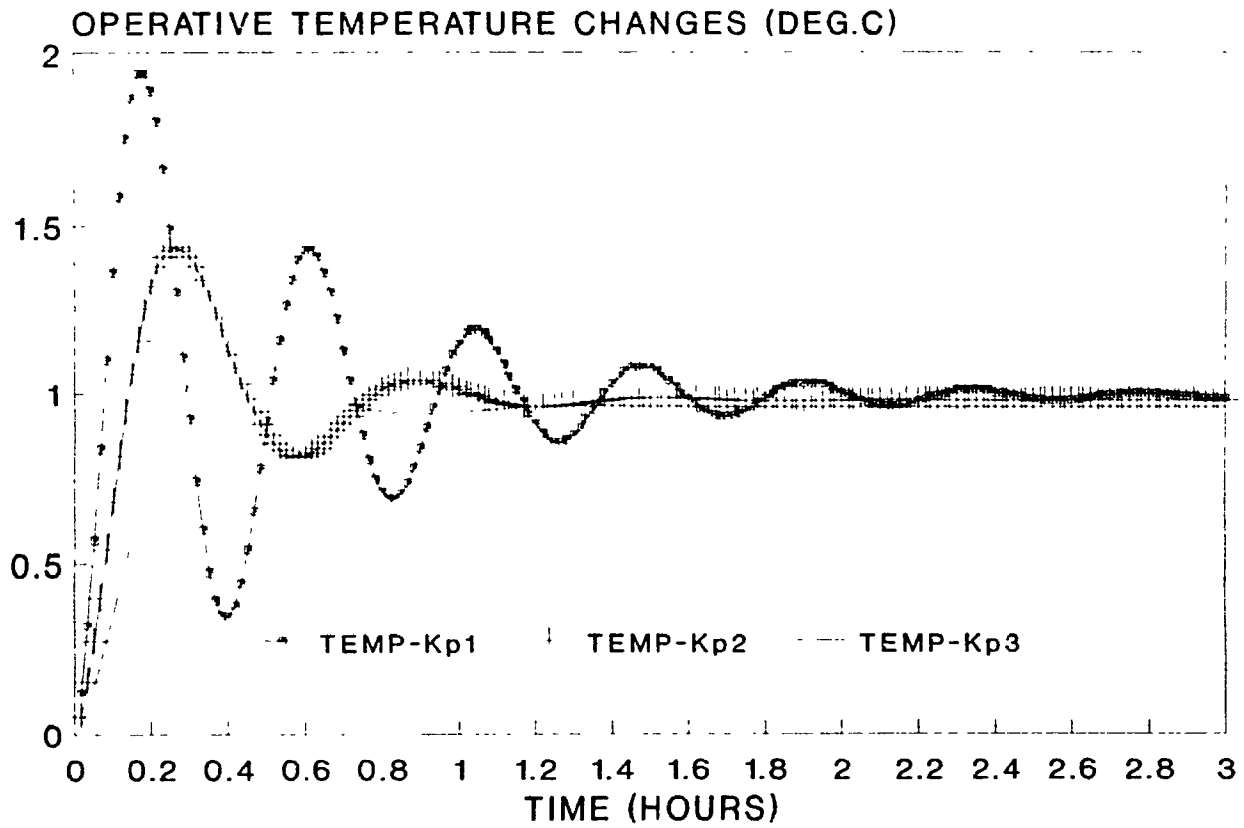

Kp1=2210 W/DEG.C
Kp2=1000 W/DEG.C
Kp3=500 W/DEG.C

Figure 4.7 Simulation results of operative temperature changes due to one degree setpoint change for a radiant ceiling heating system with different proportional gains.

and 0.2°C, respectively. For radiant ceiling heating with proportional gains of 2,210 W/°C, 1,000 W/°C and 500 W/°C (figure 4.7), the rise time is 4.8 minutes, 7.2 minutes and 15 minutes, respectively. The temperature overshoot for the three cases is 1.9°C, 0.5°C and 0.2°C, respectively. The radiant heating system with the proportional gain 2,210 W/°C has a settling time of 2 hours (the time required for a step response to stay within 5 percent of its setpoint). In general, the room air temperature for the baseboard heating rises faster than the operative temperature for the radiant heating because of the smaller time constants for the baseboard and air temperature sensor. For radiant heating, the operative temperature control with large proportional gains may result in system oscillation because of the large time constant of the sensor.

The simulation results indicate that the dynamic characteristics of a radiant heating system is significantly different from that of a baseboard heating system. Generally, a baseboard heating system with air temperature control operates in a stable manner. A fast response of the system can be expected with larger proportional gains. However, with radiant ceiling heating, the requirements of speed and stability of the system are often contradictory, i.e., a change made in proportional gain to improve the speed of response could adversely affect the stability of the system. Hence, the controller parameters of such systems should be selected to suit the applications in terms of control, comfort and energy conservation.

CHAPTER 5

CONTROL OF RADIANT PANEL HEATING

5.1 Introduction

Radiant panel heating systems have seen steadily increasing applications in both residential and commercial buildings. The design and the control of radiant heating systems have been based on the room air temperature, which is usually the controlled variable for convective heating systems. However, it is known that the room air temperature may differ significantly from the room mean radiant temperature. Several studies concerning the thermal comfort and physiological response of occupants in radiant-heated buildings have been conducted (LeBrun 1978; Fanger et al. 1980; Berglund et al. 1982). The results suggested that it would be more rational to control the operative temperature (approximately equal to the average of the room air temperature and mean radiant temperature) for radiant heating. However, limited efforts have been made so far to study the transient response of radiant heating system with operative temperature control.

Generally, six principal comfort components should be taken into consideration in HVAC system design: air temperature, mean radiant temperature, humidity, air movement, activity of the occupant and thermal resistance of clothing. One of the most overlooked is the effect of the mean radiant temperature (MRT) on comfort conditions. When the temperatures of the interior surfaces start to deviate excessively from the air temperature of the space, it becomes much more difficult for a convective heating system,

such as a baseboard heating system, to counteract the discomfort due to the cold surfaces. By contrast, a radiant heating system can neutralize the deficiency and minimize the excessive radiation losses from the body by raising the surface temperatures. What is desired is not a constant air temperature in a conditioned space, but a constant comfort, which may be achieved in part by using operative temperature control.

In this study, the program HEATCON has been employed to simulate a radiant heating system with air temperature or operative temperature control. The analytical results of air temperature or operative temperature response to the step changes in the setpoint (step response) are compared with the experimental measurements. Changes in the setpoint are the standard tests for investigating dynamic system behaviour and control performance. They are important in implementation of energy saving measures, such as the use of thermostat setpoint night setback. The tests were conducted with the electric radiant heating systems installed in the test-room on the roof of the Centre for Building Studies. The thermal properties and the air exchange rate of the room were measured as built. The detailed results of the test is presented following the description of the experimental facilities.

In order to evaluate the performance of the radiant heating system with air temperature control or operative temperature control, a series of preliminary experiments were conducted with the radiant heating systems using proportional control. The controller gains calculated by HEATCON were tested in the experiments.

5.2 Test facilities

A full-scale insulated outdoor test-room has been set up on the roof of the Centre for Building Studies for building heating and control studies under real weather conditions. The floor of the room has been left unfinished, which provides the flexibility to add floor heating panels or to change the thermal storage capacity with different materials. The structure of the room is shown in figure 5.1. The south wall includes a relatively large double glazed window. The interior lining on vertical walls and on the ceiling is a 13 mm thick gypsum board, while the floor lining is 16 mm plywood.

The radiant heating systems under consideration are two types of electric radiant panels - low intensity radiant floor panels and high intensity radiant ceiling panels. They were provided by CanRay Ltd.. The panels basically consist of an insulation layer, heat storage materials and electric resistance heating wires embedded in the heat storage materials shown in figure 5.2. The maximum temperature and total heating capacity of the high intensity ceiling panels were about 85°C and 800 W, respectively. The maximum temperature and total heating capacity of the low intensity floor panels were about 40°C and 1,000 W, respectively. In addition, a baseboard heater, which had a heating capacity of 1,000 W was also installed in the test room.

The window produced an asymmetric radiant field during the period of low ambient temperature by virtue of its low thermal resistance and low interior surface temperature. The comfort of occupants is affected by the air temperature in the space, as well as by the surface temperatures of the envelope. A single index to represent the thermal sensation is the operative temperature defined by (ASHRAE Standard, 1981)

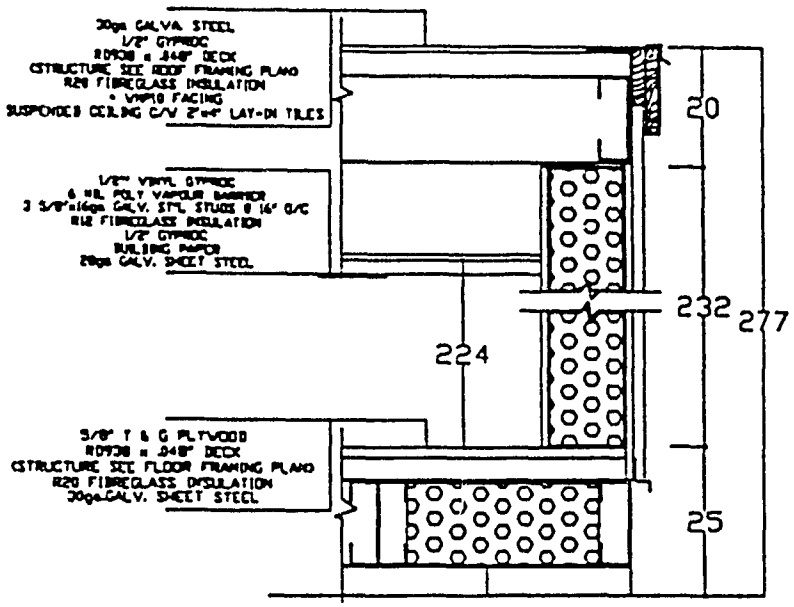

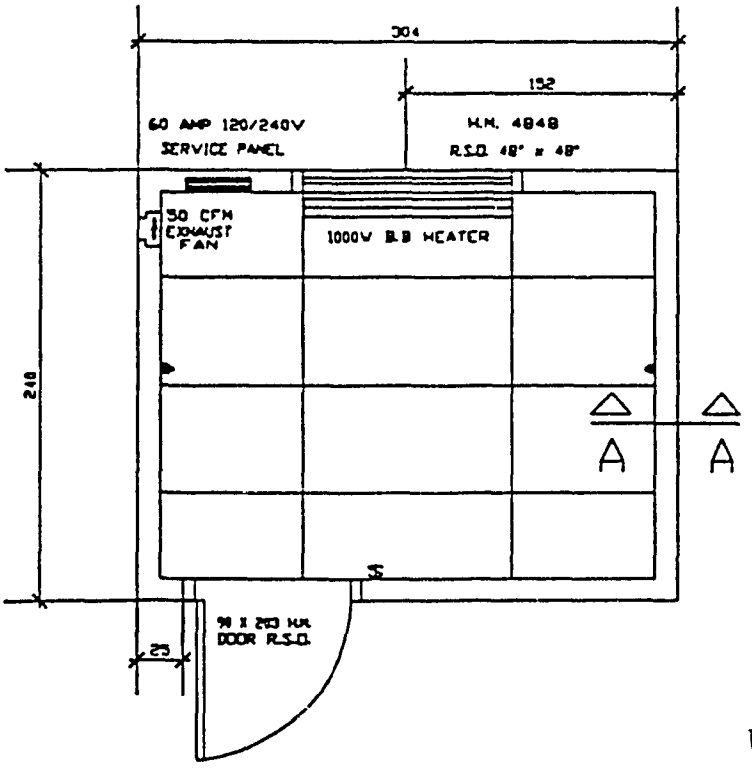

Unit = cm.

5.1 Structure of the test room.

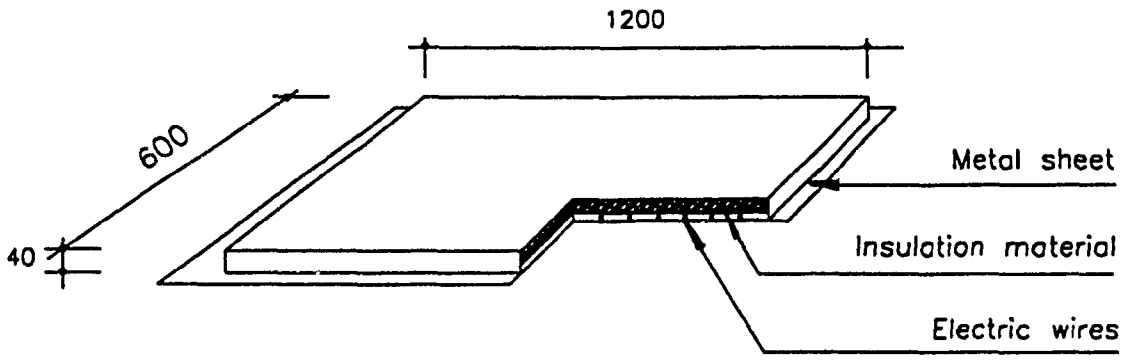

(a) High Intensity Radiant Ceiling Panel

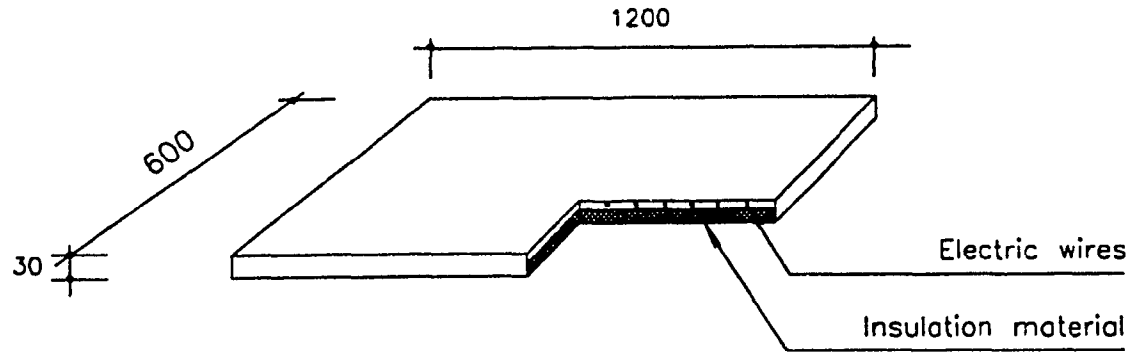

(b) Low Intensity Radiant Floor Panel

Unit = mm.

5.2 Schematic of a radiant ceiling panel and a radiant floor panel used in the tests.

$$T_e = \frac{(h_r\ T_{mr} + h_c\ T_{air})}{h_t} \qquad (5.1)$$

where T_e = operative temperature; T_{mr} = mean radiant temperature; T_{air} = dry bulb air temperature; h_r = linear radiation heat transfer coefficient; h_c = convective heat transfer coefficient; h_t = combined heat transfer coefficient or $h_t = h_r + h_c$.

Under normal conditions in which the inside air movement is less than 0.4 m/s, h_r is approximately the same as h_c. Therefore, T_e is equal to the average of MRT and T_{air}. This means that for every degree the MRT is increased, the dry bulb temperature can be decreased an equal amount without affecting the comfort level of the space. Therefore, operative temperature control is necessary to closely monitor and control the comfort level. An operative temperature sensor has been developed by Berglund et al. (1982). However, in this study, a globe temperature sensor had to be used to approximate the operative temperature measurement because the operative temperature sensor was not available to us. A globe temperature sensor consists of a hollow, black sphere with a thermocouple in the centre. In the actual environment, there is a balance between the heat exchange due to radiation and convection:

$$Q_r = Q_c \qquad (5.2)$$

where Q_r = heat flow due to radiation and Q_c = heat flow due to convection.

When the globe is in balance with the environment, the temperature inside the globe is measured, which includes the effects of air temperature and mean radiant temperature:

$$h_{r,g}\ (T_{mr} - T_g) = h_{c,g}\ (T_g - T_{air}) \qquad (5.3)$$

$$T_g = \frac{h_{r,g}\ T_{mr} + h_{c,g}\ T_{air}}{h_{r,g} + h_{c,g}} \qquad (5.4)$$

where $h_{r,g}$ = globe radiation heat transfer coefficient and $h_{c,g}$ = globe convective heat transfer coefficient. For these preliminary experiments, the operative temperature is approximated by the globe temperature.

The temperature sensors used for control purpose -- the room air temperature sensor and the globe temperature sensor -- were located in the centre of the room at a height of 1.2 meters. An additional globe thermometer, which was placed at the window, was used to measure the temperature asymmetry. Figure 5.3 indicates the placement of the heating panels and the locations of the two globe sensors in the room. Surface temperatures of the walls were also continuously measured at several locations (see Appendix C). Solar radiation was also measured.

Monitoring and controlling of the radiant heating system was accomplished with the computerized data acquisition and control system as shown in figure 5.4. The analog input signal of the control loop was scaled into a 0 - 100% range to allow the operation without direct use of units. The control algorithm computed the desired output power level in percentage which corresponds to output level of a D/A (digital to analog) converter specified in counts. The zero count always corresponded to the minimum D/A value of the range, while the 4095 count always corresponded to the maximum D/A value, regardless of voltage or current range was selected. If the controller being driven with the analog signal needed only certain range of signal (e.g. 4 - 20 mA), the range of

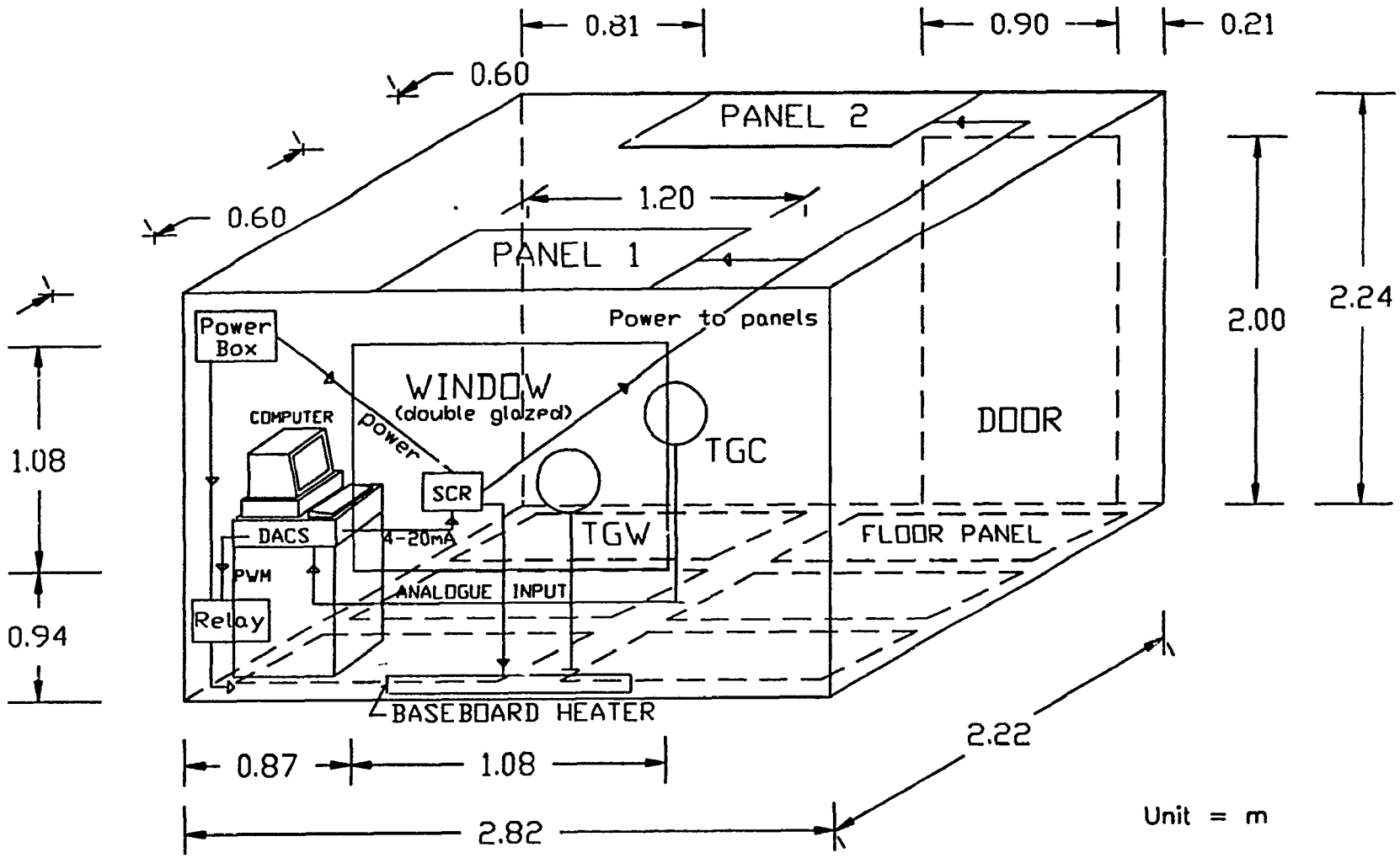

5.3 Schematic of the test room.

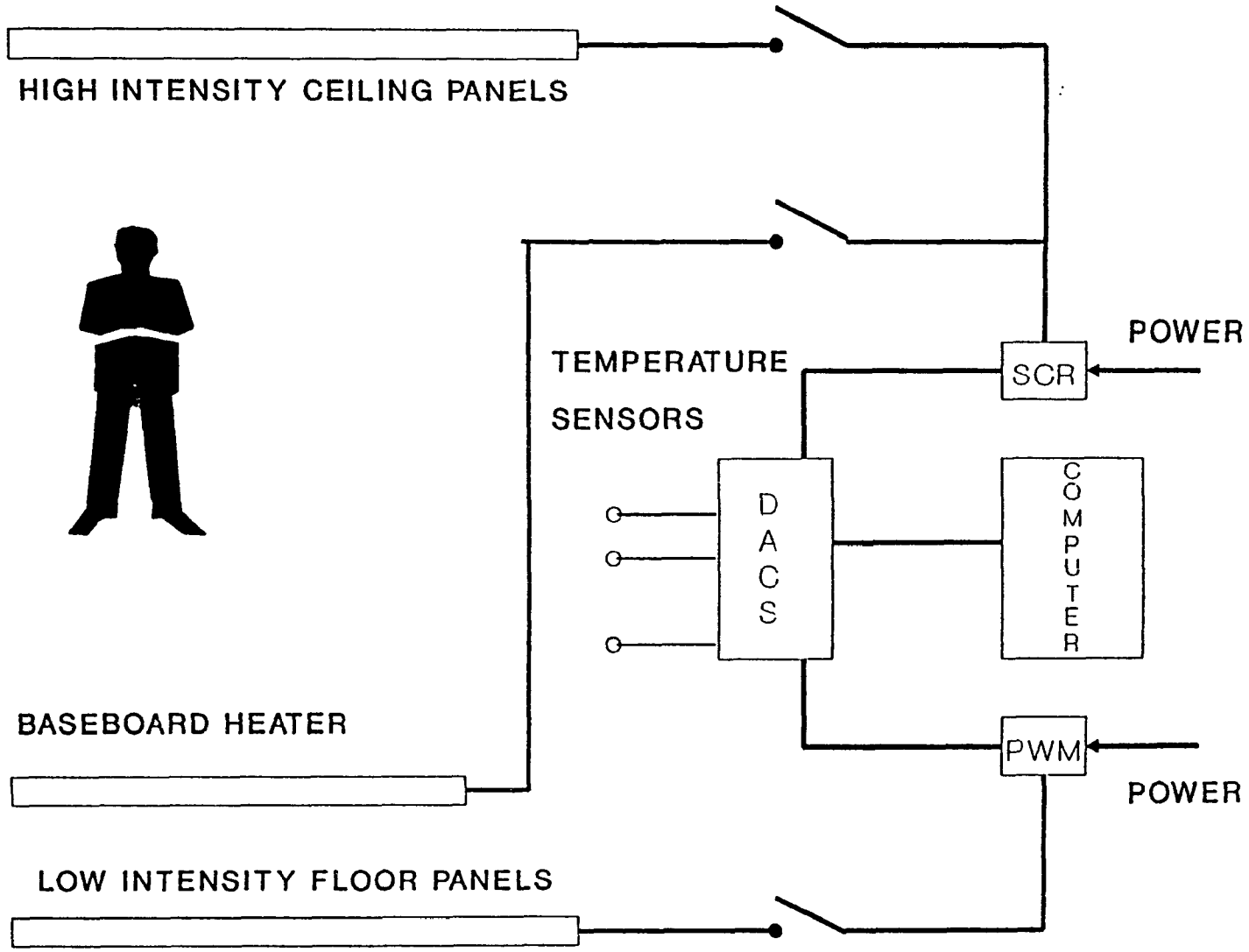

Figure 5.4 Computerized data acquisition and control system in the test room

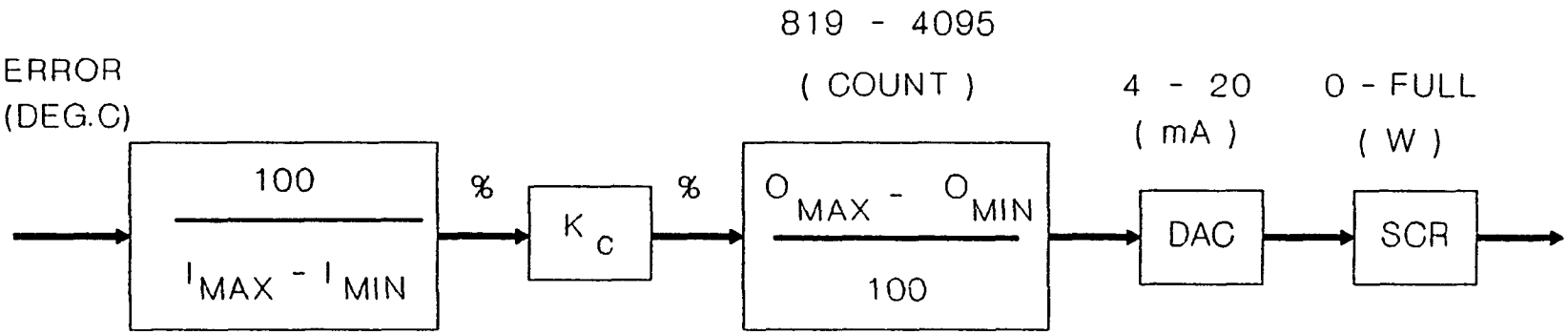

Figure 5.5 Block diagram of control action

the D/A converter was limited by selecting the correct minimum and maximum count values. For example, to limit SCR input signal to the range 4 - 20 mA, the counts should be from 819 minimum to 4095 maximum. The control action is shown by a block diagram in figure 5.5.

A general purpose software package (Gen200) was used for data acquisition and control applications. It contained features which made it an appropriate choice for our research that required continuous measurement, data storage and computer control. Another advantage of this package was that it was fully menu driven, supported multi-task measurements and controls, allowed real-time modifications of system setup parameters, such as a programmable setpoint profile, and simplified the operation of the system.

5.3 Response of radiant heating systems to setpoint changes

Prior to the step response of the heating control system, some parameters were necessary to be measured as built: (1) typical infiltration rate of the room, (2) thermal conductance of the envelope and (3) time constants of the heating panels and the temperature sensors. The thermal properties of the materials were considered uniform and homogeneous.

The tracer gas measurement of air exchange rate was performed by mixing tracer gas (CO_2) throughout the test room and monitoring the decay in concentration as a function of the time. The result indicates that the infiltration rate was about 0.6 air changes per hour (see Appendix B). The heat flow through each wall and its surface temperature were measured with a combined thermocouple-heat flux sensor. The thermal

conductances of the envelope were estimated by dividing the heat flow with the surface temperature difference. It was found that the R-value was 2.2 RSI for the vertical walls and 3.6 RSI for the ceiling and floor. The time constants of radiant panels and temperature sensors were estimated by plotting their temperature responses to step changes, such as applying constant heat to the panels or placing the temperature sensors into two different temperature environment. The time required to reach 63% of the steady state response from the initial condition is taken as a time constant. For the radiant ceiling panels it is 280 seconds, while for radiant floor panel, the time constant is 2,500 seconds because of its larger thermal mass. The time constants of the air temperature sensor (simple thermocouple) is 16 seconds and that of the globe temperature sensor is 270 seconds.

A proportional controller has two variables which can be set: the setpoint that is the value of the controlled variable which the controller is set to maintain, and the proportional gain. Normally, the proportional gain is replaced by an alternative, known as the proportional band (throttling range). It may be defined as the change in the controlled variable required to make the final control element move through its full operating range or stroke. The proportional band δ is closely related to the capacity of the heating system and inversely proportional to its proportional gain:

$$\delta = \frac{K_h}{K_p} \qquad (5.5)$$

where K_h is the total capacity of the heating system and K_p is the proportional gain.

The larger the proportional gain, the smaller the proportional band. The proportional control may not be precisely executed if the band is too small as compared with the instrument errors involved. On the other hand, a large proportional band implies longer response time, with which the step response will be affected by large variation of ambient temperature. In order to have a comparable condition for analytical and experimental studies, a proportional band of 2°C was employed in the step response experiments, and the corresponding proportional gain for radiant ceiling panels and radiant floor panels were 400 W/°C and 500 W/°C, respectively. The transfer function technique is based on a steady state initial condition. In the experiment, the initial condition was approximated by natural cooling of the test room. The step responses were conducted with 2°C set-up change of the temperature setpoint, which is actually the proportional band. During the test, the variation of ambient temperature should be minimum and any tests with ambient temperature fluctuation over ±0.5°C had to be abandoned. In order to simplify the modelling by eliminating other heat sources, such as the solar heat gain, all the tests were carried out from 16:00 to 24:00.

The step response tests of the radiant heating system with proportional control were carried out during February and March, 1991. The computer simulations of the responses were also conducted using the program HEATCON, which were compared with the experimental results. Figure 5.6 shows both predicted and measured air temperatures for radiant ceiling heating with air temperature control. Similar plots are also given in figure 5.7 which compares the simulated and measured results for radiant ceiling

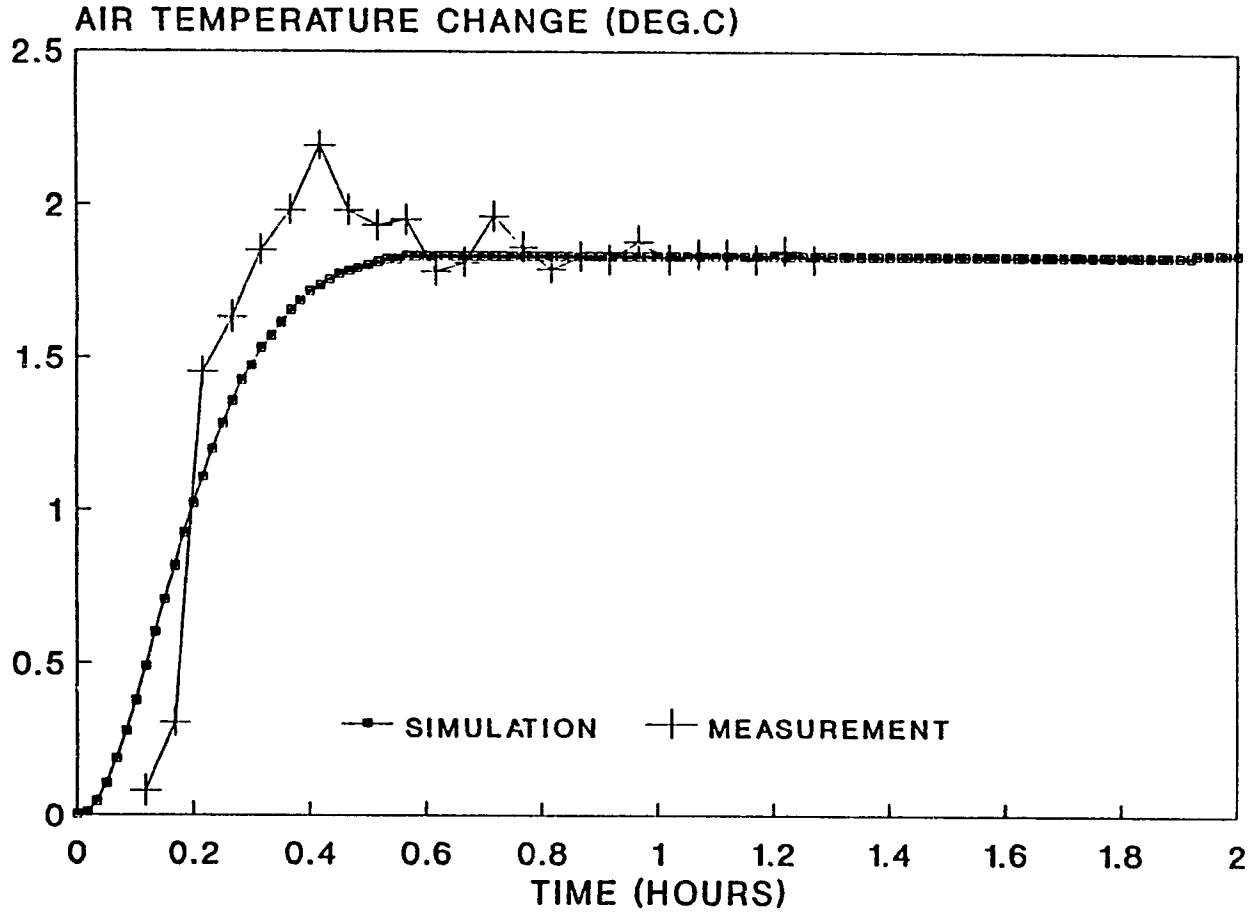

Figure 5.6 Room air temperature response (change) to 2 degree C step rise in the setpoint -- with air temperature sensor and proportional control (ceiling heating system).

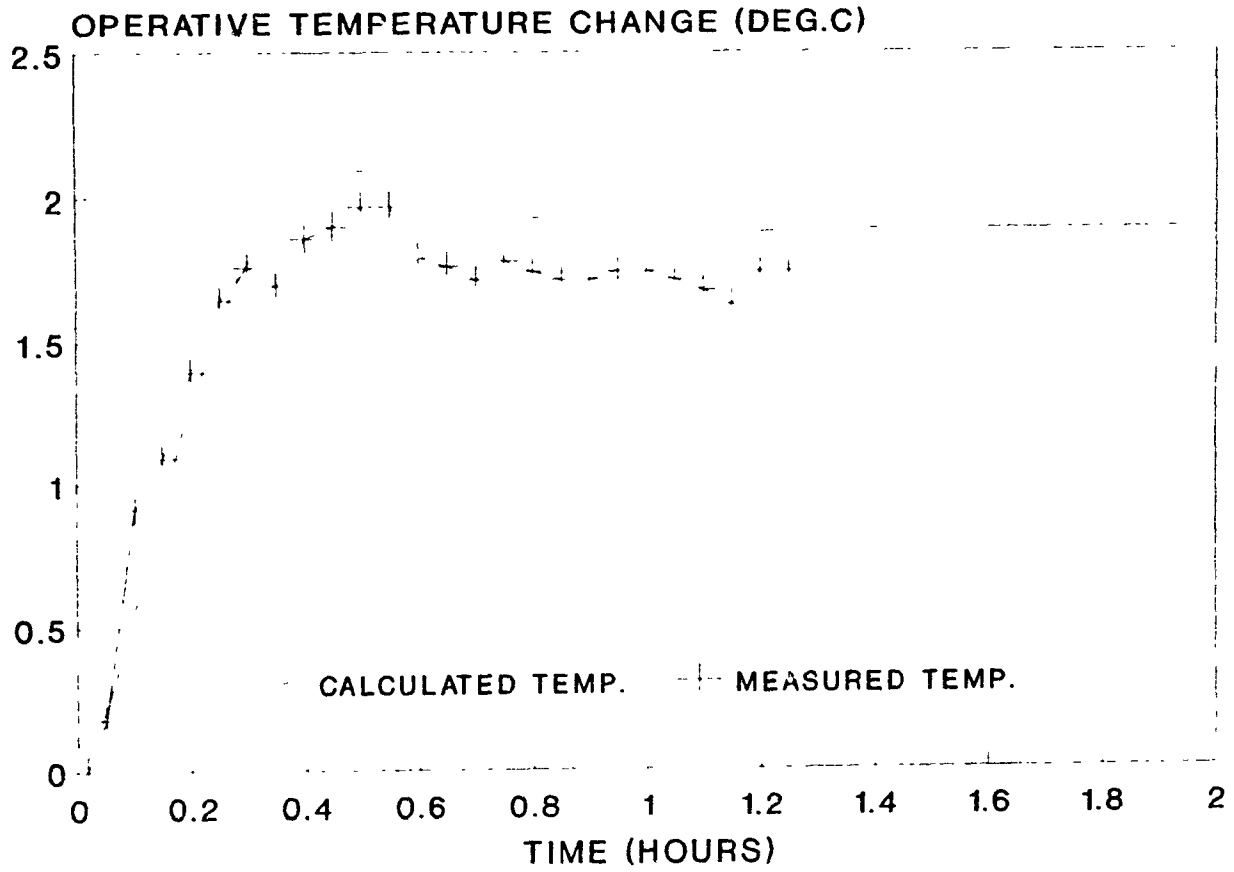

Kp=400 W/DEG.C

Figure 5.7 Operative temperature response (change) to 2 degree C step rise in the setpoint -- with operative temperature sensor and proportional control (ceiling heating system).

heating with operative temperature control. Both figures indicate that the analytical results predicted the transient response measured in the experiments reasonably well. The overshoot measured for air temperature control may be caused by insufficient mixing of the room air. The air temperature sensor was placed in the centre of the room where higher room temperature was expected. For radiant floor heating with either the air temperature control or the globe temperature control, a reasonable agreement between the calculated and measured results is also observed as shown in figures 5.8 and 5.9. However, some discrepancy has been noticed where an overshoot is predicted with the analytical method. In the tests, the predicted overshoot actually never occurred. This difference may be due to the attenuation of the panel temperature by the plywood board protecting the floor panels. However, the general tendencies of the transient responses for different applications are reflected by the calculated results with HEATCON. For instance, the slower response of the radiant floor heating system is indicated by both analytical and experimental results. The large thermal capacity of the radiant floor panels may delay the heat flow into the space, while the large time constant for the operative temperature sensor delays the control action.

The power consumption for radiant ceiling and floor heating was also estimated experimentally, as well as theoretically. The results are plotted in figures 5.10, 5.11, 5.12 and 5.13. The total energy consumption during the transient response (1 hour) are estimated by the program HEATCON and experimental measurements for the test room. The analytical results indicate that the energy consumption may be reduced 12.4% for the radiant ceiling heating with operative temperature control. However, this energy saving

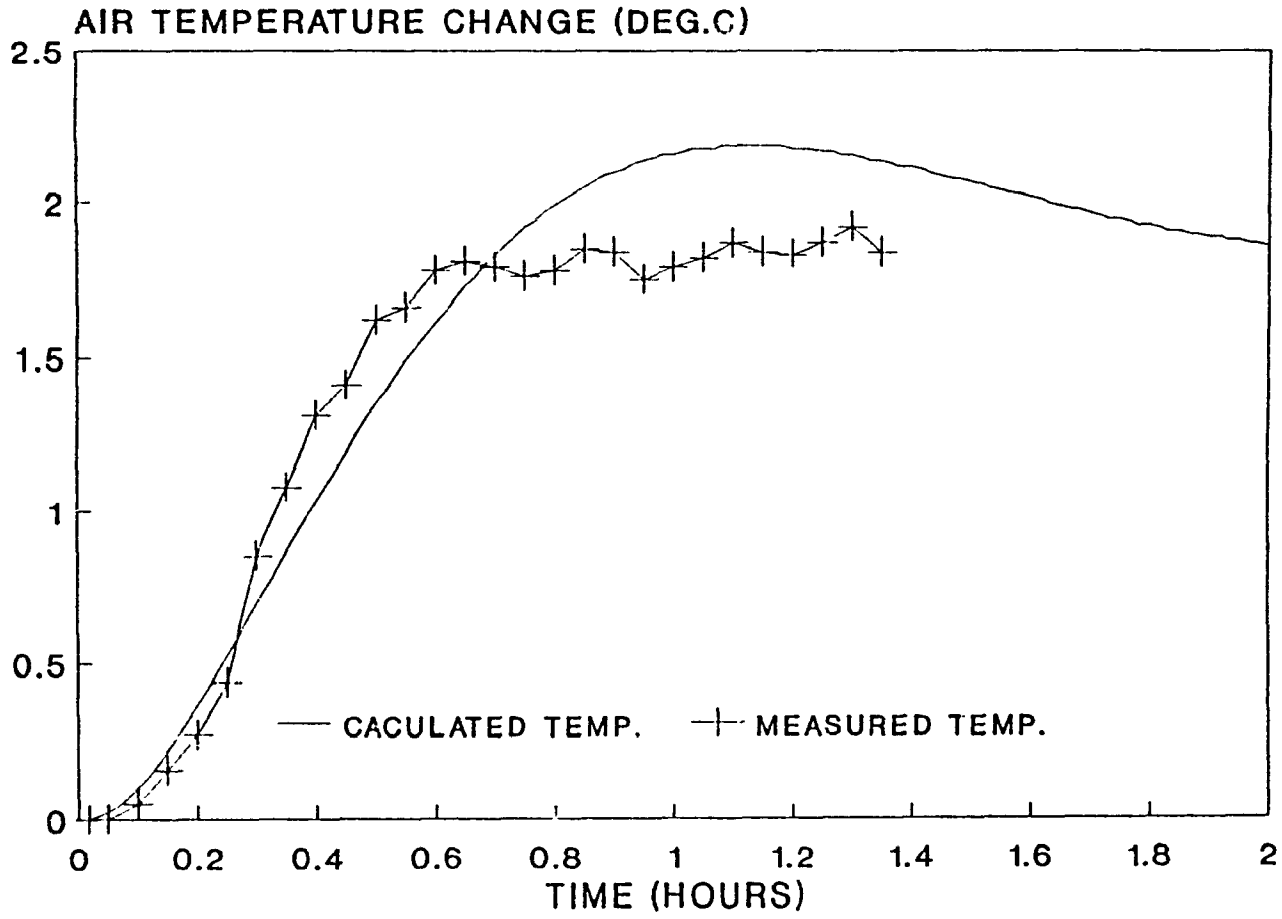

Figure 5.8 Room air temperature response (change) to 2 degree C step rise in the setpoint -- with air temperature sensor and proportional control (floor heating system).

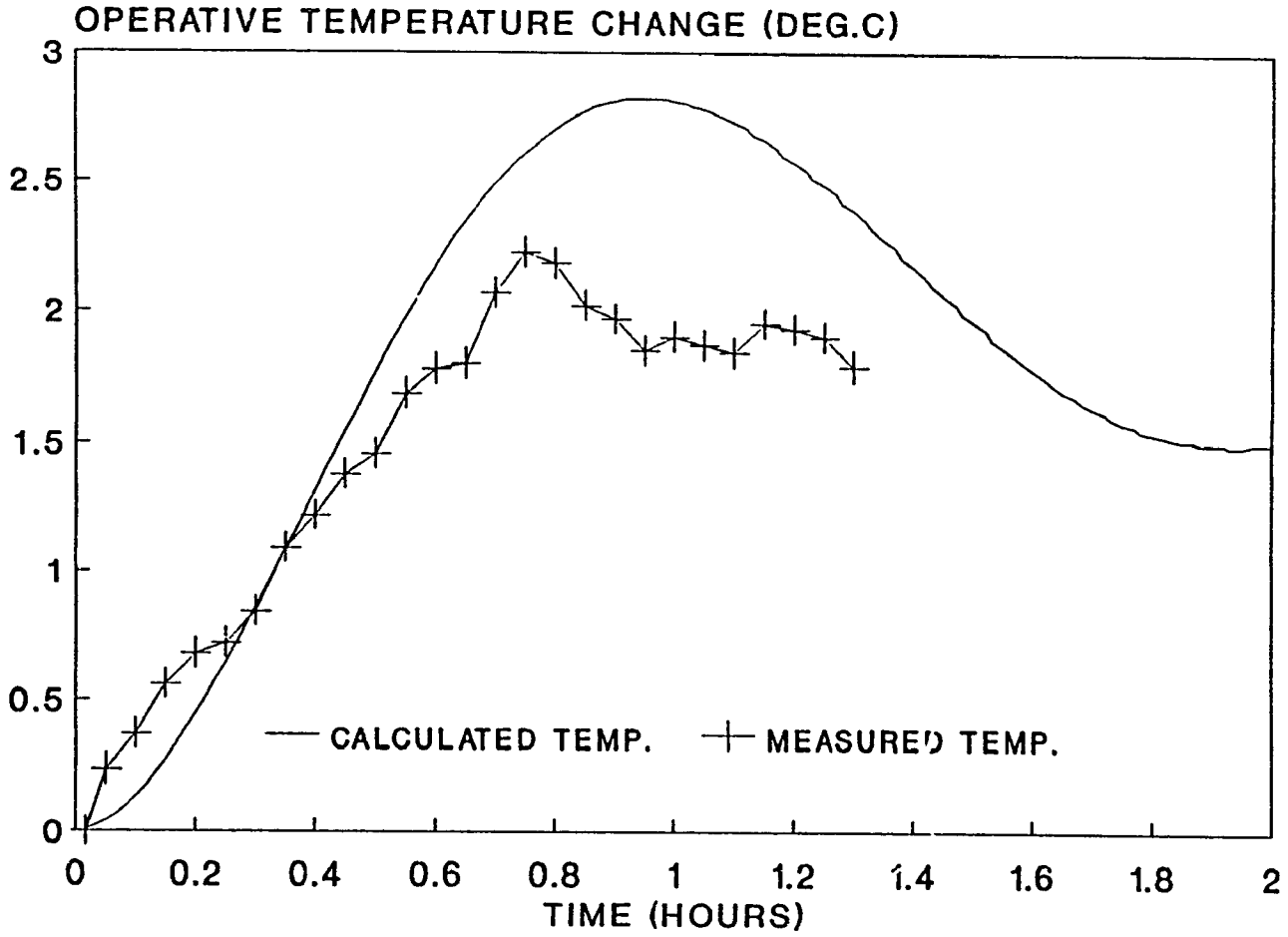

Figure 5.9 Operative temperature response (change) to 2 degree C step rise in the setpoint -- with operative temperature sensor and proportional control (floor heating system).

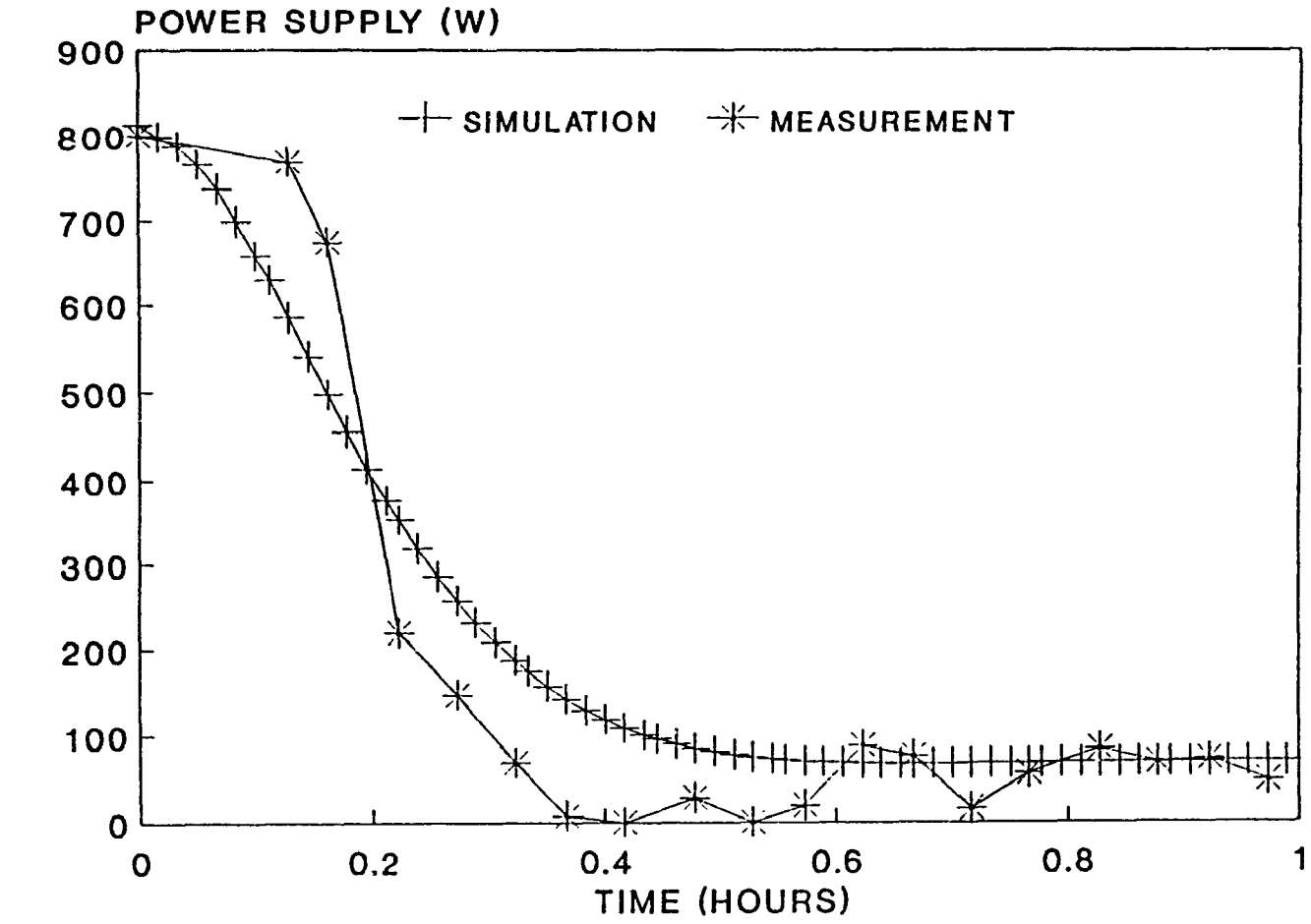

Figure 5.10 Power consumption for radiant ceiling heating with air temperature control (corresponding to Figure 5.6).

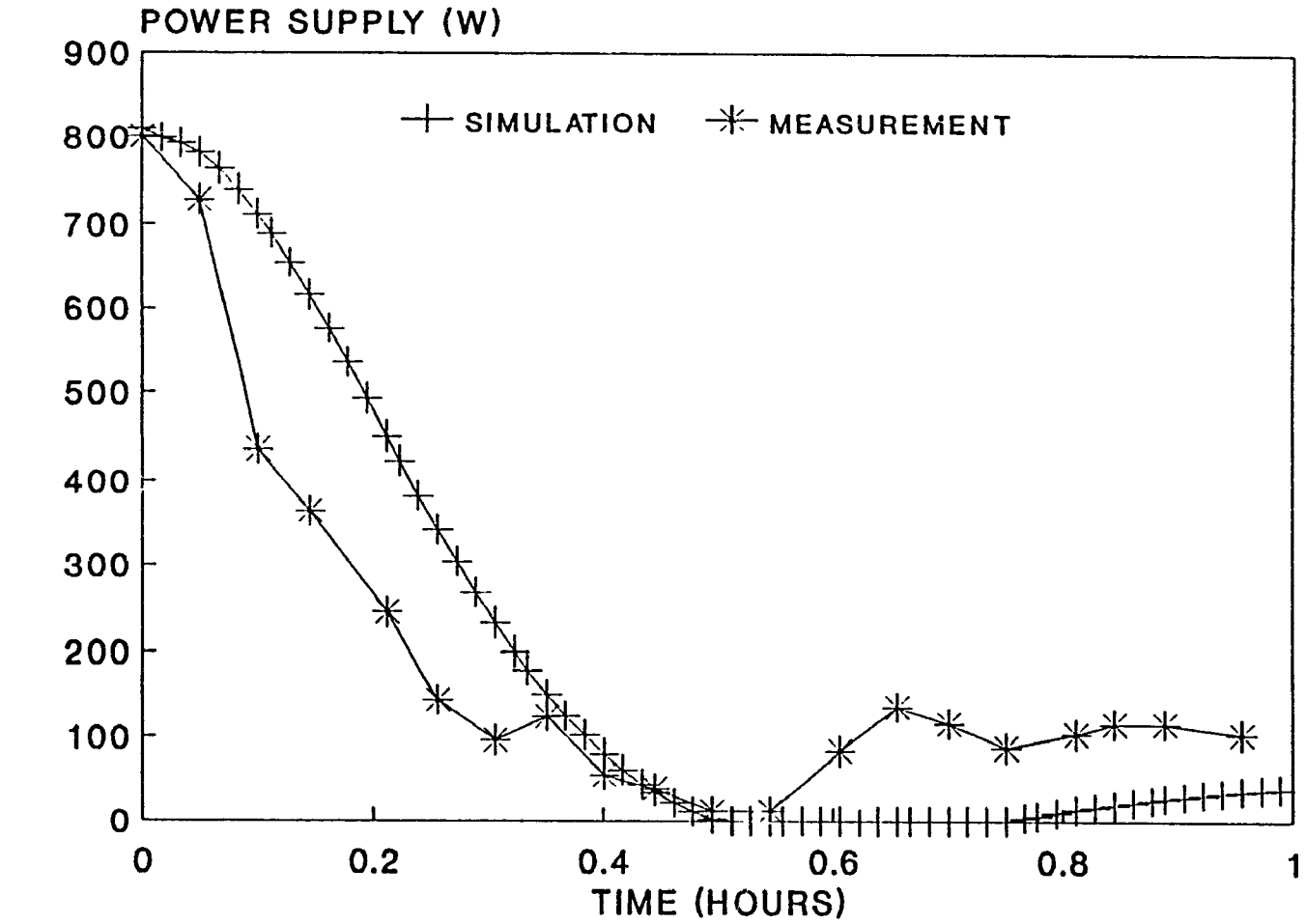

Figure 5.11 Power consumption for radiant ceiling heating with operative temperature control (corresponding to Figure 5.7).

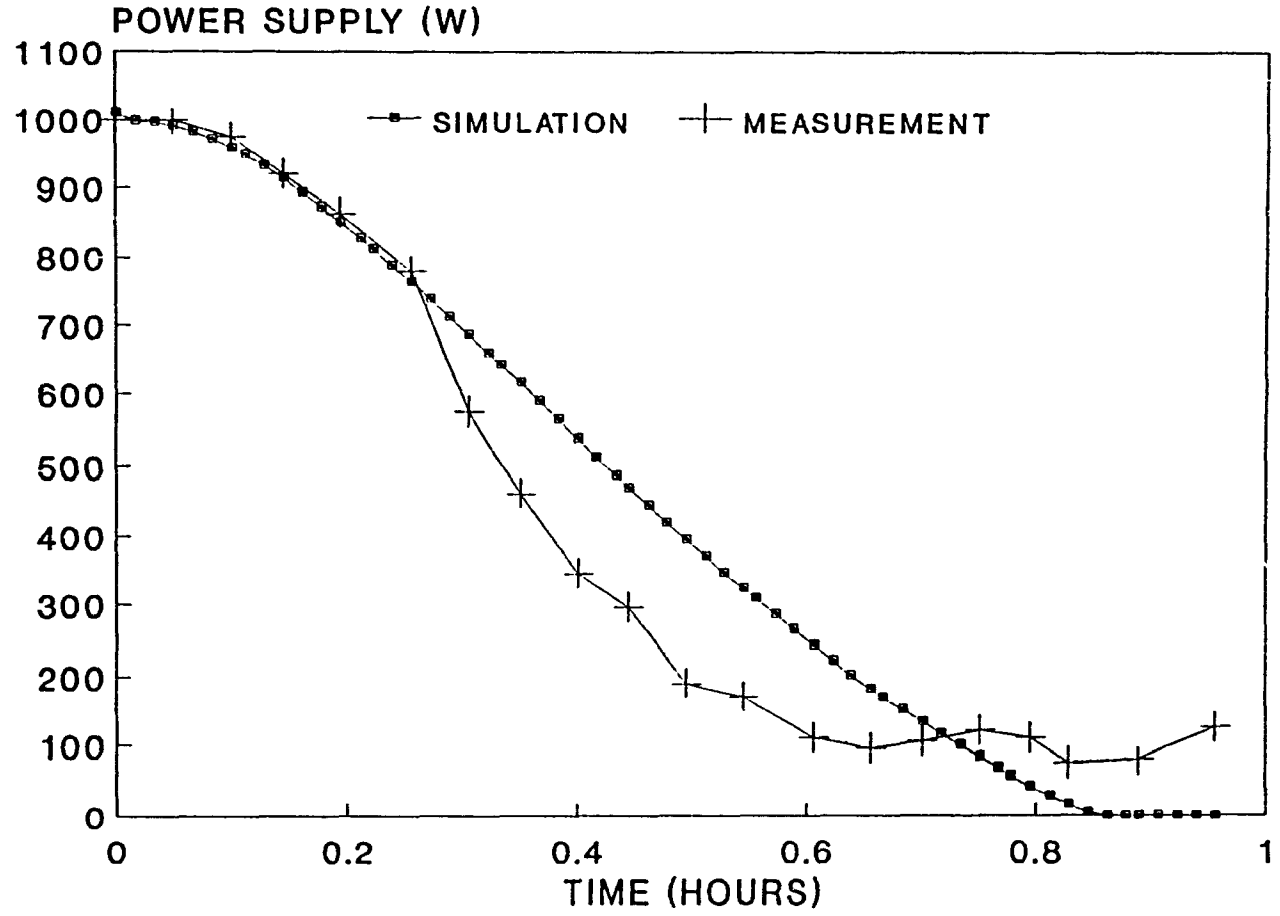

Figure 5.12 Power consumption for radiant floor heating with air temperature control (corresponding to Figure 5.8).

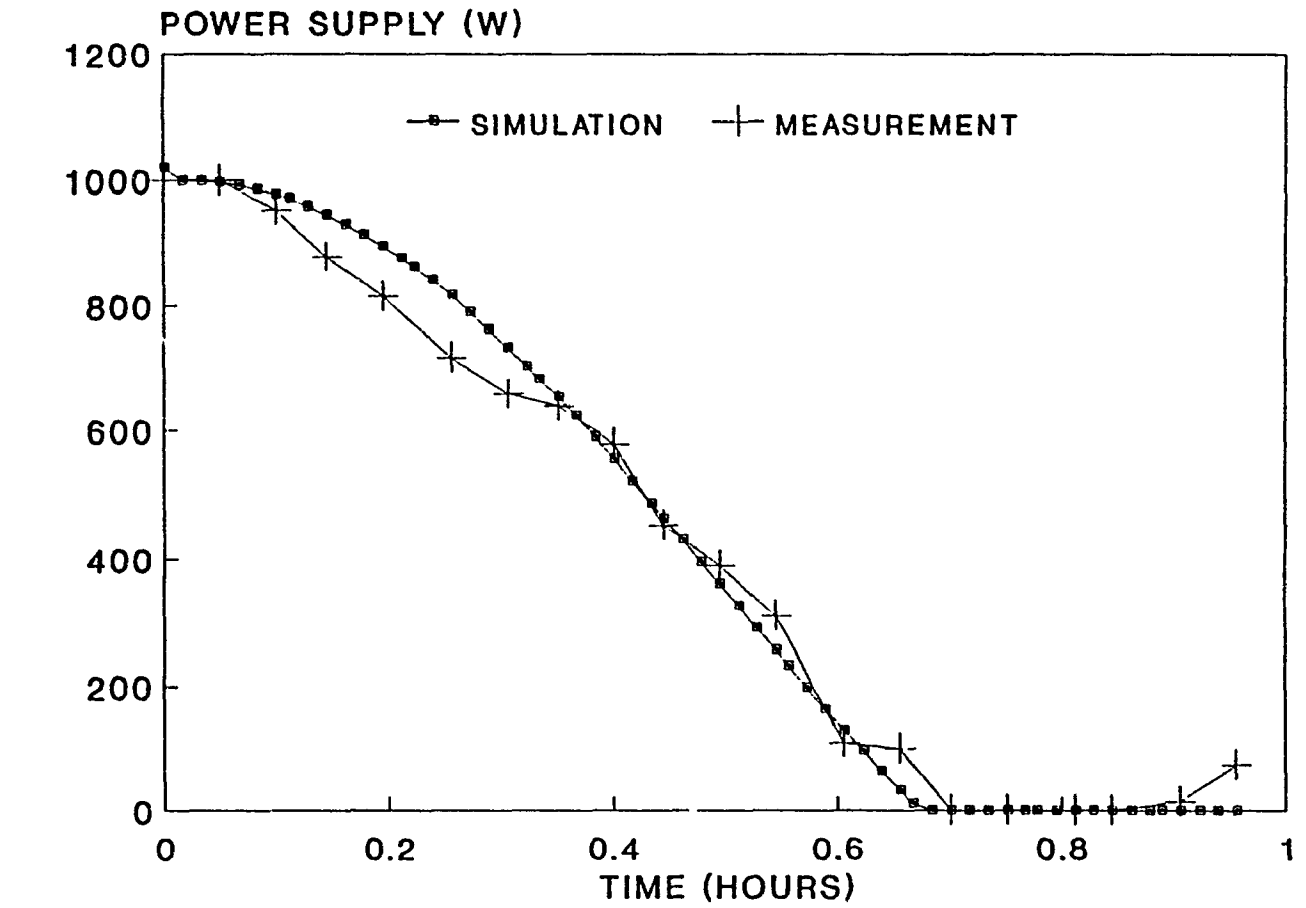

Figure 5.13 Power consumption for radiant floor heating with operative temperature control (corresponding to Figure 5.9).

was not supported by the actual measurements. The results are summarized in table 5.1.

Table 5.1 Comparison of energy consumptions for radiant ceiling heating evaluated with HEATCON and measurements.

ENERGY CONSUMPTION FOR RADIANT CEILING HEATING (KJ)			
AIR TEMPERATURE CONTROL		OPERATIVE TEMPERATURE CONTROL	
SIMULATION	MEASUREMENT	SIMULATION	MEASUREMENT
780	650	694	624

The energy saving measured was only 4.2% for the radiant ceiling heating with operative temperature control. The difference could be caused by many factors in the experiments, such as the difficulty in establishing required initial conditions. Ideally, two identical test rooms are needed to conduct more accurate experimental comparison of energy consumption between two types of heating control systems; or the test room should be located in an environmental chamber.

5.4 Proportional control of radiant heating systems

Radiant heating systems generally provide better thermal environment than convective heating methods, such as the baseboard heating. A more uniform temperature

distribution in the room was achieved with the radiant floor heating in comparison with the baseboard heating (see Appendix C). However, the large time constant of the operative temperature sensor, together with the effect of thermal mass stored in the radiant floor panels, results in slow response of the room temperature as shown in figure 5.14. This delays the thermal control action and may cause system oscillation and instability. In order to ensure that a radiant heating system has the desired response, a proper proportional gain is needed to modulate the heat output level. The study of the effects of the different magnitudes of the gains in air temperature control or operative temperature control is very important.

Figure 5.15 shows both air temperature and operative temperature responses when the test room was heated with radiant ceiling panels, using air temperature control. In order to study the effect of different controller gains on the system performance, a large proportional gain 4 KW/°C was used. The room air temperature was raised from 14 to 18 °C. The operative temperature overshoot of 1°C was observed during the transient response, though there was no system oscillation. As expected, the application of air temperature control in radiant heating system cannot properly control the thermal comfort level.

The same proportional gain 4 KW/°C was also applied in radiant ceiling heating with operative temperature control, and the temperature setpoint was set up form 16 to 20°C. Figure 5.16 indicates that the operative temperature was continuously oscillating around 20°C. Actually, this proportional gain is very close to the ultimate gain for the radiant ceiling heating system, with which the stability limit is reached.

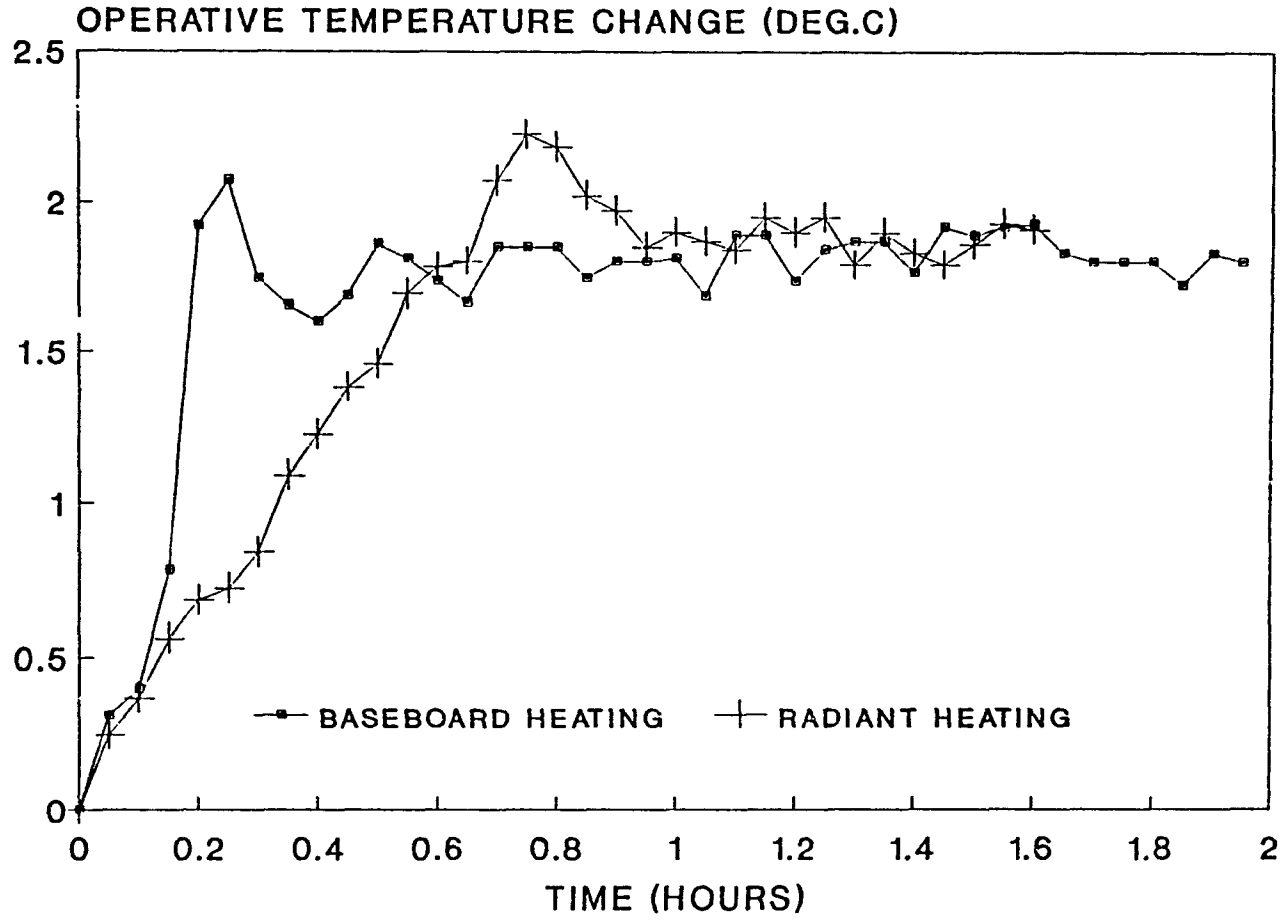

Kp = 500 W/DEG.C

Figure 5.14 Operative temperature respnse (change) for baseboard heating and radiant floor heating with operative temperature control (2 degree C setup rise in the setpoint).

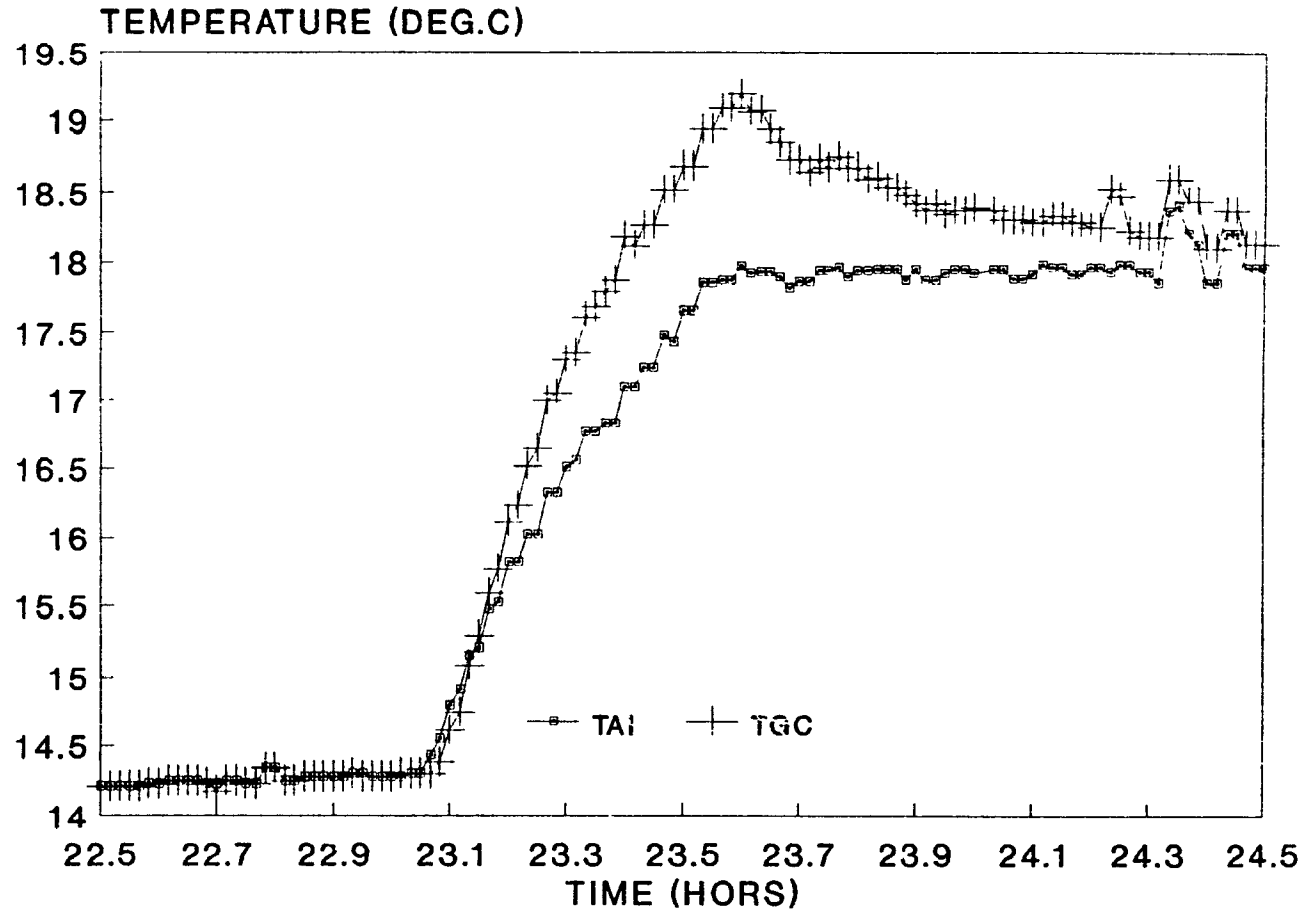

Figure 5.15 Air temperature and operative temperature for radiant ceiling heating with air temperature control (step change in the setpoint, proportional gain 4 kW/DEG.C)

Similar tests were also conducted with the radiant floor heating system. For air temperature control, there was no unstable operation even with extremely high proportional gain (10 KW/°C) shown in figure 5.17. However, the oscillation of the temperature is indicated in figure 5.18 when operative temperature control was used with proportional gain equal to 3.6 KW/°C. It is seen that a radiant heating system with operative temperature control starts oscillation at a relatively low proportional gain. Unlike the air temperature control, the operative temperature sensor has a larger time constant which contributes a large phase lag between the operative temperature feedback and the control action. Due to the phase lag, oscillation may occur in operative temperature control with a relatively small proportional gain. Similarly, large thermal storage in the room may increase the tendency for unstable operation of the heating system. This is evidenced by the fact that the oscillation occurred with the smaller proportional gain for the radiant floor heating than for the radiant ceiling heating.

Cyclic operation of a heating system not only affects the thermal comfort control, but may destroy the control valve if a hydraulic system is used. It is crucial to tune the control parameters of a radiant heating system and to choose a proper proportional gain. If the value of the gain is too low, it will take the system a long time to bring the controlled variable to the desired setpoint since low power is supplied, resulting in uncomfortable conditions for long time periods. On the other hand, if the gain is higher than necessary, the output will rise fast even with a small error and the temperature may exceed the setpoint, resulting in a high overshoot (temperature swing) and discomfort. If the gain is too high, the controlled variable may start to oscillate back and forth around

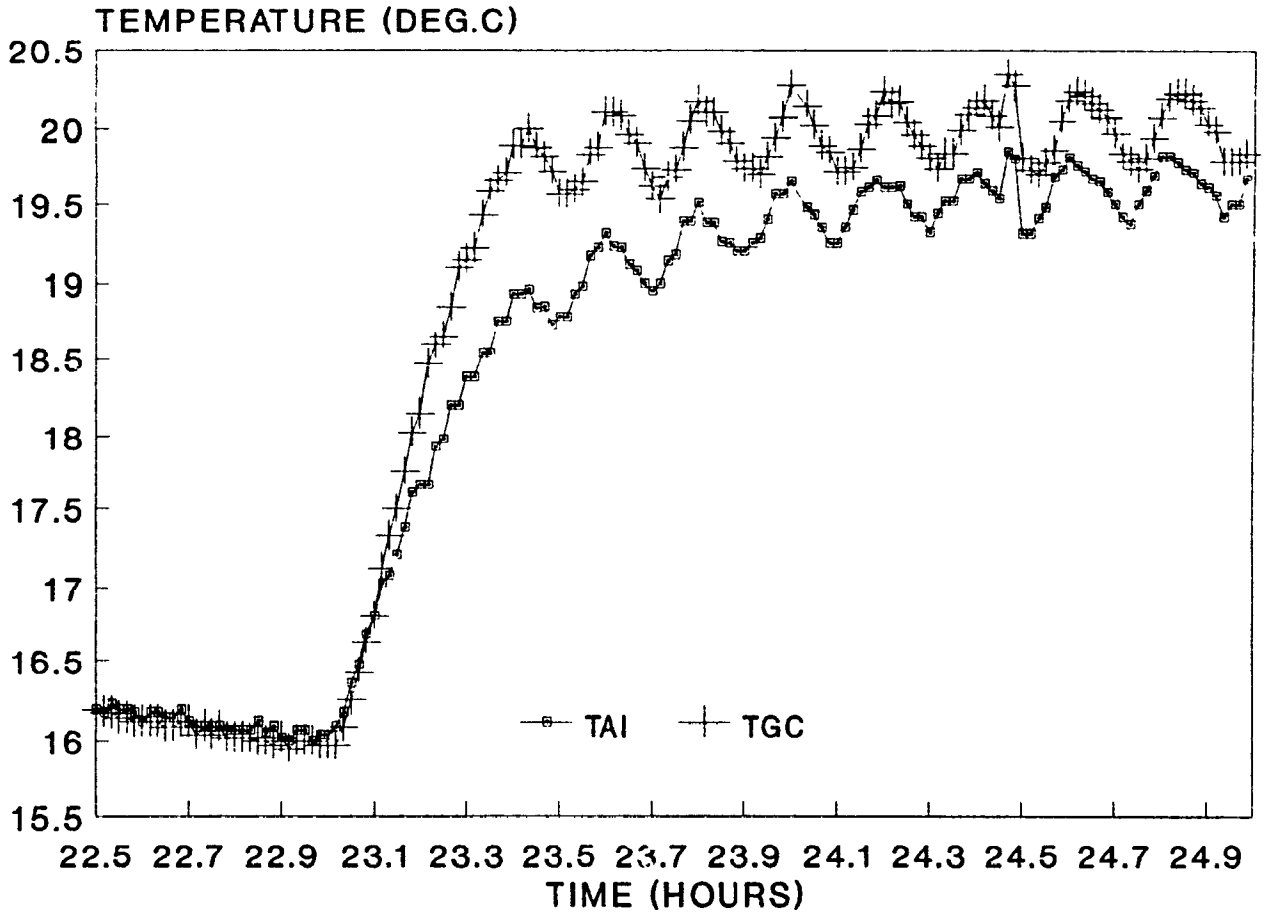

Figure 5.16 Air temperature and operative temperature for radiant ceiling heating with operative temperature control (step change in the setpoint, proportional gain 4 kW/DEG.C)

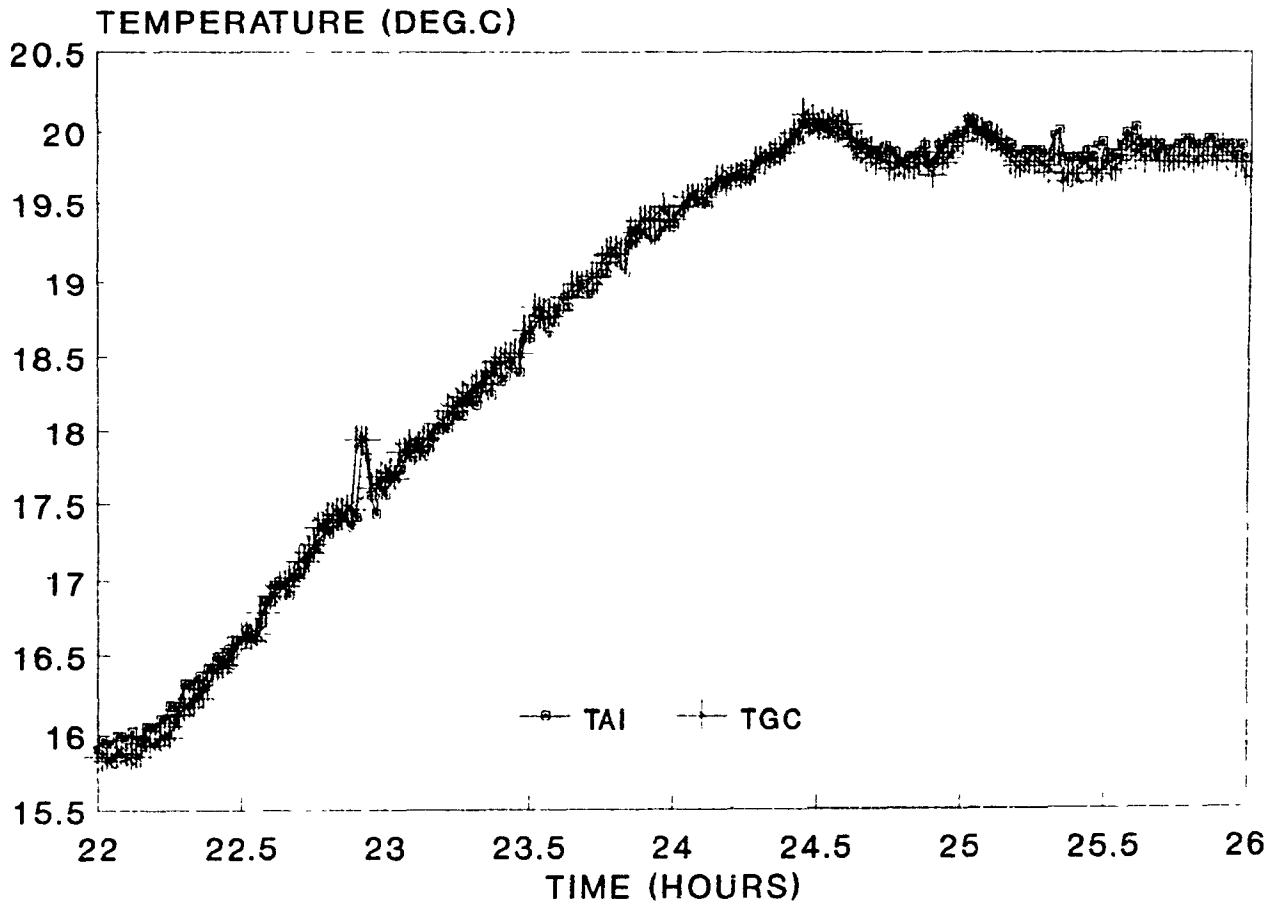

Figure 5.17 Air temperature and operative temperature for radiant floor heating with air temperature control (step change in the setpoint, proportional gain 10 kW/DEG.C).

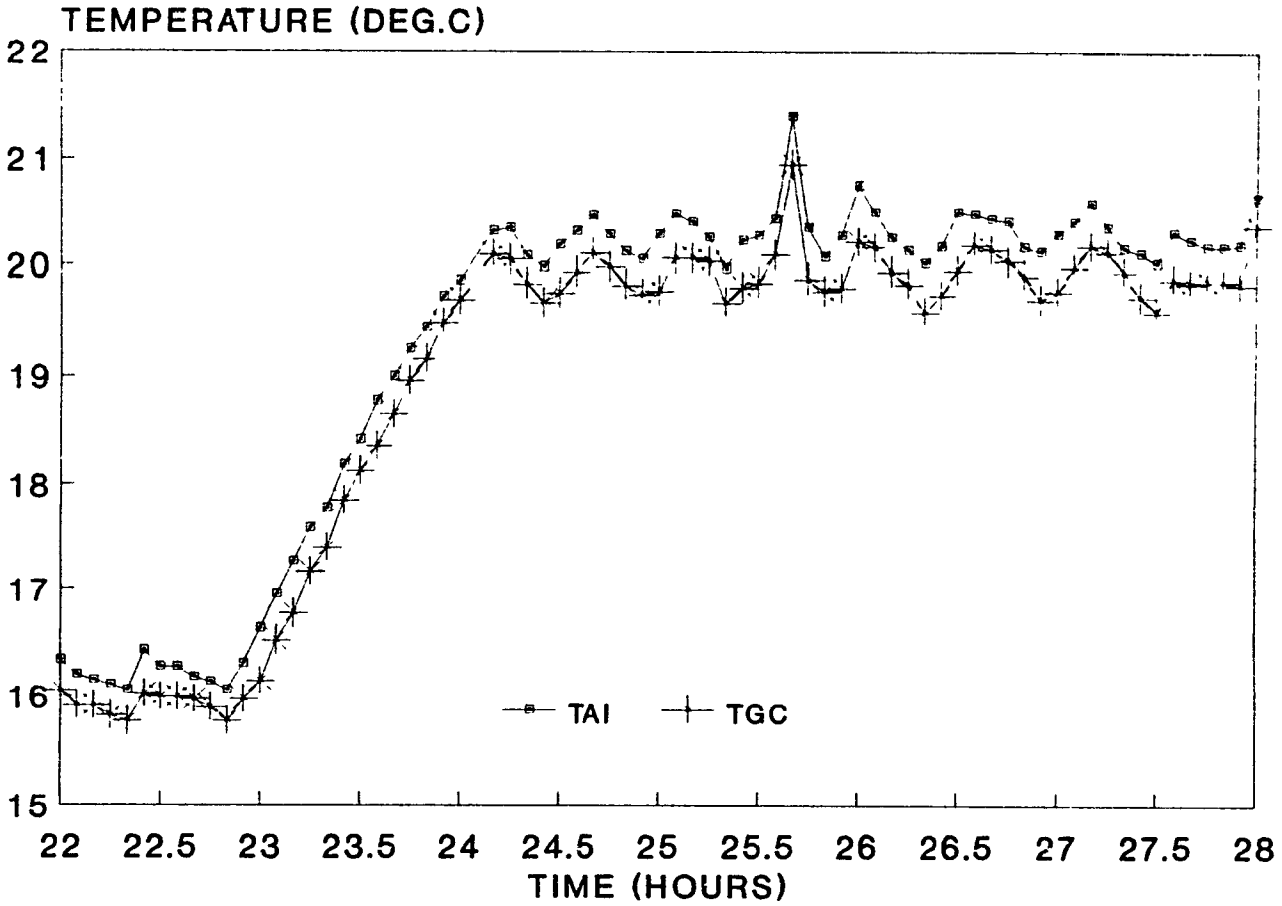

Figure 5.18 Air temperature and operative temperature for radiant floor heating with operative temperature control (step change in the setpoint, proportional gain 3.6 kW/DEG.C).

the setpoint. A compromise is necessary to balance the fast response with acceptable error. It is usually achieved through tuning by trial and error in the field. The computer program HEATCON utilizes the Ziegler-Nichols tuning technique to estimate the controller parameters. The controller proportional gains for the radiant ceiling and radiant floor heating are summarized in Table 5.2.

Table 5.2 Ziegler-Nichols tuning of system controller gains for radiant heating systems (W/°C).

TYPE OF CONTROL	RADIANT CEILING HEATING	RADIANT FLOOR HEATING
AIR TEMPERATURE CONTROL	3,905	27,704
OPERATIVE TEMPERATURE CONTROL	2,210	1,778

The proportional gains tuned for operative temperature control of radiant ceiling and radiant floor heating systems are 2.2 KW/°C and 1.8 KW/°C, respectively. The two controller gains have been applied to the heating systems. Figure 5.18 and 5.19 indicate that stable operation of the heating systems with operative temperature control is obtained.

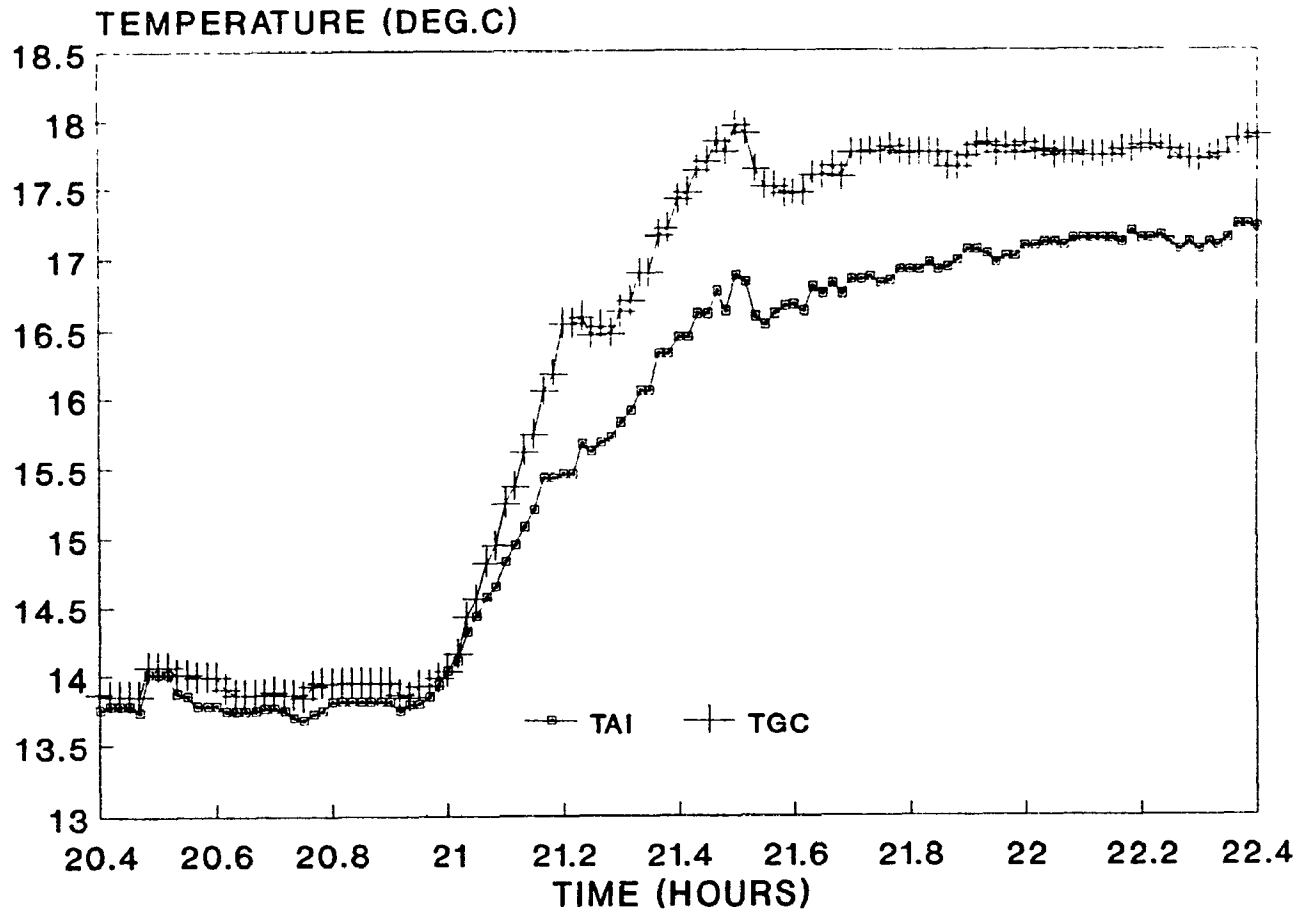

Figure 5.19 Air temperature and operative temperature for radiant ceiling heating with operative temperature control (step change in the setpoint, proportional gain 2.2 kW/DEG.C)

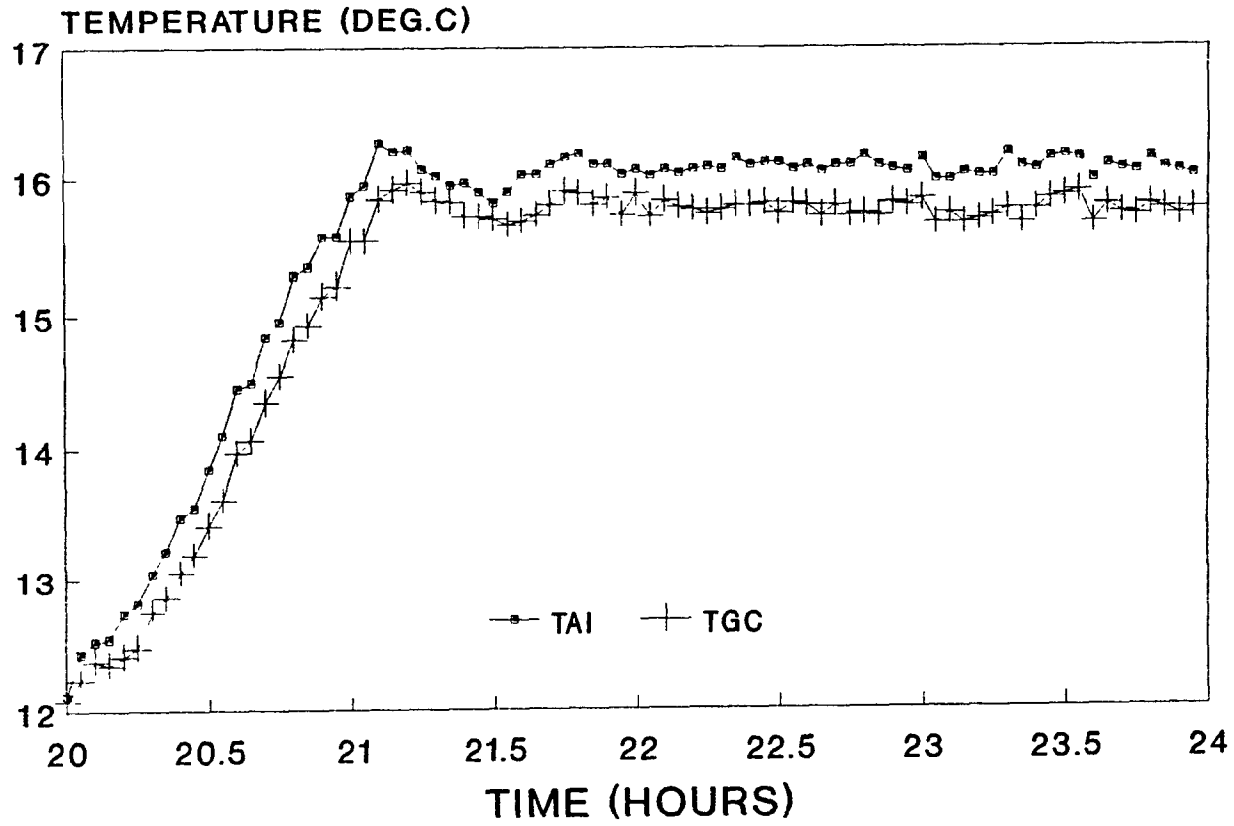

Figure 5.20 Air temperature and operative temperature for radiant floor heating with operative temperature control (step change in the setpoint, proportional gain 1.8 kW/DEG.C)

For air temperature control, the proportional gains tuned with the Ziegler-Nichols method are very large, i.e., 3.9 KW/°C for the radiant ceiling heating and 27 KW/°C for the radiant floor heating. These results are consistent with the experimental measurements. No oscillation was observed for the radiant ceiling heating or radiant floor heating with air temperature control. In reality,a heating system is usually limited by its capacity and that the proportional control band will be extremely small if a large controller gain is used. In the case of the radiant floor heating with the proportional gain of 10 KW/°C and the heating capacity of 1 KW, the proportional band was only 0.1 °C, with which the heating system was essentially operating in on/off mode.

Generally, a heating system with air temperature control has larger stable margin because of the faster response of the air temperature sensor. By contrast, special consideration to system stability should be given in the design of the radiant heating system with operative temperature control. The Ziegler-Nichols tuning method provides a general guideline to choose a proper proportional gain to obtain a stable operation of a radiant heating system. A fast response operative temperature sensor, such as the one developed recently by Markel et al. (1989), will enhance the performance of radiant heating systems.

CHAPTER 6

CONCLUSIONS AND RECOMMENDATIONS FOR FUTURE WORK

6.1 Summary

A computer technique for the dynamic analysis of a heating system and its control has been developed. It is based on the Laplace transfer function technique, with which linear components can be modelled efficiently. For the complex thermal processes in a building, a detailed room model is employed. Both the distributed parameter elements and the lumped elements are considered in the model, as well as the radiant heat exchanges. The continuous form of the Laplace transfer function for the room is determined through a modified least-squares fitting to the discrete frequency response data, which are obtained by inverting the admittance matrix of the room thermal network. The building envelope, the heating system and its control are treated as the elements of an integrated thermal system in which the thermal interactions between each element are considered.

The overall system Laplace transfer function is obtained by using block diagram algebra, including the transfer functions for the building, the heating system and the control components. Significant insight into the heating system may be achieved through frequency domain analysis. Stable operation of the system can be obtained by the proper selection of the controller gains based on the Ziegler-Nichols tuning method. The time domain response of the overall transfer function is determined by means of an efficient numerical Laplace transform inversion technique.

The computer program HEATCON was developed to conduct the analysis of a

heating control system. The procedure employed can be summarized as follows:

1. The discrete frequency response of a building is determined with the general Building Environment and Energy Program (BEEP) which uses a detailed thermal network room model;

2. The continuous form of the room transfer functions in the Laplace domain is determined accurately with an iterative fitting technique;

3. The overall system transfer function is obtained by the integration of component transfer functions, such as the transfer functions for room, heating system and control elements with block diagram algebra.

4. Frequency domain analysis of the overall transfer function is conducted for the estimation of control parameters, such as the proportional gain which will ensure stable operation of the system.

5. The transient response of the system is investigated by means of a stepwise numerical Laplace transform inversion technique.

The transient responses to thermostat setpoint changes determined with HEATCON have been compared with the experimental results of the radiant heating systems installed

in the test room on the roof of the Centre for Building Studies. Reasonable agreement is generally observed between the analytical and experimental results. The computer technique developed provides an efficient tool for studies of the thermal interactions between the building, the heating system and the control components. This assists us in choosing proper control parameters, as well as for evaluating design options based on the relative comparisons. These design options may include building envelope thermal mass, window sizes, heating system types and control methods.

6.2 Contributions and recommendations for future work

In this study, a unified analysis approach to a heating system and its control has been developed and applied to a specific type of heating system --- the electric radiant panel heating.

It was found that the thermal comfort may be improved by the control of a radiant heating system based on the operative temperature, which includes the influence of the air temperature and the mean radiant temperature. However, given a proportional control gain, the radiant heating with operative temperature control has much higher potential to incur an unstable operation of the system. This is due to the slow response of the operative temperature sensor (a globe temperature sensor) and the radiant heating panels coupled with the effects of the thermal storage mass in the building. Recently, a newly developed radiometer-based sensor was developed which will solve this problem because of its fast response.

The comparison between the test results and computer simulations showed that the

Ziegler-Nichols method is an appropriate technique for tuning a radiant heating system. The technique implemented on a personal computer will greatly help an engineer in tuning the controller. This reduces the time required to properly tune and commission a heating control system to a minimum.

In summary, the main contributions of this work are the following:

1. A modified least squares fitting method has been applied to derivation of the Laplace transfer functions of a room from a detailed thermal network model. These transfer functions can be used both for building thermal control studies and energy analysis;

2. A stepwise algorithm has been employed for the calculation of the transient response with a numerical Laplace transform inversion technique. The method provides an efficient tool for the incorporation of the frequency domain analysis and time domain response in a unified program;

3. Experimental study of radiant panel heating systems with operative temperature control has been conducted in a full-scale outdoor test room. The numerical results from the program HEATCON are generally consistent with the experimental results. It has been found that special attention to system stability should be paid for a radiant heating system with operative temperature control.

Presently, this study has been confined to a one zone heating system. In future work, the room model should be extended to a multizone system including cooling. More extensive experimental measurements would be desirable in a better controlled environment. The experimental comparison of the power consumption of the systems with different types of control could be conducted in two identical rooms or in an environmental chamber.

It is obvious that the inclusion of a fast response sensor for the operative temperature in the control system will enhance the system operation. Such efforts should be made to develop a type of intelligent sensor to timely reflect occupant's comfort.

This study has also shown that a radiant heating system has slow response which may result in overheating during the warm up period or cause large temperature fluctuations with intermittent heating. One possible solution would be the combination of feedback and feedforward control. The capability of the control system to integrate the HVAC system and the building dynamics, and to predict the weather several hours or days in advance, would have significant benefit in both system performance and energy savings.

REFERENCE

Al-assadi, S.A.K., "An iterative method for simplification of discrete system", Journal of the Franklin Institute, vol. 326, no. 4, pp. 587-607, 1989.

ASHRAE Handbook-1987,"HVAC systems and applications".

ASHRAE Standard 88-81, "Thermal environment condition for human occupancy", 1981.

Athienitis, A.K., "A predictive control algorithm for massive buildings", ASHRAE Trans., Vol.94, Pt.2, 1988.

Athienitis, A.K.,Chandrashekar, M. and Sullivan, H.F., "Modelling and analysis of thermal network through subnetworks for multizone passive solar buildings", Appl. Math. Modelling, vol.9, pp. 109-116, 1985.

Athienitis, A.K. and Dale, J.D., "A study of the effects of window night insulation and low emissivity coating on heating load and comfort", ASHRAE Trans. Vol. 93, Part 1A, pp. 279-294, 1987.

Athienitis, A.K., Sullivan, H.F. and Hollands, K.G.T., "Passive solar simulation for multizone

buildings: a frequency domain approach", Proc. Solar Energy Society of Canada Conference, pp. 107-112, 1986.

Athienitis, A.K. Sullivan, H.F. and Hollands, K.G.T., "Discrete Fourier series models for building auxiliary energy loads based on network formulation techniques", Solar Energy, vol. 39, no. 3, pp. 203-210, 1987.

Athienitis, A.K., Stylianou, M. and Shou, J., "A methodology for building thermal dynamics and control applications", ASHRAE Trans., vol.96, part 2, pp. 839-848, 1990.

Athienitis, A.K. and Shou, J., "A general method for estimation of building transfer functions from detailed thermal models and applications", Proc. of ASME International Computers in Eng., pp.403-410, 1990.

Athienitis, A.K. and Shou, J., "Control of radiant heating based on the operative temperature", Proc. ASHRAE Tran. Vol.97, part 2, 1991 (in the press).

Berglund, L., "Radiant heating and control for comfort during transition condition", ASHRAE Trans., part 2, pp. 765-775, 1982.

BLAST, "Building load analysis and system thermodynamics program", Support office, Department of Mechanical Engineering, University of Illinois, Urbana-Champaign, 1983.

Borresen, B.A., "HVAC control process simulation", ASHRAE Trans., vol.87, part 2, PP. 871-882, 1981.

Borresen, B.A., "Thermal room models for control analysis", ASHRAE Trans., vol. 87, part 2, pp. 251-261, 1981.

Bryan, W., "Comparative energy requirements of radiant space heating", ASHRAE Trans., vol. 87, pp. 106-115, 1981.

Chen, Q., "Comfort and energy consumption analysis in buildings with radiant panels", Energy and Buildings, 14, pp. 247-287, 1990.

Clark, D., Hurley, C.W. and Hill, C.R.,"Dynamic models for HVAC system components", ASHRAE Trans., part 1b, pp. 737-751, 1985.

Curtis, R., et al., "The DOE-2 building energy use analysis program", Lawrence Berkley Laboratory, 1984.

Dexter, A.L., "Control system simulation - computer control", Energy and Buildings, vol. 10, pp. 203-211, 1988.

Fanger, P.O., "Thermal comfort",Mcgraw-Hill, 1972.

Gondal, I.A., "Linear analysis of an air-temperature control loop", ASHRAE Trans., part 2, pp. 736-745, 1987.

Haghighat, F. and Athienitis, A.K., "Comparison between time domain and frequency domain computer program for building energy analysis", Computer-aided design, vol.20, no.9, 1988.

Hartman, T.B., "Dynamic control: fundamentals and considerations", ASHRAE Trans., part 1, pp. 599-609, 1988.

Hittle, D.C., "The building loads analysis system thermodynamics (BLAST) program, version 2.0: users manual", 1979.

Hunt, King and Trechsel, "Building air change rate and infiltration measurements", American Society for Testing and Materials, 1980.

Jones, B.W., Niedringhaus, W.F. and Imel, M.R., "Field comparison of radiant and convective heating in vehicle repair buildings", ASHRAE Trans., part 1, pp. 1045-1051, 1989.

Kalisperis, L.N., "Automated design of radiant heating system based on MRT", ASHRAE Trans., Vol. 96, Part 1, pp. 1288-1295, 1990

Kelly, G.E., "Control system simulation in North America", Energy and Building, vol. 10, pp.

193-202, 1988.

Kimura, K., "Scientific basis of air conditioning", Applied Science Publisher LTD., 1977.

Levy, E.C., "Complex-curve fitting", IRE Trans., AC-4, pp. 37-43, 1959.

Markel, M.L., et al., United States Patent No.: 4,863,279., 1989.

Mehta, D.P., "Dynamic performance of PI controllers: experimental validation", ASHRAE Trans., part 1, pp. 1775-1785, 1987.

Miller, D.E., "A simulation to study HVAC process dynamics", ASHRAE Trans., vol. 88, pp. 809-825, 1982.

Olesen, B.W., et al., "Thermal comfort in a room heated by different methods", ASHRAE Trans., vol. 86, part 1, pp. 34-48, 1980.

Olesen, B.W., et al., "Methods for measuring and evaluating the thermal radiation in a room", ASHRAE Trans., Part 1, pp.1028-1044, 1989.

Park, C., Bushby, S.T. and Kelly, G.E., "Simulation of a large office building system using HVACSIM$^+$ program", ASHRAE Trans., 1986.

Park, C., Clark, D.R. and Kelly, G.E., "An overview of HVACSIM+, a dynamic building/HVAC/control systems simulation program", Proc. of Building Energy Simulation Conf., pp. 175-184, 1985.

Shavit, G. and Brandt, S.G., "The dynamic performance of a discharge air - temperature system with PI controller", ASHRAE Trans., vol. 88, pp. 826-838, 1982.

Singhal, K. and Vlach, J., "Computation of time domain response by numerical inversion of the Laplace transform", Journal of the Franklin Institute, vol. 299, no. 2, 1975.

Stephanopoulos, G., "Chemical process control, an introduction to theory and practice, Prentice-Hall.

Thompsom, J.G.,"The effect of room and control systems dynamics on energy conservation", ASHRAE Trans., vol.87, part 2, pp. 883-896, 1981.

Vlach, J. and Singhal, K., "Computer methods for circuit analysis and design", Van Nostrand Reinhold Company, 1983.

Zaheer-uddin, M., "Combined energy balance and recursive Least square method for the identification of system parameters", ASHRAE Tran., vol. 96, part 2, pp.239-244, 1990.

Zmeureanu, R., Fazio, P. and Haghighat, F., "Thermal performance of radiant heating panels", ASHRAE Trans., vol. 94, part 2, 1988.

Zhang, X. and Warren, M.L., "Use of a general control simulation program", ASHRAE Trans., part 1, pp. 1776-1791, 1988.

APPENDIX A

NUMERICAL LAPLACE TRANSFORM INVERSION

The inverse Laplace transform v(t) of a transfer function V(s) is given by

$$v(t) = \frac{1}{2\pi j}\int_{c-j\omega}^{c+j\omega} V(s)\, e^{st}\, ds \qquad \text{(A-1)}$$

The exact inverse, however, is only possible if the poles of V(s) are known. To avoid root finding, Vlach and Singhal (1969,1983) substitute st with z

$$v(t) = \frac{1}{2\pi j}\int_{c'-j\omega}^{c'+j\omega} V(z/t)\, e^{z}\, dz \qquad \text{(A-2)}$$

and subsequently approximate e^z by a Padé rational function

$$R_{M,N}(z) = \frac{P_N(z)}{Q_M(z)} = \frac{\sum_{i=0}^{N} (M+N-i)!\,\binom{N}{i} z^i}{\sum_{i=0}^{M} (-1)^i (M+N-i)!\,\binom{M}{i} z^i} \qquad \text{(A-3)}$$

where $P_N(z)$ and $Q_M(z)$ are polynomials of orders N and M respectively. The first M+N+1 terms of this function's Taylor expansion are equal to those of the Taylor's expansion of e^z and when (A-3) is inserted in (A-2), the approximation v'(t) to v(t) becomes

$$v'(t) = \frac{1}{2\pi j}\int_{c'-j\omega}^{c'+j\omega} V(z/t)\, R_{M,N}(z)\, dz \qquad \text{(A-4)}$$

Using residue calculus, it can be shown that $R_{M,N}(z) = \sum_i K_i/(z-z_i)$ (with i=1-M) where K_i are residues and z_i are poles. Closing the path of integration around the poles of $R_{N,M}$ in the right

half plane, it can be shown that

$$v'(t) = -\frac{1}{t}\sum_{i=1}^{M} K_i V(z_i/t) \qquad \text{(A-5)}$$

which is the basic inversion formula. Real time functions can now be evaluated by using only the poles z_i in the upper half plane, thus reducing the computations to one half. If M is even and the bar denotes complex conjugate, then

$$\begin{aligned} v'(t) = &-\frac{1}{t}\sum_{i=1}^{M'} K_i V(z_i/t) - \frac{1}{t}\sum_{i=1}^{M'} K_i \bar{V}(\bar{z}_i/t) \\ &-\frac{1}{t}\sum_{i=1}^{M'} Re\,[K'_i\ V(z_i/t)] \end{aligned} \qquad \text{(A-6)}$$

where M'=M/2 and $K'_i=2K_i$. Values for K'_i and z_i for different M and N have been calculated and tabulated by Vlach and Singhal (1983).

APPENDIX B

INFILTRATION MEASUREMENT OF THE TEST ROOM

The measurement of infiltration rates may be performed by releasing tracer gas (CO_2) throughout the ventilated space and monitoring the decrease in concentration as a function of time. A method for data analysis has been suggested by Hunt et al.(1980), based on relative concentrations. The equation for the air infiltration rate may be expressed as:

$$I = -\frac{1}{t_m} \ln \frac{c_n}{c_n - 1} \qquad \text{(B-1)}$$

where

I = infiltration rates, times/hour.

t_m = time interval between measurement of c_{n-1} and cn, hours.

c_{n-1} = concentration of tracer at the beginning of time interval, ppm.

c_n = concentration of tracer at the end of the time interval, ppm.

The air infiltration rate in the test room was measured on January 11, 1991. A CO_2 analyzer (HORIBA) was used to measure the tracer gas (CO_2) concentration during the test. The CO_2 concentration as a function of time is given in Figure B-1. The concentration at the beginning of the test was 3910 ppm, while, at the end, it was 510 ppm. According to Equation (B-1), the air infiltration of the test room is found:

$$I = -\frac{1}{t_m} \ln \frac{c_n}{c_{n-1}}$$

$$= -\frac{1}{3.5} \ln \frac{510}{3910}$$

$$= 0.58 \quad .$$

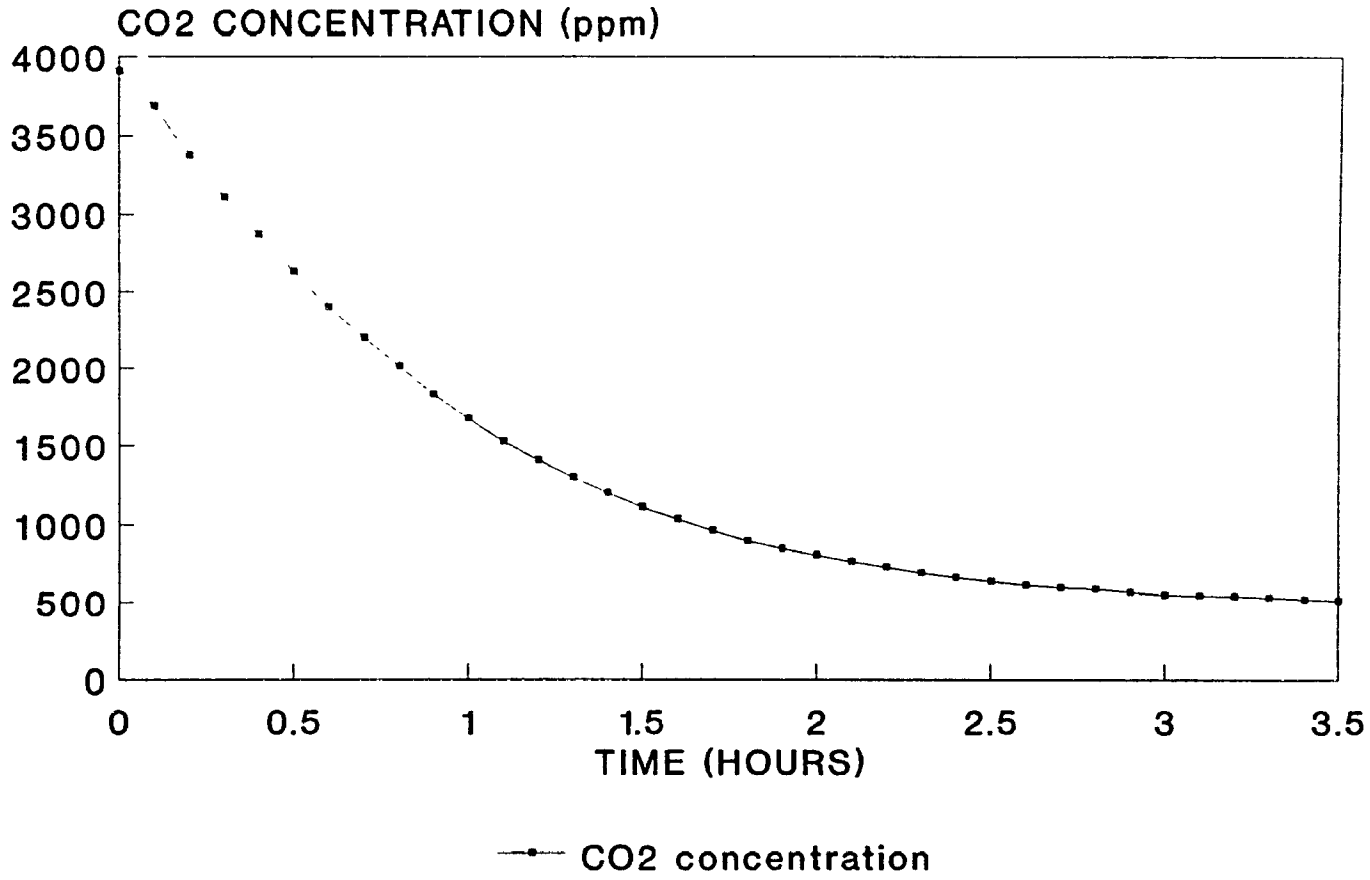

Figure B-1 CO2 concentration during infiltration test

APPENDIX C

TEMPERATURE MEASUREMENTS IN THE TEST ROOM

A test room for heating control study was set up in November, 1990, on the roof of Centre for Building Studies (CBS). Experiments were conducted with both an electric baseboard heater and electric radiant panel heating systems with proportional control during the period from November 1990 to March 1991.

The three heating systems installed in the test room are the high intensity radiant ceiling panels with the capacity of 800 W, the low intensity electric radiant floor panels with the capacity of 1,000 W and the electric baseboard heater with the capacity of 1,000 W. The heating system control and data acquisition is accomplished with a computer control and data acquisition system run by a software package Gen200.

There are a total of 32 channels for the data acquisition. 24 channels were used for thermocouples, 2 for thermistors, 2 for pyranometers (DC Voltage), 2 for heat flux sensors (DC Voltage) and 2 for light meters (DC Voltage). The following table lists each measured parameter and the associated channel number. Figure C-1 describes the locations of the surface temperature sensors in the test room.

Channel number	Label	Parameter
0	TO	Outdoor air temperature.
1	TAI	Room air temperature at centre.
2	TGC	Globe temperature at room centre.
3	TGW	Globe temperature at window.
4	TPANSF	Front surface temperature of the south ceiling panel.
5	TPANSB	Back surface temperature of the south ceiling panel.

Channel number	Label	Parameter
6	TPANNF	Front surface temperature of the north ceiling panel.
7	TPANNB	Back surface temperature of the north ceiling panel.
8	TIWALS1	Interior surface temperature of the south wall at location number 1.
9	TIWALS2	Interior surface temperature of the south wall at location number 2.
10	TIWALS3	Interior surface temperature of the south wall at location number 3.
11	TIWALS4	Interior surface temperature of the south wall at location number 4.
12	TIWALW	Interior surface temperature of the west wall.
13	TIWALE	Interior surface temperature of the east wall.
14	TDOOR	Interior surface temperature of the door.
15	TFLR2B	Back surface temperature of floor panel at location number 2.
16	TFLR5B	Back surface temperature of floor panel at location number 5.
17	TFLR2T	Top surface temperature of floor panel at location number 2.
18	TFLR5T	Top surface temperature of floor panel at location number 5.
19	N/A	
20	N/A	
21	TAIT	Room air temperature located 10 cm from the ceiling.
22	TCEIL	Interior surface temperature of the ceiling.

Channel number	Label	Parameter
23	N/A	
24	SOLIN	Solar radiation through the window.
25	SOLOUT	Solar radiation outside the test room.
26	N/A	
27	TIWALN	Interior surface temperature of the north wall.
28	N/A	
29	N/A	
30	N/A	
31	N/A	

Two globe temperature sensors were used to measure the temperature asymmetry in the test room, one of which was placed in the centre of the room at a height of 1.2 m, while another one was placed adjacent to the window at the same height. To measure the vertical air temperature distribution, four thermocouples were placed at 0.1 m, 1.1 m, 1.7 m and 2.0 m from the floor level in the centre of the test room.

During the operation of the baseboard heating or radiant floor heating system, which have the same heating capacity of 1 KW, the globe temperatures and vertical air temperatures were measured. Typical results are shown in tables C-1 and C-2. As can be seen the radiant floor heating system provided a more uniform thermal environment in comparison with baseboard heating.

Table C-1. Globe temperature difference (°C) between globe near window and centre globe (TGW - TGC).

Heating type	Globe temperature difference
Baseboard heating	+1.6
Radiant floor heating	-0.9

Table C-2. Vertical air temperature difference (°C) at different heights in comparison with the air temperature (°C) at the height of 0.1 m.

Heating type	1.1 m	1.7 m	2.0 m
Baseboard heating	2.4	2.2	2.6
Radiant floor heating	1.3	0.5	1.5

The surface temperatures of heating panels, walls, floor, window and door were also measured. A representative result of the measurements with radiant floor heating are shown in figure C-2.

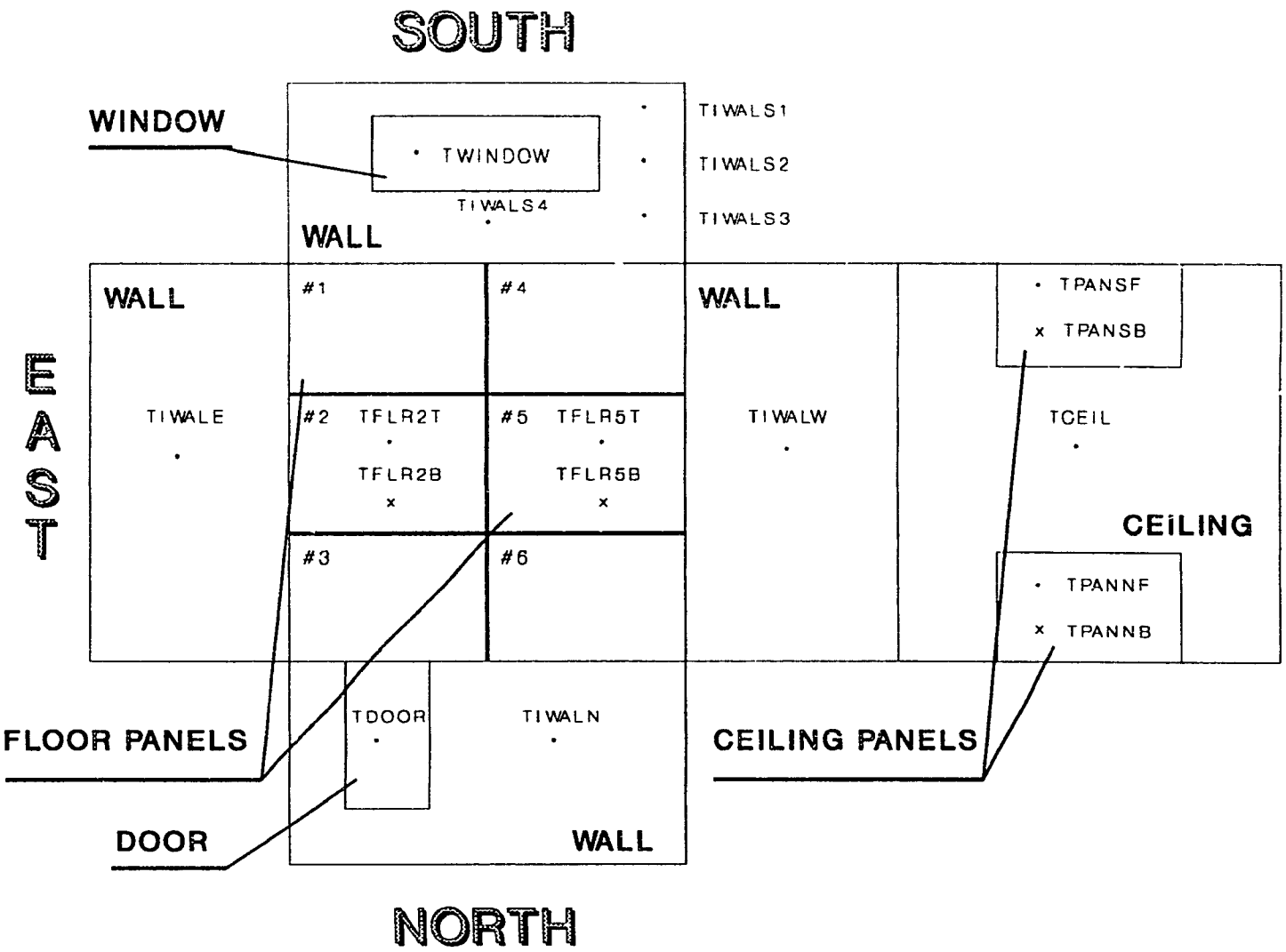

C-1 Locations of the surface temperature sensors in the test room.

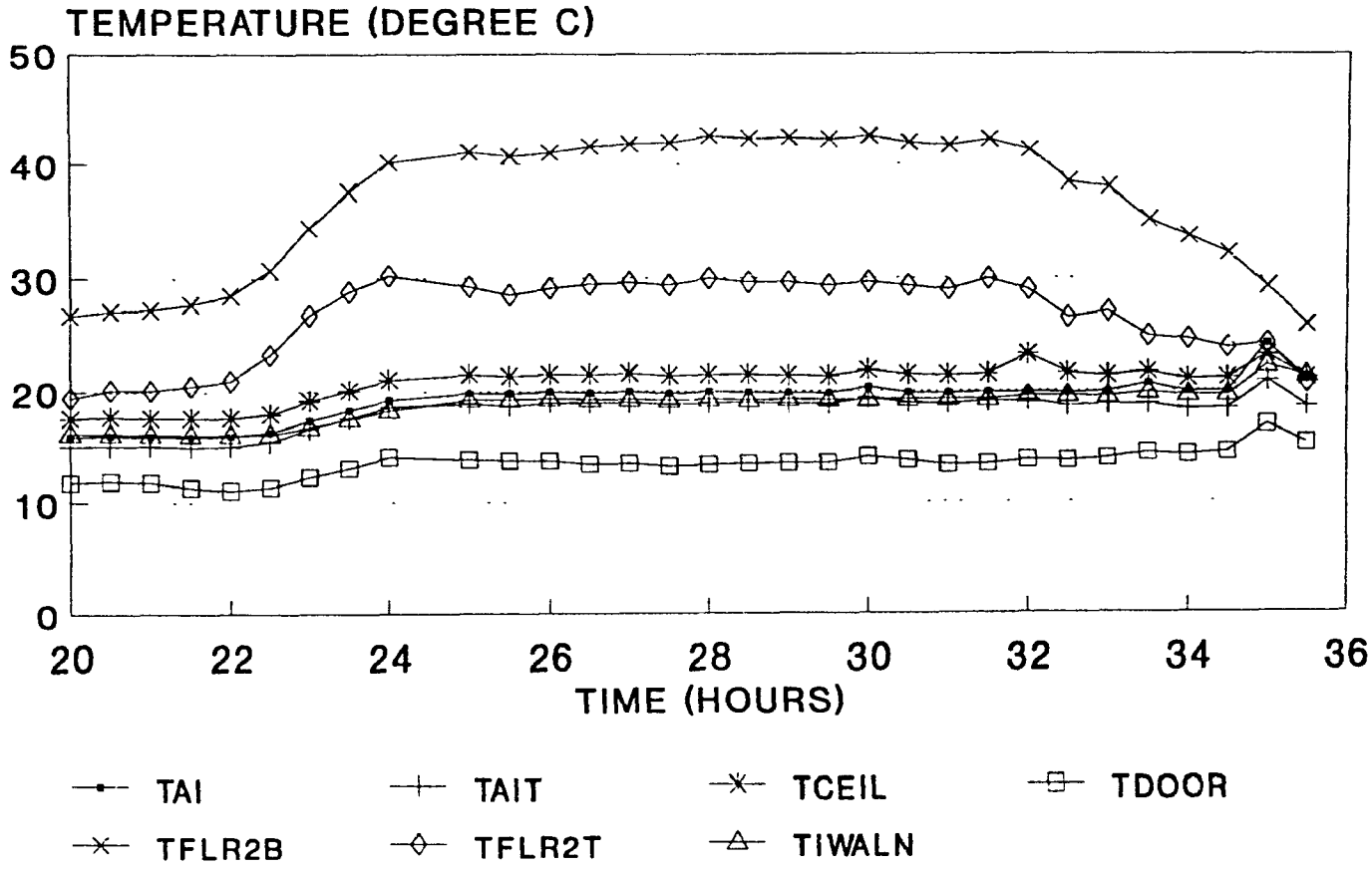

C-2 Representative temperatures of the test room with radiant floor heating.